DUDLEY KNOX LIBRARY
NAVAL POSTGRADUATE SCHOOL
MONTEREY, CALIFORNIA 93943

NPS 68-85-009

NAVAL POSTGRADUATE SCHOOL
Monterey, California

THESIS

TEMPORAL AND SPATIAL DISTRIBUTIONS OF
ARCTIC SEA ICE THICKNESS
AND PRESSURE RIDGING STATISTICS

by

Robert P. Garrett

March 1985

Thesis Advisor: Robert H. Bourke

Approved for Public Release; Distribution Unlimited

Prepared for:
Naval Surface Weapons Center, White Oak
Silver Spring, Maryland 20902

T224624

NAVAL POSTGRADUATE SCHOOL
Monterey, California

Commodore R. H. Schumaker
Superintendent

D. A. Schrady
Provost

This thesis prepared in conjunction with research sponsored in part by Naval Surface Weapons Center, White Oak, Silver Spring, Maryland under N6092185WR0084. Reproduction of all or part of this report is authorized.

Released by:

SECURITY CLASSIFICATION OF THIS PAGE (When Data Entered)

REPORT DOCUMENTATION PAGE

READ INSTRUCTIONS BEFORE COMPLETING FORM

1. REPORT NUMBER: NPS 68-85-009	2. GOVT ACCESSION NO.
3. RECIPIENT'S CATALOG NUMBER	
4. TITLE (and Subtitle): Temporal and Spatial Distributions of Arctic Sea Ice Thickness and Pressure Ridging Statistics	5. TYPE OF REPORT & PERIOD COVERED: Final, Master's Thesis Dec 1983-March 1985
	6. PERFORMING ORG. REPORT NUMBER: NPS 68-85-009
7. AUTHOR(s): Robert P. Garrett in conjunction with R. H. Bourke	8. CONTRACT OR GRANT NUMBER(s): N-60921-85-WR-0084
9. PERFORMING ORGANIZATION NAME AND ADDRESS: Naval Postgraduate School Monterey, California 93943	10. PROGRAM ELEMENT, PROJECT, TASK AREA & WORK UNIT NUMBERS
11. CONTROLLING OFFICE NAME AND ADDRESS: Naval Surface Weapons Center, White Oak Silver Spring, Maryland 20902	12. REPORT DATE: March 1985
	13. NUMBER OF PAGES: 168
14. MONITORING AGENCY NAME & ADDRESS (if different from Controlling Office)	15. SECURITY CLASS. (of this report): UNCLASS
	15a. DECLASSIFICATION/DOWNGRADING SCHEDULE

16. DISTRIBUTION STATEMENT (of this Report)

Approved for public release; distribution unlimited

17. DISTRIBUTION STATEMENT (of the abstract entered in Block 20, if different from Report)

18. SUPPLEMENTARY NOTES

19. KEY WORDS (Continue on reverse side if necessary and identify by block number)

Arctic, Arctic Ice, Sea Ice, Arctic Ocean, Ice Thickness, Pressure Ridge

20. ABSTRACT (Continue on reverse side if necessary and identify by block number)

Data from the unclassified literature were reviewed to determine the regional and seasonal distributions of sea ice thickness, pressure ridging statistics, frequency of occurrence of polynyas, and keel/sail height ratios. Seasonal and regional maps and histograms of these properties were constructed. The majority of the data were obtained from submarines equipped with a narrow-beam, upward-looking sonar.

DD FORM 1 JAN 73 1473 EDITION OF 1 NOV 65 IS OBSOLETE

S/N 0102-LF-014-6601

SECURITY CLASSIFICATION OF THIS PAGE (When Data Entered)

As determined from an analysis of 17 submarine cruises, the overall mean thickness of Arctic sea ice above 65°N, including both deformed and undeformed ice, is 2.9 m with a standard deviation of 1.8 m. The overall seasonal mean ranges from approximately 2.4 m in spring to 3.3 m in summer. Local mean ice thicknesses ranged from less than 1 m near the marginal ice zone to greater than 7 m to the north of the Canadian Archipelago. Histograms of sea ice thickness reflect a bimodal distribution in winter and spring, an effect of the presence of thin first year ice. Due to ice melt in summer and autumn only a single mode of much thicker multi-year ice is observed.

S/N 0102-LF-014-6601

Approved for public release; distribution is unlimited.

Temporal and Spatial Distributions of Arctic Sea Ice Thickness and Pressure Ridging Statistics

by

Robert P. Garrett
Lieutenant Commander, United States Navy
B.A., University of New Mexico, 1976
M.M.A., University of Rhode Island, 1982

Submitted in partial fulfillment of the
requirements for the degree of

MASTER OF SCIENCE IN METEOROLOGY AND OCEANOGRAPHY

from the

NAVAL POSTGRADUATE SCHOOL
March 1985

Thesis
G203
c.1

ABSTRACT

Data from the unclassified literature were reviewed to determine the regional and seasonal distributions of sea ice thickness, pressure ridging statistics, frequency of occurrence of polynyas, and keel/sail height ratios. Seasonal and regional maps and histograms of these properties were constructed. The majority of the data were obtained from submarines equipped with a narrow-beam, upward-looking sonar.

As determined from an analysis of 17 submarine cruises, the overall mean thickness of Arctic sea ice above 65°N, including both deformed and undeformed ice, is 2.9 m with a standard deviation of 1.8 m. The overall seasonal mean ranges from approximately 2.4 m in spring to 3.3 m in summer. Local mean ice thicknesses ranged from less than 1 m near the marginal ice zone to greater than 7 m to the north of the Canadian Archipelago. Histograms of sea ice thickness reflect a bimodal distribution in winter and spring, an effect of the presence of thin first year ice. Due to ice melt in summer and autumn only a single mode of much thicker multi-year ice is observed.

TABLE OF CONTENTS

I. INTRODUCTION 14

A. PURPOSE AND OBJECTIVES 14

B. BACKGROUND 16

1. Sea Ice and Pressure Ridge Formation Processes 16

2. Distribution, Deformation, and Drift of Sea Ice 19

3. Mean Ice Thickness 23

4. Level Ice 25

5. Pressure Ridging 26

6. Leads and Polynyas 29

II. DATA 32

A. SOURCES OF DATA 32

1. Methods of Measurement 32

B. TREATMENT OF DATA 45

1. Mean Ice Thickness 46

2. Pressure Ridging 48

3. Polynyas 49

III. DISCUSSION AND RESULTS 51

A. ARCTIC BASIN 51

1. Mean Annual Ice Thickness 51

2. Mean Annual Pressure Ridging 53

3. Seasonal Ice Thickness Distribution . . . 54

B. REGIONAL DISCUSSION 73

1. Central Arctic Basin 76

2. Chukchi Sea 81

3. Beaufort Sea 85

4. Canadian Archipelago 88
5. Baffin Bay and Davis Strait 91
6. Greenland Sea. 93
7. Eurasian Seas 96
IV. CONCLUSIONS 112
APPENDIX A: SUBMARINE TRANSECT DATA FROM LESCHACK (1983) 114
APPENDIX B: SUBMARINE TRANSECT DATA FROM WADHAMS . . 120
APPENDIX C: MEAN ICE THICKNESS AND KEEL DRAFT MAPS. . 122
LIST OF REFERENCES 146
BIBLIOGRAPHY 151
INITIAL DISTRIBUTION LIST 157

LIST OF TABLES

I	Data from Various Submarine Cruises 1960-1982 . .	37
II	Seasonal Partitioning of Data	47
III	Geographic Partitioning of Data	47
IV	Seasonal Mean Ice Thickness and Standard Deviation	66
V	Regional Mean Ice Thickness	74
VI	Ice Conditions in the Central Arctic Basin	78
VII	Ice Conditions in the Chukchi and Beaufort Seas	83

LIST OF FIGURES

1.1 Major drift patterns of ice in the Arctic Ocean (after Weeks, 1978) 21
1.2 Probability density functions of ice draft, along a transit from 85° to 90°N at 70° W (after Wadhams, 1981b) 30
1.3 Relation between mean ice draft and the percentage of level ice per 100 km (after Wadhams, 1983a) 30
1.4 Probability density function of level ice from GURNARD in the Beaufort Sea (after Wadhams and Horne, 1980) 31
1.5 Trafficability diagram for M'Clure St. (after McLaren, 1984) 31
2.1 Typical underice profile. Depths are marked in ft. Note the large keel extending to 97 ft (29.5m) 39
2.2 Distribution of keel spacings. Results are plotted for keels deeper than 5 and 9 m (after Wadhams and Horne, 1980) 41
2.3 Geographical sampling regions for laser data (after Tucker et al., 1979) 45
2.4 Contours (percent) of the area containing open water in the Arctic Ocean (after LeSchack, 1983) 50
3.1 Arctic mean ice thickness distribution. 53
3.2 Pressure ridge keel depth distribution in the Arctic Ocean 54
3.3 Mean ice thickness(m) in spring derived from submarine underice profile data 57

3.4 Mean ice thickness(m) in summer derived from submarine underice profile data 58
3.5 Mean ice thickness(m) in autumn derived from submarine underice profile data 59
3.6 Mean ice thickness(m) in winter derived from submarine underice profile data 60
3.7 Contours(m) of mean annual ice thicknesss. Dashed lines represent conditions in April 1977 (after LeSchack, 1980) 61
3.8 Arctic spring mean ice thickness distribution. . . 63
3.9 Arctic summer mean ice thickness distribution. . . 64
3.10 Arctic autumn mean ice thickness distribution. . . 64
3.11 Arctic winter mean ice thickness distribution. . . 65
3.12 Summer pressure ridging intensity from BIRDSEYE data (after Weeks, 1971) 68
3.13 Winter pressure ridging intensity from BIRDSEYE data (after Weeks, 1971) 69
3.14 Spring pressure ridge keel distribution from submarine underice data 70
3.15 Summer pressure ridge keel distribution from submarine underice data 71
3.16 Autumn pressure ridge keel distribution from submarine underice data 71
3.17 Winter pressure ridge keel distribution from submarine underice data 72
3.18 Regional locater map for the Arctic Ocean 75
3.19 Location of regions of frequently occurring polynyas. 97
3.20 Frequency distribution of mean ice thickness in the Central Arctic Basin 100
3.21 Percentage of keels of different drafts in the Central Arctic Basin 100
3.22 Histograms of sea ice drafts in the Central Arctic Basin (after Weeks et al., 1981) 101

3.23 Percentage of keels of different drafts in the Central Arctic from 2 submarine cruises (after Weeks et al., 1981) 101
3.24 Regional variation in ridging intensity from the one-parameter model (after Hibler et al., 1974) 102
3.25 Frequency distribution of mean ice thickness in the Chukchi Sea 103
3.26 Percentage of keels of different drafts in the Chukchi Sea 103
3.27 Summer frequencies of ridge heights and number of ridges per nautical mile (after Weeks et al., 1981) 104
3.28 Winter frequencies of ridge heights and number of ridges per nautical mile (after Weeks et al., 1981) 104
3.29 Frequency distribution of mean ice thickness in the Beaufort Sea 105
3.30 Percentage of keels of different drafts in the Beaufort Sea 105
3.31 Route of the USS GURNARD, 7-10 April 1976 (after Wadhams and Horne, 1980) 106
3.32 Frequency distribution of mean ice thickness in the Canadian Archipelago 106
3.33 Percentage of keels of different drafts in the Canadian Archipelago 107
3.34 Frequency distribution of mean ice thickness in Baffin Bay and Davis Strait 107
3.35 Percentage of keels of different drafts in Baffin Bay and Davis Strait 108
3.36 Percentage of level ice in Davis St. with respect to mean ice draft with linear regression (after Wadhams, 1985) 108

3.37 Track of HMS SOVEREIGN, October 1976. The numbers refer to the 100 km sections used by Wadhams (1981b) 109
3.38 Contours of mean ice draft in Fram Strait in April-May 1979 (after Wadhams, 1981b) 110
3.39 Frequency distribution of mean ice thickness in the Greenland Sea 111
3.40 Percentage of keels of different drafts in the Greenland Sea 111
C.1 Mean ice thickness(m) in spring, 84°N-90°N . . . 122
C.2 Mean ice thickness(m) in spring, 65°N-85°N, 010°W-100°E 123
C.3 Mean ice thickness(m) in spring, 65°N-85°N, 070°E-180°E 124
C.4 Mean ice thickness(m) in spring, 65°N-85°N, 100°W-010°E 125
C.5 Mean ice thickness(m) in spring, 65°N-85°N, 180°W-070°W 126
C.6 Mean ice thickness(m) in summer, 84°N-90°N . . . 127
C.7 Mean ice thickness(m) in summer, 65°N-85°N, 010°W-100°E 128
C.8 Mean ice thickness(m) in summer, 65°N-85°N, 070°E-180°E 129
C.9 Mean ice thickness(m) in summer, 65°N-85°N, 100°W-010°E 130
C.10 Mean ice thickness(m) in summer, 65°N-85°N, 180°W-070°W 131
C.11 Mean ice thickness(m) in autumn, 84°N-90°N . . . 132
C.12 Mean ice thickness(m) in autumn, 65°N-85°N, 010°W-100°E 133
C.13 Mean ice thickness(m) in autumn, 65°N-85°N, 070°E-180°E 134
C.14 Mean ice thickness(m) in autumn, 65°N-85°N, 100°W-010°E 135

C.15 Mean ice thickness(m) in autumn, 65°N-85°N, 180°W-070°W 136
C.16 Mean ice thickness(m) in winter, 84°N-90°N . . . 137
C.17 Mean ice thickness(m) in winter, 65°N-85°N, 010°W-100°E 138
C.18 Mean ice thickness(m) in winter, 65°N-85°N, 070°E-180°E 139
C.19 Mean ice thickness(m) in winter, 65°N-85°N, 100°W-010°E 140
C.20 Mean ice thickness(m) in winter, 65°N-85°N, 180°W-070°W 141
C.21 Mean keel drafts(m) for spring, 65°N-90°N 142
C.22 Mean keel drafts(m) for summer, 65°N-90°N 143
C.23 Mean keel drafts(m) for autumn, 65°N-90°N 144
C.24 Mean keel drafts(m) for winter, 65°N-90°N 145

ACKNOWLEDGEMENTS

The assistance of Commander John King, USN and Mr. Meyer Kleinerman of the Naval Surface Weapons Center, Washington D.C. is gratefully acknowledged. Also the assistance of Dr. W. F. Weeks of the United States Army Cold Regions Research and Engineering Laboratory, Hanover, N.H. and Dr. Alan Beal of the Arctic Submarine Laboratory, Naval Oceans Systems Center, San Diego, Ca. is gratefully appreciated. Special thanks go to Professor Robert Bourke, Naval Postgraduate School, for his guidance in preparation of this thesis.

I. INTRODUCTION

A. PURPOSE AND OBJECTIVES

The purpose of this study is to provide the United States Navy and the scientific community with current information on the temporal and spatial distribution of sea ice thickness and sea ice features in the Arctic Ocean. Important sea ice features include the seasonal and regional distributions of mean ice thickness, pressure ridge frequency, sail height and keel depth, leads and polynyas, and deformed and undeformed ice thickness.

Operations in the Arctic Ocean, whether military or purely scientific, often rely upon a knowledge of the thickness of the sea ice for any particular region during any season within a predetermined degree of certainty. Prior knowledge of sea-ice thickness is important in the development of items such as ice penetration devices; i.e., sonobuoys, air launched weapons, and scientific sea-ice data collectors which measure not only ice thickness but salinity and density. Also, the success rate of penetration devices prior to deployment may be ascertained, allowing the most efficient number of devices to be used for a particular operation. The safety of submarine operations under the ice (e.g., to surface through the ice during an emergency or routine evolution) is dependent upon a prior knowledge of lead and polynya frequency as well as knowledge of those areas where ice can be expected to be relatively thin. Knowledge of areas of extremely thick ice with deep keel drafts is also important because such areas represent possible dangers to the safe navigation of the submarine, especially in shallow or restricted water. The success of

Anti-Submarine Warfare (ASW) in the Arctic is completely dependent upon knowledge of the environment. Knowing where the underside of the ice is rough or where keel drafts tend to be either deep or shallow dictates the success of detecting the enemy or being detected by his sonar. Additionally, examination of climatological changes over a long period depends upon the knowledge acquired of current sea-ice conditions. Armed with this knowledge, scientists may then gain an understanding about past and future ice conditions.

Current analyses of Arctic sea-ice conditions are generally confined to a particular region for a given time period per study. In order to gain an understanding of all the available information on Arctic sea-ice conditions, one must be familiar with many different papers and publications; even then a complete knowledge of ice conditions may not be obtained. Much of the data which has been collected has not been analyzed and only portions of many other data sets have been actually analyzed and published. The major portion of Arctic sea-ice data comes from submarine underice sonar profiles and from laser profilometers obtained during Arctic reconnaisance flights. A principal effort of this thesis was to compile all currently analyzed Arctic sea-ice data, as well as introducing the previously untapped data source of United States submarine commanding officer's cruise reports, into a combined data set, in order to provide temporal and spatial ice thickness statistics and distributions for the entire Arctic Ocean.

To accomplish the purposes of this research the following objectives were pursued:

1. To compile all of the available previously analyzed submarine underice data sets and reconnaisance flight ice surface data sets into one reference.

2. To produce statistics, maps, and histograms of mean ice thickness, pressure ridge, and polynya distributions on a regional and seasonal basis.

3. To incorporate findings from the current literature to reinforce, contrast, and compare with that of this study.

4. To produce an extended bibliography consisting of the current studies and papers which provide information on Arctic sea ice conditions.

B. BACKGROUND

1. Sea Ice and Pressure Ridge Formation Processes

Sea ice is formed over the Arctic Ocean as a result of the freezing of surface waters by the cool (-20° to -40°C) air temperatures of this region. Ice initially begins to form when sea surface temperatures are cooled to the equilibrium freezing temperature, a function of the local surface salinity (Zubov, 1943). For the typical Arctic surface salinity of 32.5 to 34.2 parts per thousand (ppt) sea water will begin to freeze when surface temperatures are between -1.5° and -1.78° C (Stanford, 1984). For this to occur, the air temperature must be even lower. Ice grows as crystals composed of plates, where each plate is partially separated by an array of brine pockets. Ice then grows downward into the underlying sea water.

The strength of ice is determined primarily by the amount of ice-to-ice connections between the plates (Weeks, 1978). As the ice thickens and ages, brine percolates downward out of the ice. At the end of a year's growth the ice has an average salinity of 4-5 ppt (Weeks, 1978). The most rapid change in salinity of ice occurs during the first summer's melt season when low salinity surface melt water

(0-1 ppt) drains down through the ice sheet. This process produces a salinity profile within the ice mass starting at about zero near the surface and increasing with depth to 2-3 ppt near the bottom of the ice. This is the characteristic salinity profile for multi-year ice. The brine volume is the principal parameter controlling the large variations in the strength of sea ice.

The differences in properties between first-year and multi-year sea ice are based upon strength and subsequently brine content (Weeks, 1978; Zubov, 1943; and Weeks and Ackley, 1982). First-year ice is thin (0-2 m), being limited by the amount of ice growth possible during one winter. Multi-year ice is generally thicker (2-4 m), with the limiting thickness determined from the balance between ice growth in winter and ice melt in summer. The surface and interior temperatures of the thicker multi-year ice are invariably colder during the winter. In addition, because of the extensive desalinization process which occurs during the summer melt period, multi-year ice has a lower mean salinity than first-year ice (0-2 ppt vs. 4-5 ppt) (Weeks et al., 1971). Some multi-year ice may have also recrystallized which results in a different texture than first-year ice. Sea ice can therefore be classed by age: first-year ice is thinner and weaker than the thicker, stronger multi-year ice.

Other important aspects of the Arctic ice pack are produced primarily by the surface forces that are exerted on the ice by the atmosphere and the ocean which cause the ice to diverge and converge (Weeks, 1978). Cracks in sea ice occur frequently and on many different scales. When a long narrow crack opens up, the resulting open water area is called a lead. During most of the year a newly opened lead freezes within 5-15 days depending upon the meteorological conditions (Weeks, 1978). When divergence of the ice stops

and the ice pack begins to converge, it is the thinner ice that is crushed and pushed into ridges which characterize the deformed ice pack. This is the procedure which is responsible for the formation of large pressure ridges which are found throughout the Arctic Ocean. Areas of pressure ridging are generally referred to as deformed ice. Forms of deformation include rafting, ridging, and hummocking. Alternately, undeformed ice refers to sheets of relatively flat ice which have not been subjected to converging processes.

Most ridges develop from the deformation of thinner, generally first-year ice, floes which form in leads, or during the freezing season along the peripheries of the permanent ice edge. The type of ridging varies with the relative thickness of the interacting ice sheets and with the type of motion occurring between the ice sheets, whether compression or shear. Through these motions and interactions, the ice sheets fracture forming large angular blocks which pile up forming hummocks or pressure ridges. The portions of the pressure ridges and hummocks which are above the water line are referred to as sails while the below water line portions are called keels (Zubov, 1943). Some of these ridges are immense accumulations of deformed ice; sails as high as 13 m and keels as deep as 47 m represent the maximum observed to date for free-floating ice features (Kovacs, et al., 1972). First-year ridges are commonly poorly frozen together, a jumble of angular blocks full of air/snow pockets, and are much less resistant to penetration by ships and mechanical penetration devices used for ice measurements than multi-year ridges, which are massive pieces of low-salinity ice (Weeks, 1984).

In addition to the ice features discussed above, when large pieces of ice break away from the Arctic ice shelf or from a glacier, they result in ice islands and

icebergs, respectively. Ice islands usually have a thickness of 30 to 50 m, an area from a few thousand square meters to several hundred square kilometers, and a regular undulating upper surface (Weeks, 1978; Zubov, 1943). An Arctic iceberg is somewhat smaller in size than an ice island and is of greatly varying shape with a freeboard of more than 5 m (Weeks, 1978).

2. Distribution, Deformation, and Drift of Sea Ice

At its maximum extent Arctic sea ice covers 15,100,000 km² (Weeks, 1978). Maps depicting the maximum and minimum seasonal extent of sea ice are given in Chapter 3. Most of the ice, and almost all of the heavy multi-year ice, is contained within the essentially land-locked Arctic Ocean and its marginal seas. The more southerly seas in the Arctic region contain primarily first-year ice. The one exception is the shelf waters off the coast of East Greenland which serves as the main exit for thick multi-year ice leaving the Arctic Ocean. The thickest and most deformed ice in the Arctic is found along the northern coast of Greenland, in the Lincoln Sea, and along the west coast of the Canadian Archipelago (Wadhams, 1983a). The thinnest ice is found towards the Soviet side of the Arctic Ocean. Because of the land-locked nature of the Arctic Ocean, the seasonal variation of the ice extent in the Arctic is only 20-25% of the maximum (Weeks, 1982).

A summary of information collected by the U.S. Navy "BIRDSEYE" ice reconnaisance flights over the Arctic Ocean provides the most detailed compilation of airborne sea-ice characteristics presently available (Wittman and Schule, 1966). The data obtained from the BIRDSEYE flights have been useful to identify at least three ice provinces in the Arctic Ocean which are characteristic of certain ice types and illustrate the distribution of ice in the Arctic Ocean (Weeks et al., 1971, p.16):

1. A Coastal Province consisting of a zone of shore-fast ice bordered by a flaw zone of disturbed ice and in some locations a recurring flaw lead.

2. An Offshore Province mainly composed of relatively unstable first-year ice which has usually experienced a considerable amount of deformation.

3. A Central Arctic Basin Province which is by far the largest province of the three and is primarily composed of multi-year ice. The amount of deformation in this province is commonly thought to be less than in areas closer to shore.

All of these provinces can undoubtedly be further sub-divided as more information becomes available. For instance, in the Central Arctic Basin Province the surface topography of the ice in the Transpolar Drift Stream appears to be significantly rougher (angular ridges and hummocks) than the topography of the ice in the Beaufort Gyre (gentle rounded hummocks) (Koerner, 1970).

The drift features of the Arctic Ocean are illustrated in Figure 1.1. The drift pattern is in direct response to the atmospheric circulation pattern which dominates the Arctic region throughout much of the year. A high pressure cell is almost continuously centered over the Beaufort Sea causing the generally anticyclonic rotation of the Arctic drift system, in particular the Beaufort or Pacific Gyre (Zubov, 1943). Two dominant drift features are readily evident. The Transpolar Drift Stream flows from the East Siberian Sea across the North Pole to the northeast of Greenland. It transports ice from the cold shallow waters off the Siberian continental shelf (Weeks, 1982). Because this area is ice free in summer and because of the cold off-shore Siberian winds, it undergoes rapid ice growth every fall. This area also is an area of rapidly growing ice

even in winter due to the northward movement of the ice. The transpolar trip across the Arctic Ocean takes about 5 years to complete (Dunbar and Wittman, 1963; Weeks, 1978; Zubov, 1943).

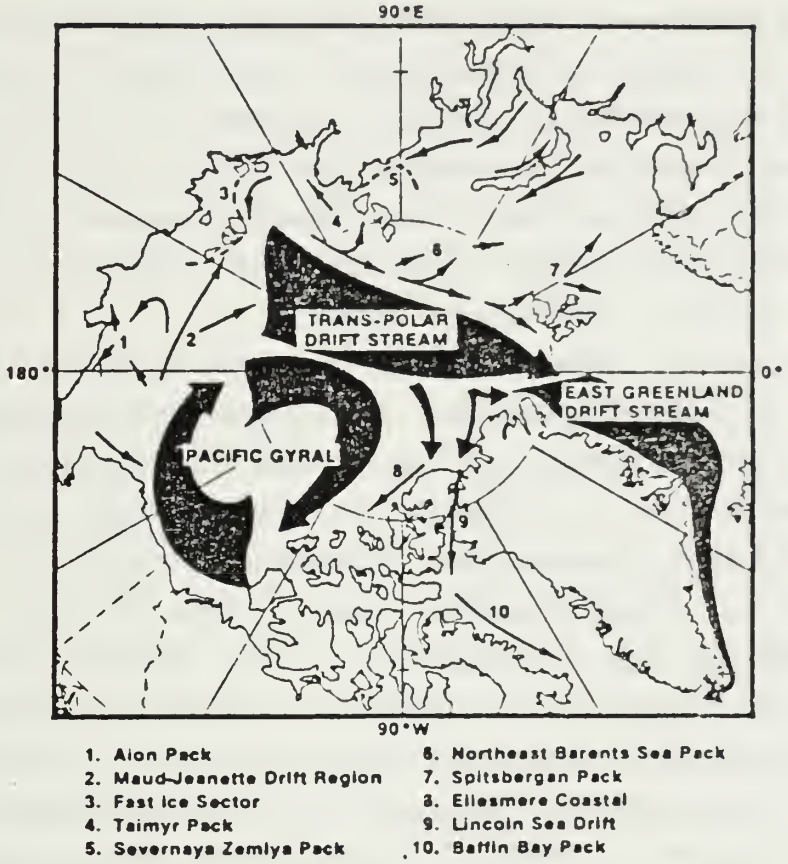

Figure 1.1 Major drift patterns of ice in the Arctic Ocean (after Weeks, 1978).

The second major drift feature is the Beaufort Gyre. It is a region of generally closed clockwise drift located between the Canadian Archipelago, the Alaskan north coast, and the North Pole (Weeks, 1982). The oldest and thickest ice in the Arctic Ocean is located in this region. Floes have been known to last in the gyre for more than 20 years, although 10 years is more common (Weeks, 1978; Zubov, 1943). In comparison, the average age of the sea ice in the Arctic Ocean is between 4 and 6 years (Zubov, 1943). The ice in

this region circulates about the Beaufort Gyre working its way towards the periphery and is eventually exported out of the Arctic where it gradually melts (Colony and Thorndike, 1985).

The principal exit for ice from the Arctic Ocean is by way of the East Greenland Current or Drift Stream (Weeks, 1982). The most intense ridging in the Arctic Ocean occurs just off the coast of northern Greenland. This is the area where ice that splits away from the Transpolar Drift Stream moves westward to rejoin the Beaufort Gyre and is forced around the northern Greenland coast.

Mean drift rates for the ice pack vary from 0.4 to 4.8 km per day (Weeks, 1982). Monthly average values may be as high as 10.7 km/day. Under rare conditions, maximum drift velocities of 32.2 km/day have been recorded for short periods of time (Dunbar and Wittman, 1963). Both the highest and the lowest drift rates in the Arctic Ocean have been recorded within the domain of the Beaufort Gyre. The highest drift rates were observed in the southern part of the gyre with the highest net rate of 7 km/day being observed at the southern edge of the ice pack during summer (Dunbar and Wittman, 1963). The slowest drift rates, less than 1 km/day, are observed toward the northern limits of the Beaufort Gyre between Ellesmere Island and the North Pole due to the divergence in this area between the Beaufort Gyre and the Transpolar Drift Stream (Dunbar and Wittman, 1963).

In addition tc the effect on ice distribution by the oceanic flow, surface winds blowing across the ice have a smoothing and a slight pushing effect on the ice. Mean wind speeds remain fairly constant throughout the year. The average wind speed observed throughout most of the Arctic Basin is less than 5 m/s (Weeks, 1982). October is the windiest month with wind speeds averaging less than 7 m/s.

The wind is also the cause of wave induced fracturing of the ice pack at its outer limits.

3. Mean Ice Thickness

Ice profiles are obtained from either above or below the ice pack. Submarines transiting the Arctic Ocean are a valuable source of underice profiles. These are obtained through the use of the submarine's onboard echo-sounding equipment. Reconnaissance aircraft equipped with laser profilometers provide the chief source of surface or topside ice profiles.

The simplest ice statistic which can be obtained from such profiles is mean ice thickness or draft (Wadhams, 1983a). Mean ice draft is a function of the mean ice density and the density of the water in which it is floating. Mean ice thickness is a direct measure of vertical ice extent from the surface to the bottom. Mean ice draft can be converted to mean ice thickness by multiplying by 1.12, the approximate density ratio of water to ice (Wadhams, 1983a). Since the maximum difference between the two values is generally less than 0.5 m, no attempt has been made to convert the various data sets used in this study to a common standard. Some recent Arctic ice studies have used the root mean square to describe mean ice thickness, e.g. LeSchack and Chang (1977) and LeSchack and Lewis (1983). This definition of mean ice thickness is not used in this study.

When calculating mean ice thickness from submarine underice profiles, several factors must be considered. First, the sonar beam-width must be taken into consideration for reasons which will be discussed in Chapter 2. Next, statistical reliability must be considered, although little can be done to correct this if a problem arises. The length of track over which the mean ice thickness measurement is

made is an important factor. If the length of track is too long, the possibility of including another ice regime could influence the calculation; if the length is too short, the measurement may be influenced by an uncharacteristic feature of the particular region. Typically, lengths of 50 km or 100 km are used and have proven to yield satisfactory measurements of mean ice thickness (Kozo, 1974; Wadhams, 1983a; LeSchack, 1983; McLaren et al., 1984). For purposes of contouring values of mean ice thickness, the position of the measurement is placed at the geographic center of the track length for which the mean value was computed. In some areas, such as coastal zones, mean ice thickness changes rapidly (Wadhams, 1983a). In these areas even track lengths of 50 km are not satisfactory to resolve a measurement of mean ice thickness. In areas such as these the accuracy of any ice thickness measurement becomes much lower.

Probability density functions are commonly used to determine the distribution of ice thickness from submarine underice profiles. Wadhams (1983a) defines the probability density function P(h) of ice thickness such that P(h) dh is the probability that a random point has a thickness between h and h+dh. It varies both seasonally and geographically primarily being influenced by the amount of thin and first year ice present.

A typical set of P(h) functions, obtained from the track of the submarine HMS SOVEREIGN in the central Arctic Ocean, is shown Figure 1.2. The submarine's track was segmented into 100 km sections. The distributions show clearly a peak at less than 1 m thickness which is indicative of first-year, young thin ice. A second major peak appears, after a gap, at about 3 m which is indicative of thicker first-year ice and multi-year ice. A tail then extends towards extreme ice thickness values which represent ice accummulations due to pressure ridging. The gap which

appears after the thin ice peak illustrates that ice with a thickness less than 1 m is easily crushed and goes directly into the formation of pressure ridges. Thin ice, less than 1 m, is usually found in leads and polynyas which are highly susceptible to convergence of the ice pack and is therefore short-lived. Most of the thin first-year ice is therefore represented in the tail of the distribution in the form of pressure ridging. The twin peaks in the major peak at 3 m demonstrate the presence of both first-year and multi-year ice.

4. Level Ice

It is often necessary to be able to separate the different features of the ice pack into various categories, such as ice formation in leads and polynyas. As observed in Figure 1.2, the major peak in P(h) lacks significant detail to be able to discern between the features associated with undeformed first-year ice and multi-year ice (Wadhams, 1983a). Newly formed ice in leads and polynyas tends to be smooth and flat and provide ideal sites on which to land aircraft if the ice is sufficiently thick or to penetrate from above or below if sufficiently thin. Ice in these regions is termed level or undeformed ice and is defined as ice with a local gradient of less than 1 in 40 (Williams et al., 1975). More restrictively, it may also be defined as a point where the draft differs from a point 10 m to either side by less than 25 cm (Wadhams et al., 1985). By isolating sections of level ice along a track, the mean ice thickness of both undeformed first-year ice and multi-year ice may be found (Wadhams, 1983a).

Figure 1.4 shows a probability density function of level ice thickness, based upon the more restrictive definition of level ice, taken from the 1,400 km underice track profile of the submarine USS GURNARD (Wadhams, 1983a). Two

young, thin ice peaks are visible at 0.3-0.4 m and 0.8-0.9 m. The main peak also shows two peaks which are recognizable as undeformed first-year ice at 2.1 m and multi-year ice at 2.7 m.

In heavily ridged regions, the local level ice thickness is a difficult parameter to measure and has been empirically determined by Wadhams (1983a) to be 2.5 m. This value has been applied to sonar and laser profiles alike, to define the local level ice bottom (McLaren et al., 1984; Lowry and Wadhams, 1979; Tucker et al., 1979; Wadhams, 1977, 1980a, 1980b, 1981a, 1981b; Wadhams and Horne, 1980; and Williams et al., 1975).

The percentage of the sea surface covered by level ice varies inversely with the total mean ice thickness of a particular region (Wadhams, 1983a). This is because a high mean ice thickness value implies a large degree of ice deformation and pressure ridging. Conversely, as mean ice thickness decreases, the amount of level ice per unit area increases. This is illustrated in Figure 1.3 which shows that level ice constitutes 27-40% of the heavily ridged ice canopy (5 m mean ice thickness) offshore of northeastern Greenland and up to 60% of the total ice cover in the Greenland Sea marginal ice zone (3.5 m mean ice thickness).

5. Pressure Ridging

Characterizing the distribution of ridging over time and space in the Arctic is difficult. New ridges are continuously being generated, and once formed, drift laterally with the general motion of the ice pack. Brine drainage, sublimation and melting will, during the spring and summer, cause significant changes in the geometry and properties of the upper portions of ridges. It is quite possible that a similar modification of the geometry of ridge keels occurs, but on a much longer time scale, although information on this subject is almost nonexistent (Weeks et al., 1971).

In order to ascertain accurate measurements of pressure ridging from profiles of the Arctic ice pack, equations have been developed to calculate pressure ridging parameters directly from the ice profiles. The frequency of occurrence of pressure ridges in a particular region as well as the actual thickness of pressure ridges are important parameters which may be obtained from ice profiles.

To arrive at pressure ridge distribution statistics, Hibler et al. (1972) showed that the distribution of spacings between pressure ridges is given by:

$$Pr(x)\,dx = u \exp(-ux)\,dx \qquad \text{(eqn 1.1)}$$

where u is the mean number of ridges per unit length and Pr(x)dx is the probability that a given spacing lies between x and (x+dx). In the event of two overlapping pressure ridges (no noticable trough between the two ridges), Lowry and Wadhams (1979) derived an equation which effectively separates the two pressure ridges. If the two ridges have reliefs h and h', where h is greater than h', with a triangular cross-section of the ridges having a slope of 'a', then the distance x which allows h and h' to be determined independently is given by:

$$X(crit) = h \cot a \qquad \text{(eqn 1.2)}$$

Equations have also been derived to calculate pressure ridge thickness, e.g., Wadhams (1977, 1983a), Wadhams and Horne (1980), Hibler et al. (1972), and LeSchack (1983). Since these equations generally reflect local and regional effects and characteristic features of the observed pressure ridging, the interested reader is referred directly to the above references.

In addition to the equations that are applied to sea ice profiles, efforts have also been made by various researchers to provide methods of reconstructing ice thickness statistics through the application of keel/sail height ratios (LeSchack, 1983; Williams et al., 1975; Wittman and Schule, 1966; Kovacs, 1972; Wadhams, 1983a; and Wright, 1978). There are presently two keel to sail ratios which are applied to obtain pressure ridge statistics. The first value of 3.3/1, based upon the Makorov-Wittman pressure ridge model (Wittman and Schule, 1966), appears to be somewhat low for first-year pressure ridges, although it does appear to satisfy the ratio for multi-year ridges (Kovacs,1972). This ratio has been supported by data from the SARGO and SEADRAGON cruises of 1960 (Kovacs, 1972). Wright et al. (1978) expanded the data set with actual physical measurements of individual pressure ridges and found a keel/sail height ratio of 3.28/1 which indicates a slight change to the earlier derived ratio. They also found that multi-year pressure ridge keel/sail height ratios ranged from 1.3/1 to 3.8/1 whereas first-year pressure ridge keel/sail height ratios ranged from 3/1 to 9/1. The keel/sail height ratio of 3.3/1 is accepted as the appropriate ratio to be applied to submarine underice profile data obtained with a narrow-beam sonar and data acquired from reconnaisance flights such as BIRDSEYE data. A ratio of 8/1 is generally accepted as appropriate for underice profiles obtained with a wide-beam sonar and has been applied to the AIDJEX Beaufort Sea data by LeSchack (1983) and Wadhams (1983a). This ratio takes into account the difference between the profiles produced by wide-beam and narrow-beam sonars and when applied to wide-beam data the same degree of accuracy asssociated with the narrow-beam sonar is obtained. These differences will be discussed in detail in Chapter 2.

6. Leads and Polynyas

The terms lead and polynya are used interchangeably throughout the ice literature. For purposes of computer analysis, a lead was defined to be a continuous stretch of ice at least 5 m in length where the ice is no greater than 1 m thick (Wadhams and Horne, 1980). This definition has generally been employed by most ice researchers in the past but recently McLaren (personal communication, 1985) has used 1 ft (0.3 m), supposedly being more useful for submarine underice penetration.

There is presently no mathematical function available which is able to determine the distribution of lead width on any scale (Wadhams, 1983a). The accepted method of displaying leads, from the information given by an ice profile, is by the use of trafficability diagrams (Figure 1.5). The ordinate gives the distance between encounters of leads while the abscissa is the observed lead width. From diagrams such as these one can readily ascertain the average spacings of leads encountered along a particular track. In general, polynyas of large width are not encountered frequently. Polynyas of 2 to 4 km in width generally occur at intervals of 1 to 10 km along the track. However, polynyas of sufficient size for a submarine to surface in, approximately 100-200 m wide, occur about every 3 km. It is also observed that the frequency of lead occurrence in winter as compared to summer is a factor of 10:1 in M'Clure Strait, 1960. In winter many more narrow leads are observed in the ice pack as a result of the movement of ice along the Canadian Archipelago coast. Wadhams (1983a) also observed that leads are much more frequent in the marginal ice zones than in the interior of the Arctic Ocean.

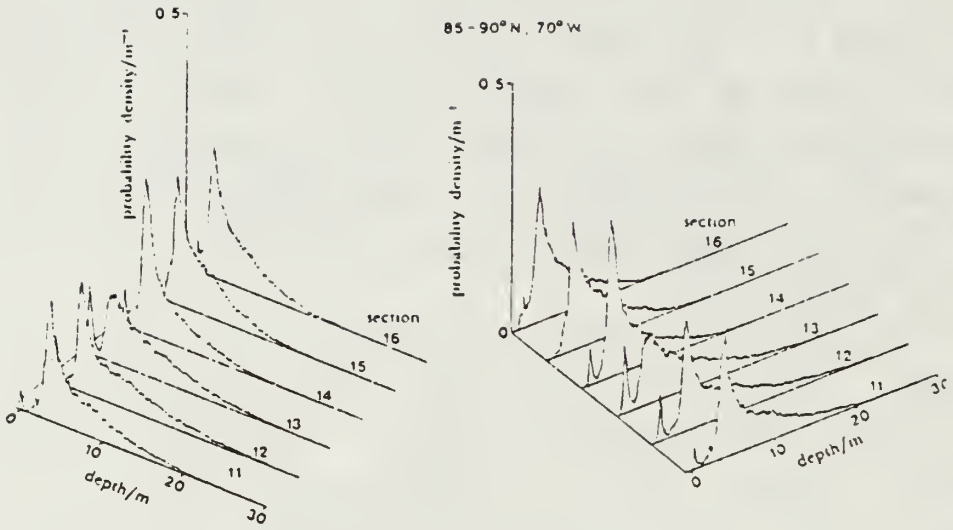

Figure 1.2 Probability density functions of ice draft, along a transit from 85° to 90°N at 70° W (after Wadhams, 1981b).

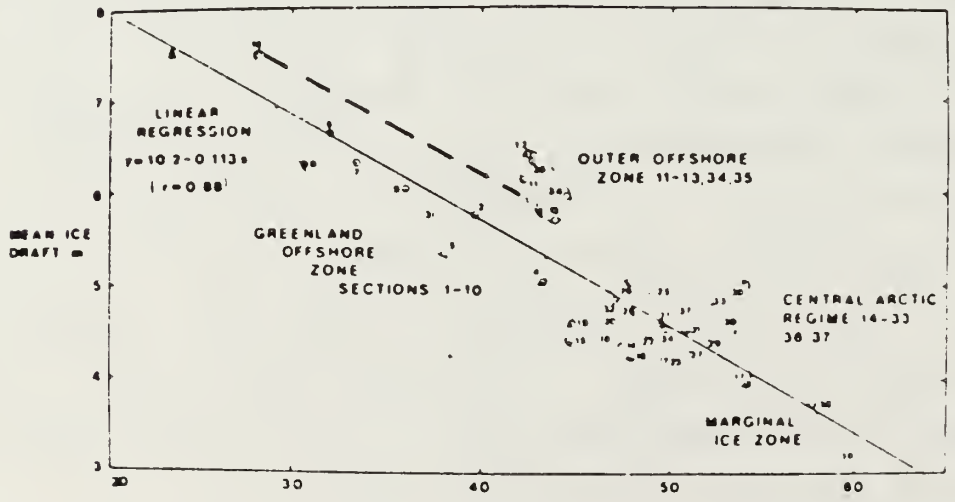

Figure 1.3 Relation between mean ice draft and the percentage of level ice per 100 km (after Wadhams, 1983a).

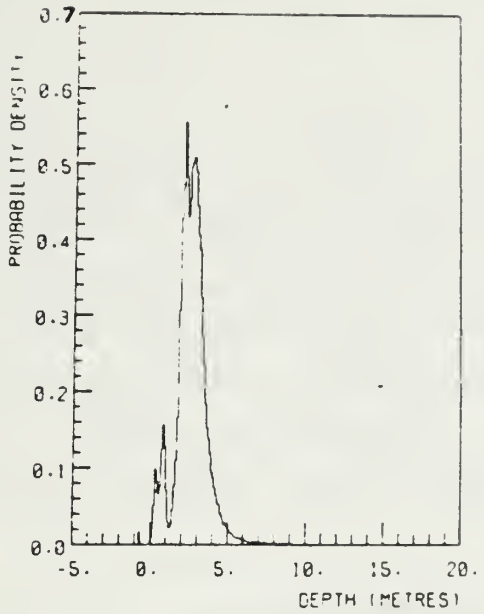

Figure 1.4 Probability density function of level ice from GURNARD in the Beaufort Sea (after Wadhams and Horne, 1980).

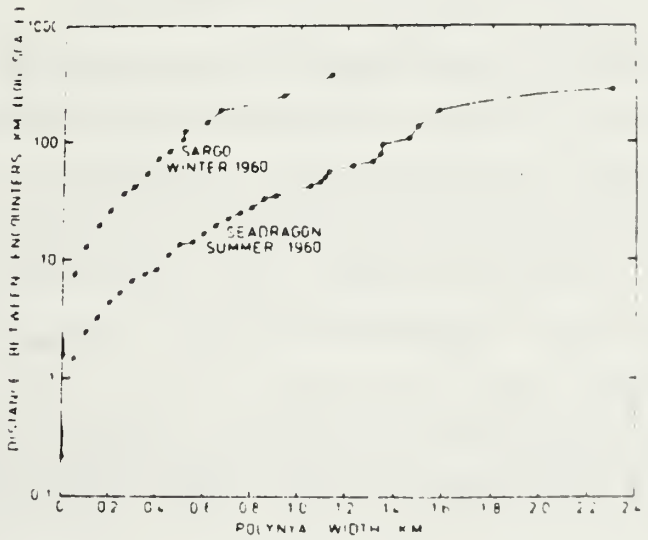

Figure 1.5 Trafficability diagram for M'Clure St. (after McLaren, 1984).

II. DATA

A. SOURCES OF DATA

Sea ice thickness data for the Arctic Ocean are sparse, and the data that are available can be considered coarse and subject to various errors (LeSchack, 1983). It is therefore difficult to develop an accurate data base for the entire Arctic region. This problem becomes more complicated when strong regional variations are considered. However, the data that are currently available do provide a reasonable basis for making judgements on the spatial and temporal thickness of sea ice.

1. Methods of Measurement

Three methods have generally been employed to develop an understanding of ice thickness, distributions, and texture (Blidberg et al., 1981). They are:

(1) Ice corings and physical measurements.

(2) Submarine sonar measurements, generating profiles of the bottom of the ice relative to sea level.

(3) Aircraft laser measurements, generating profiles of the surface of the ice relative to sea level.

The data for this study are mainly from submarine underice cruises and analyzed BIRDSEYE flight data since they represent the vast majority of the data currently available and are generally acccepted as accurate (Weeks et al., 1971). Only data north of 65°N were considered.

a. Ice Corings

Ice corings, being time consuming and expensive, represent only a small part of the total amount of data currently available (Blidberg et al.,1981). The data available from ice corings are not generally available for a particular area on a seasonal or continuous basis which can provide regional or temporal distributions of sea ice thickness. Analysis of ice cores can provide valuable information about the local physical character of the ice, such as its thickness, density, and age. These important parameters are not always the primary reason for the measurement. Often ice coring or drilling is done for other purposes, usually to obtain access to the water under the ice, i.e. diving operations, for closeup study of ridging features, bottom sampling, and for making ocean current measurements (Weeks et al., 1971).

Because of the relative paucity of this type of data and its lack of temporal and spatial distribution, ice core data have not been used extensively in this study. Most ice coring statistics come from studies conducted at ice camps and on ice islands. They are not used here because of their narrow distribution over time and space. However, the information gained from ice coring data has been used as ground truth to corroborate the time and spaced-averaged submarine ice thickness data before being discarded.

b. Submarine Underice Transits

The vast majority of ice thickness data are obtained from submarines equipped with a narrow-beam, upward-looking sonar. Since 1960 virtually all United States submarine transits in the Arctic Ocean have employed the use of a narrow-beam width sonar to record ice thickness and keel depth. An exception to this was the Arctic Ice Dynamics

Joint Experiment (AIDJEX), a joint international project in 1976 which involved the U.S. submarine USS GURNARD and the British submarine HMS SOVEREIGN. The SOVEREIGN was equipped with a sounder having a wide beam in the fore-and-aft plane (17°) and a narrow beam in the athwartships plane (5°) (Wadhams and Horne, 1980).

The beam-width of the wide-beam sonars in use is large (10-30°) (Wadhams, 1983a). The wide-beam sonar tends to smooth out the structure of submerged features such as the smoothing of a keel to a single wedge. Wadhams (1980a) has pointed out the errors caused by using a wide-beam sonar and has developed procedures for correcting such data. The overall effects of a wide beamwidth are (Wadhams, 1983a, p.179):

a) over-estimate of mean ice draft;

b) under-estimate of pressure ridge numbers;

c) under-estimate of the slope of a pressure ridge, and distortion of its shape especially rounding of the crest;

d) correct estimate of the absolute draft of a pressure ridge, so long as it is not 'lost' by merging with a deeper one;

e) loss of information on fine scale spatial roughness.

With the application of reconstruction equations, some of the data may be regenerated but the fine structure remains essentially lost.

Recent U.S. submarine cruises have solved most of these problems by using a narrow-beam (3°) sonar, with digital recording of depth and a zero reference provided automatically by a coupled pressure transducer. The USS GURNARD used this type of equipment on a cruise to the Beaufort Sea in 1976 and obtained an accuracy of ±0.3 m for

ice draft measurements (Wadhams and Horne, 1980). Records from this type of sonar system can be regarded as perfect representations of the ice underside, failing only in the resolution of very fine scale topographic variations (since the beam footprint is about 4 m in diameter) (Wadhams, 1983a). A narrow-beam sounder is capable of resolving much of the fine structure of the underice features by illuminating the clefts and hollows of the submerged blocks. A much greater ridge frequency results from being able to discern the many ridges and spaces in the submerged ice.

Because of the greater resolution available from a narrow-beam sonar, only submarine cruises later than 1959 were analyzed to ensure that narrow-beam sonars were used for ice thickness measurements. Seventeen submarine cruises, conducted between 1960 and 1982, provided adequate data for use in this study. The British submarines SOVEREIGN and DREADNOUGHT, included in these 17 cruises, used a wide-beam sonar in the fore and aft plane and narrow-beam sonar in the athwartships plane. These measurements, obtained from profiles from the wide-beam sonar, were then corrected to be consistent with the narrow-beam data which comprise the major portion of the total submarine underice data. The correction which was applied to the wide-beam data was obtained from Wadhams (1983a) and is given by Equation 2.1:

$$h(n)=0.84\ h(w) \qquad \text{(eqn 2.1)}$$

where h(n) and h(w) are the narrow-beam and wide-beam thicknesses, respectively. The dates and locations of these cruises are listed in Table I. Although several more submarine cruises to the Arctic have taken place during this time, their underice profile data have not been released to

the scientific community for analysis. Those cruises for which data are not available are indicated by an asterisk (*).

Almost all areas of the Arctic region are represented in this data base as well as all the Arctic seasons thus providing a good representation of both the regional and temporal distributions of mean ice thickness. The central Arctic Basin and the Chukchi, Beaufort, and Greenland Seas are the regions of the most intensive sea ice measurements. A visit to the North Pole is an objective of all submarine cruises to the Arctic Ocean. The summer season also provides a larger portion of the total information available, as is illustrated in Table I. This is due to scheduling requirements of submarines with other support platforms, such as ice camps, aircraft, and ice breakers which require periods of daylight to carry out their tasks.

Except for the data available from AIDJEX, virtually all of the current submarine data are held by the Arctic Submarine Laboratory (ASL), Naval Ocean Systems Center, San Diego, Ca. At the present time the bulk of the submarine track data is in the form of analog tapes which have not been digitized. Discussions with the Deputy Director of the Laboratory indicate that it is currently not cost effective to undertake the massive job of digitizing the more than 300,000 km of underice track records stored in the ASL archives (personal communication with Dr. Allan Beal, ASL). Limited portions of the data in high interest areas, approximately 15% of the total, have been digitized by several researchers, notably LeSchack (1975a, 1980, and 1983), LeSchack and Hibler (1972), LeSchack and Chang (1977), LeSchack and Lewis (1983), Wadhams (1977, 1980a, 1980b, 1981a, 1981b, 1983a, and 1983b), and Wadhams and Horne (1980). These analyzed data sets have been reported in various publications; those from LeSchack and Wadhams are listed in Appendices A and B, respectively.

TABLE I

Data from Various Submarine Cruises 1960-1982

Submarine	Yr	Season	Geog. Region(s)	Sonar Beam Width
USS Sargo	60	Winter	Chukchi Sea Cent. Arctic Beaufort Sea	Narrow
USS Seadragon	60	Summer	Beaufort Sea Cent. Arctic Chukchi Sea N. Laptev Sea	Narrow
USS Seadragon	62	Summer	Chukchi Sea Cent. Arctic N. Laptev Sea Beaufort Sea	Narrow
USS Skate	62	Summer	Lincoln Sea Cent. Arctic	Narrow
USS Queenfish	67	Winter	Baffin Bay	Narrow
USS Whale*	69	Spring	Cent. Arctic	Narrow
USS Pargo*	69	Spring	Cent. Arctic	Narrow
USS Skate*	69	Spring	Cent. Arctic	Narrow
USS Queenfish*	70	Summer	Cent. Arctic Siberian Shelf	Narrow
USS Hammerhead*	70	Autumn	Nares St. Cent. Arctic	Narrow
HMS Dreadnought	71	Spring	Cent. Arctic	Narrow/ Wide
USS Trepang	71	Win/Spr	Denmark Strait Greenland Sea	Narrow
USS Hawkbill	73	Win/Spr	Bering Sea	Narrow
USS Bluefish	75	Win/Spr	Greenland Sea Denmark Strait Cent. Arctic	Narrow
USS Gurnard	76	Win/Spr	Bering Sea Chukchi Sea Beaufort Sea Cent. Arctic	Narrow

Table I
Data from Various Submarine Cruises 1960-1982 (cont'd.)

Submarine	Yr	Season	Geog. Region(s)	Sonar Beam Width
HMS Sovereign	76	Autumn	Greenland Sea Cent. Arctic	Narrow/ Wide
USS Flying Fish	77	Spring	Greenland Sea Cent. Arctic Lincoln Sea	Narrow
USS Pintado	78	Autumn	Chukchi Sea Cent. Arctic Beaufort Sea	Narrow
USS Archerfish*	79	Spring	Baffin Bay Nares St.	Narrow
HMS Sovereign	79	Spring	Greenland Sea	Narrow/ Wide
USS Silversides	81	Autumn	Canadian Arch. Cent. Arctic Greenland Sea	Narrow
USS Aspro	82	Autumn	Chukchi Sea Cent. Arctic	Narrow
USS Tautog	82	Autumn	Chukchi Sea Beaufort Sea Cent. Arctic	Narrow

* indicates cruises for which data are not currently available.

In order to digitize the mean ice thickness, a line follower digitizer is generally used to trace the curvilinear analog echo sounder charts (LeSchack, 1983; Wadhams, 1983a). An example of such an echo sounder trace is shown in Figure 2.1. Digitizing is generally done in 50 km or 100 km segments with ice measurements every 1.5 meters along the underice track (see, for example, Figure 3.37) (Wadhams and Horne, 1980). The mean geographic position of each segment must be determined by reconstructing the track of the submarine from course and speed entries in the ship's log and matching the time of each segment to the ship's position. Variations in the ship's speed can alter the shape of the recorded underice profile and cause errors in the measurements.

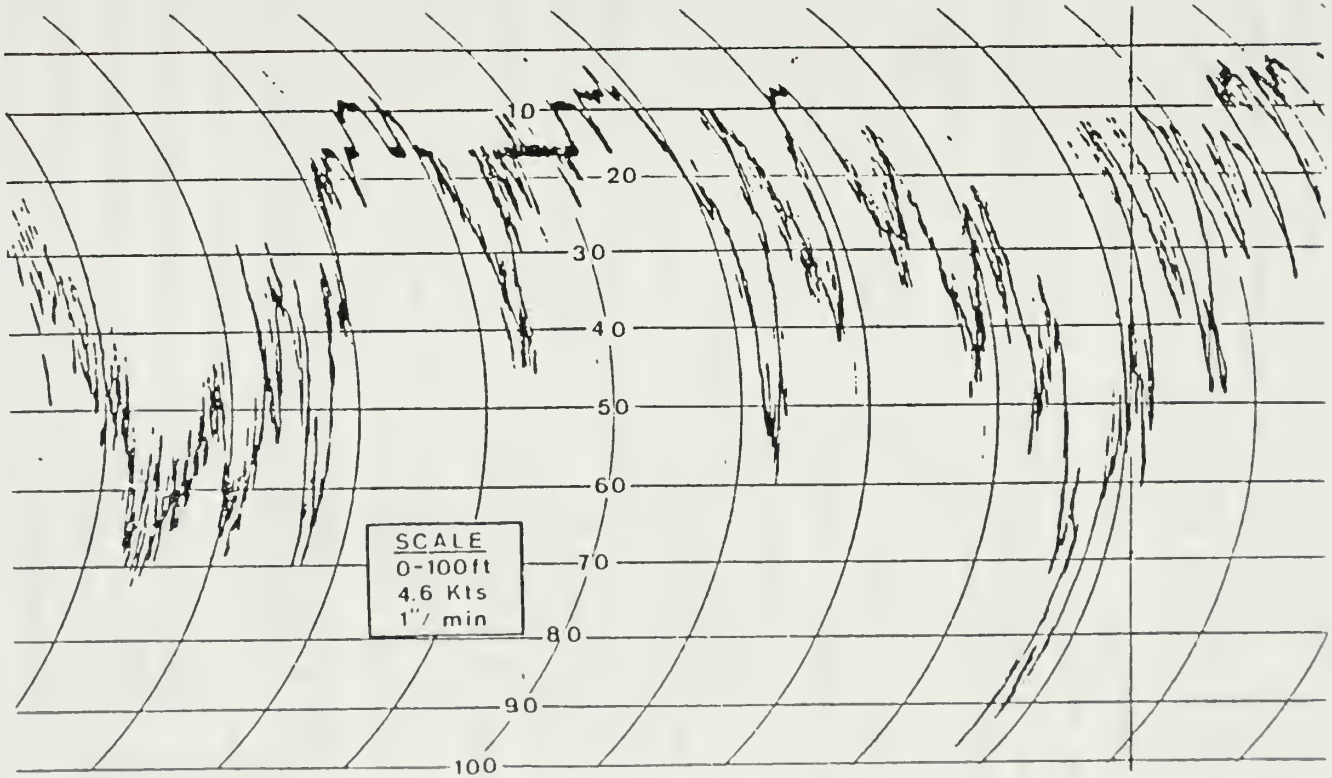

Figure 2.1 Typical underice profile. Depths are marked in ft. Note the large keel extending to 97 ft (29.5m).

These variations of the submarine's course and speed are the result of porpoising caused by the movement of the submarine through the water and are virtually uncorrectable (Wadhams, 1983a).

Another correction which must be applied to earlier data (prior to the USS GURNARD, 1976) is the uncertainty of the depth of the actual water surface, the level from which all ice depth measurements are determined. The chart is calibrated each time a lead or polynya is encountered. These features are recognized by their characteristic refection pattern. The error in determining this water line may be as much as 1 m (3 ft) (LeSchack, 1983). Since these profiles were originally recorded for navigational purposes, a high degree of accuracy in measuring absolute ice thickness was not required in the overall data collection process. As a result, the accuracy of sea ice thickness measurements along a submarine track are usually within 10% or within 1 m at any one point (LeSchack, 1975a).

Pressure ridging statistics not only include ice thickness measurements but also frequency of occurrence of pressure ridges for a given segment of the submarine track or geographical region. Two low-value cutoffs for keel drafts are normally applied, 5 m and 9 m (Wadhams and Horne, 1980; Wadhams, 1983a; Hibler et al., 1973; McLaren et al., 1984). The 9 m cutoff value for counting keels is generally accepted as being more valid because only "real" keels are recorded and the effect of keel shadowing by numerous smaller drafts is reduced (Wadhams and Horne, 1980). The result of using a 5 m or 9 m keel-cutoff value is shown in Figure 2.2. At 100 m spacings, keels with drafts of 5 m or greater are almost ten times more likely to be encountered than keels which exceed 9 m. As the spacing increment increases, the frequency of occurrence of 5 and 9 m keels becomes more nearly similar.

In addition to the echo sounder data, mean ice thickness values are also available from the submarine Commanding Officer's daily cruise report entries. These cruise reports are also held in the archives of ASL. Data from eight submarine cruises is presently available. Mean ice thickness and mean keel depth values are reported for averages determined over a specified observational period, e.g., every 4 hours. The position given for the observation is that of the current position at the time of the report.

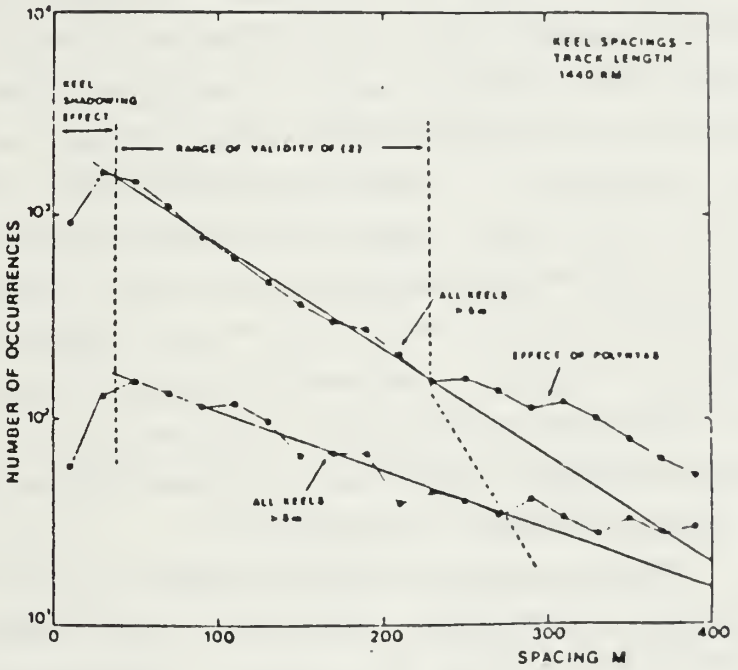

Figure 2.2 Distribution of keel spacings. Results are plotted for keels deeper than 5 and 9 m (after Wadhams and Horne, 1980).

Ice thickness and pressure ridge statistics obtained from individual ship's cruise reports incorporate various kinds of errors. Errors may result from different interpretations of mean ice thickness over a given period of time or from an inaccurate count of observed pressure

ridging over the same period by the different watches responsible for the observations. The quality of the observation is subject to human error which may have a significant effect upon the recorded measurement. The data obtained from the submarine logs indicate that errors also may be present in the temporal distribution of the recorded measurements due to unspecific or changing recording requirements from one ship to another. There may also be errors in the spatial distribution of the data due to differing interpretations of the observed measurements. Although most logs indicate that the mean ice measurement is taken over a spatial distribution of level ice, some of the logs are not so specific and an element of doubt arises for each of these data sets. The required frequency of reporting observations varies with each submarine, with the average being a report of mean ice conditions as observed over a period of 12 hours. Mean measurements were recorded, however, with a frequency as often as every 4 hours during more recent cruises and as long as every 24 hours during the earlier cruises. Due to the many changes in course and speed that a submarine makes while navigating the perilous environment of the Arctic waters, a typical distance covered in a 12 hour period cannot be estimated.

A typical observation recorded in the ship's log includes the ship's position, mean ice thickness observed over the specified period of time, amount of ridging observed, the average depth of the keels, and the deepest keel observed. The human element involved in making these types of measurement carries with it random and unpredictable errors which often are not detectable or correctable. These errors may result from the fact that this type of data collection is a secondary task assigned to the watchstanders and, because of this, is usually relegated to a lesser degree of attention. In spite of these observational

problems, the error encountered in mean ice thickness observations has been empirically determined to be, on the average, no greater than 1 m (LeSchack, 1983). This is within acceptable range for this type of study in temporal and spatial sea ice distribution.

c. Aircraft Laser Measurements/Remote Sensing

Profiles of pressure ridge sails are typically obtained using airborne laser profilometers which employ a pencil-thin beam capable of recording ice sails, troughs, and crevices (Campbell et al., 1975). This is an important method for determining regional pressure ridge distribution and, to a lesser degree, for determining the thickness of the ice by applying keel to sail height ratios. However, mean sea ice thickness information derived from this technique is not generally useful due to the many inaccuracies and inconsistencies which result from the wide range of keel/sail height ratios which have been reported.

AIDJEX data provide 81 sets of laser profilometer data, each containing 40 km of track taken at different geographical locations in the Arctic basin (Hibler et al., 1974). To study the regional and temporal variations in ridging intensity, the location of each of the 81 laser data samples was catalogued (Tucker and Westhall, 1973). The locations were found to fall in one of 26 geographical sites shown in Figure 2.3. These data are useful for determining contours of regional pressure ridge frequency. The data are displayed later in this study in its evaluated form as provided by Tucker and Westhall (1973).

In order for airborne profilometer data to provide pressure ridging statistics it must first be reduced. The reduction applies to all such airborne data, which includes AIDJEX and BIRDSEYE ice profiles obtained by reconnaisance flights. The data reduction consists of two

parts. First, laser data recorded in analog form on magnetic tape are converted to a form acceptable for digital computing by digitizing the analog record and then removing the phase shift. Second, the digitized profile is then processed to remove the aircraft altitude variation by using the three-step digital filtering process developed by Hibler (1972). This process provides a leveled profile with a zero fiducial level from which to measure ridge heights. Ridges are identified digitally by declaring a profile peak to be a ridge when the peak is at least 0.6 m (2 feet) above the minimum points located to the left and right of the peak (Hibler et al., 1974).

Data obtained from satellite systems such as LANDSAT or NOAA are important for determining the position of the ice edge and open water areas. However, attempts to determine ice thickness from this type of remotely sensed data have not proven to be fruitful (Campbell et al., 1975). Efforts have been made to reconstruct ice thickness data by equating ice thickness to ice age, i.e. first-year and multi-year ice (Naval Polar Oceanography Center, 1983). Current satellite systems are able to discern the age of sea ice but attempts to equate this parameter to ice thickness have not provided accurate statistics. Researchers are continuing to explore methods to more accurately reconstruct the ice thickness data from remotely sensed data which are becoming more increasingly available (Campbell et al., 1975; and Campbell, 1984).

The BIRDSEYE data are currently the most important source of pressure ridge statistics. Because of the nature of the data, little information can be drawn for mean ice thickness statistics. The BIRDSEYE data were collected exclusively in the Central Arctic Basin and the Chukchi, Beaufort, and Greenland Seas. Within these areas the

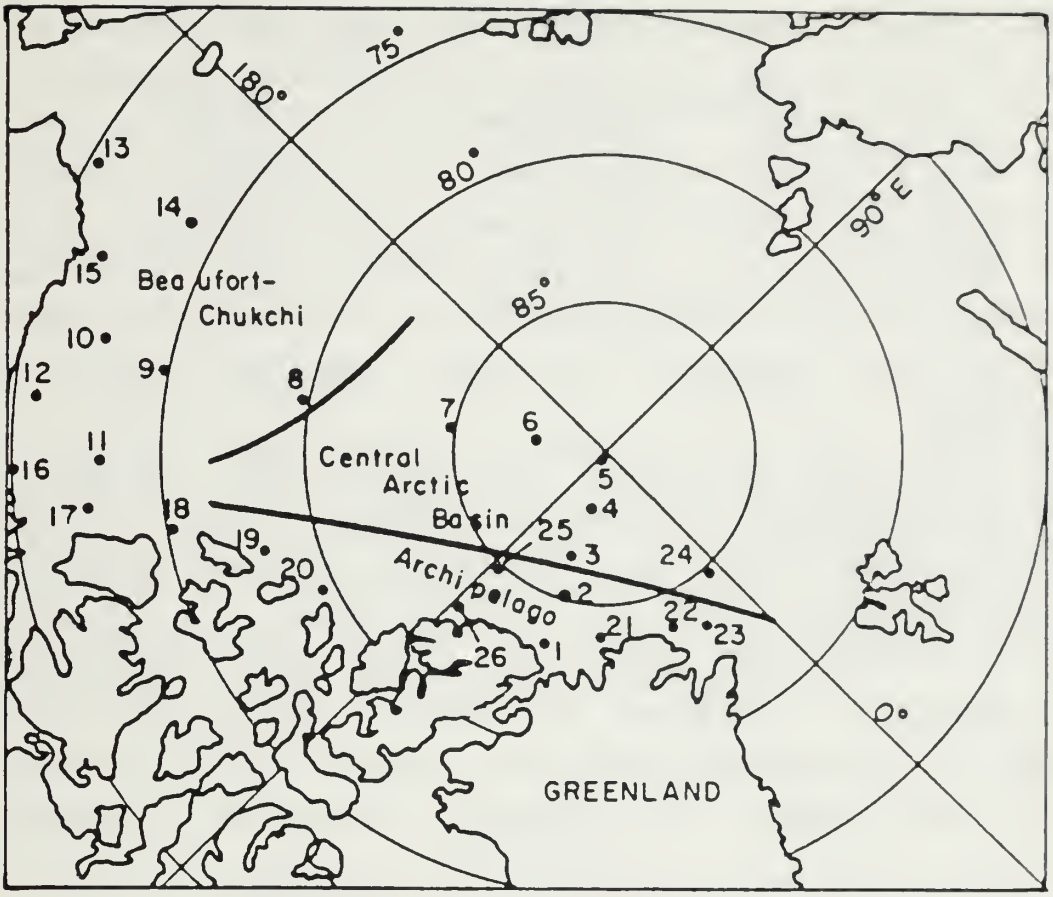

Figure 2.3 Geographical sampling regions for laser data (after Tucker et al., 1979).

BIRDSEYE data provide a wealth of information on spatial and temporal distribution of pressure ridging for the areas of coverage and thereby allow distributions of pressure ridging to be inferred for areas of sparse coverage. However, little such data are available from the Soviet Arctic.

B. TREATMENT OF DATA

The submarine underice profile data used in this study were the only data sets suitable for further analysis. These data sets, which consist of submarine cruise reports and

previously digitized underice profiles (LeSchack, 1983; Wadhams, 1983a; Wadhams and Horne, 1980; Wadhams et al., 1985), were combined to obtain an extensive temporal and regional distribution. This procedure allows one to incorporate ice measurements obtained from various submarine cruises over many years into a more extensive data set of actual ice conditions. By incorporating the interannual variability, a mean representation of long term ice conditions may be observed in the resulting maps and calculations.

The data were sorted and partitioned into respective seasons and geographic regions by a point by point evaluation of the combined data set. Data from sources other than submarine transits, such as BIRDSEYE data, are given in Chapter 3 in their evaluated form. These data, which have been previously evaluated by other researchers, are displayed for comparative analysis and for further description of ice thickness and pressure ridging on a regional basis.

The submarine underice data were partitioned into four seasons. The seasons of the Arctic region tend to lag the normal advent of seasonal transition observed in mid-latitude areas by 4-6 weeks (Zubov, 1943). To reflect this timelag the seasonal partitioning of the data has been adjusted accordingly. This timelag is a result of the polar transport of heat energy from lower latitudes and the time it takes for this transport to occur. The seasonal segmentation of the data is given in Table II.

1. Mean Ice Thickness

The submarine underice data sets were partitioned into four regions for ease of display and to permit as much of the data as possible to be shown within the finite limits of the map scale. The partitions were chosen to correspond

TABLE II

Seasonal Partitioning of Data

Season	Yearly Segment
Spring	mid April - mid July
Summer	mid July - mid October
Autumn	mid October - mid January
Winter	mid January - mid April

as closely as possible to the general geographic regions and seas of the Arctic Ocean. Some overlapping of data was necessary to achieve proper geographic coverage. The partitions are given in Table III with their respective regions of coverage. A fifth partition was made for the area of the Arctic Ocean north of 84°N in order to display this extreme northern data in an uncluttered illustration.

TABLE III

Geographic Partitioning of Data

Data Segment	Geographic Region
10°W - 100°E	Norwegian Sea Barents Sea Kara Sea
70°E - 180°E	Kara Sea Laptev Sea East Siberian Sea
180°W - 70°W	Chukchi Sea Beaufort Sea Canadian Archipelago
100°W - 10°E	Canadian Archipelago Lincoln Sea Baffin Bay/Davis St. Greenland Sea Norwegian Sea

Seasonal and regional maps of sea ice thickness are shown in Appendix C (Figures C.2 - C.16). These maps are

presented to illustrate local thickness variations as well as the distribution of the data points. The transit routes of the different submarine cruises are readily apparent. Also noticeable are the large data-sparse areas.

In addition to seasonal and regional maps of mean ice thickness, contour maps, histograms, and mean ice thickness values as well as their standard deviations were produced. Since these products were produced on a regional as well as a seasonal basis, they are presented and discussed in Chapter 3 which concerns the findings of this study.

2. Pressure Ridging

The submarine underice data sets also contain information regarding pressure ridging statistics. These include the average draft of pressure ridge keels observed along each submarine track line with a corresponding geographic location of each observation. Keel drafts remain quite constant from season to season as they are not subjected to the eroding processes which occur on the surface of the ice. Accordingly, an ice floe may appear relatively smooth on the surface while the bottom profile may indicate the presence of many keels which may have been formed at an earlier time. The major portion of the keel draft data were gleaned from the submarine underice cruise reports.
Additional data, which were available in small quantities throughout much of the literature, e.g. Wadhams and Horne (1980) and Wadhams et al. (1985), were incorporated into the combined underice data set. These data were included on a case by case basis to avoid duplication of any data points. The low-value cutoff for keel drafts applied to the data was 5 m in order to include more of the data points available from those submarine cruise reports which reported average keel drafts over the track. The total availabilty of keel

draft measurements is quite limited and is not ameniable to an extensive regional analysis.

Due to the sparseness of pressure ridge data, seasonal maps were produced which cover the entire Arctic Basin. Figures C.21-C.24 (Appendix C) illustrate the paucity of data while also drawing attention to the areas of severe or little to no pressure ridging.

Histograms were produced for areas of the Arctic Ocean where sufficient data points were available. Because these histograms reflect regional variations of keel drafts, they also are presented in the regional discussion of Arctic ice conditions in Chapter 3. Additional pressure ridge data are available in their evaluated form from the literature. These data are also presented in the general and regional discussions of Chapter 3.

3. Polynyas

Data concerning polynya distribution compose the least amount of ice distribution data currently available. LeSchack's (1983) underice profile data from five submarine cruises includes percentages of the segmented areas along the track containing open water. These five submarine cruises, which took place in 1960, 1962, and 1976, provide information on the interannual variability of leads. The data also include seasonal variability by providing measurements taken in summer, fall, and winter. These data are given in Appendix A.

A map of the areas of open water in the Arctic Ocean is shown in Figure 2.4. The data base for this map is located in Appendix A and is representative of mean yearly conditions observed in the Arctic. Areas with 20% or more open water are considered major Arctic open lead areas (LeSchack, 1983).

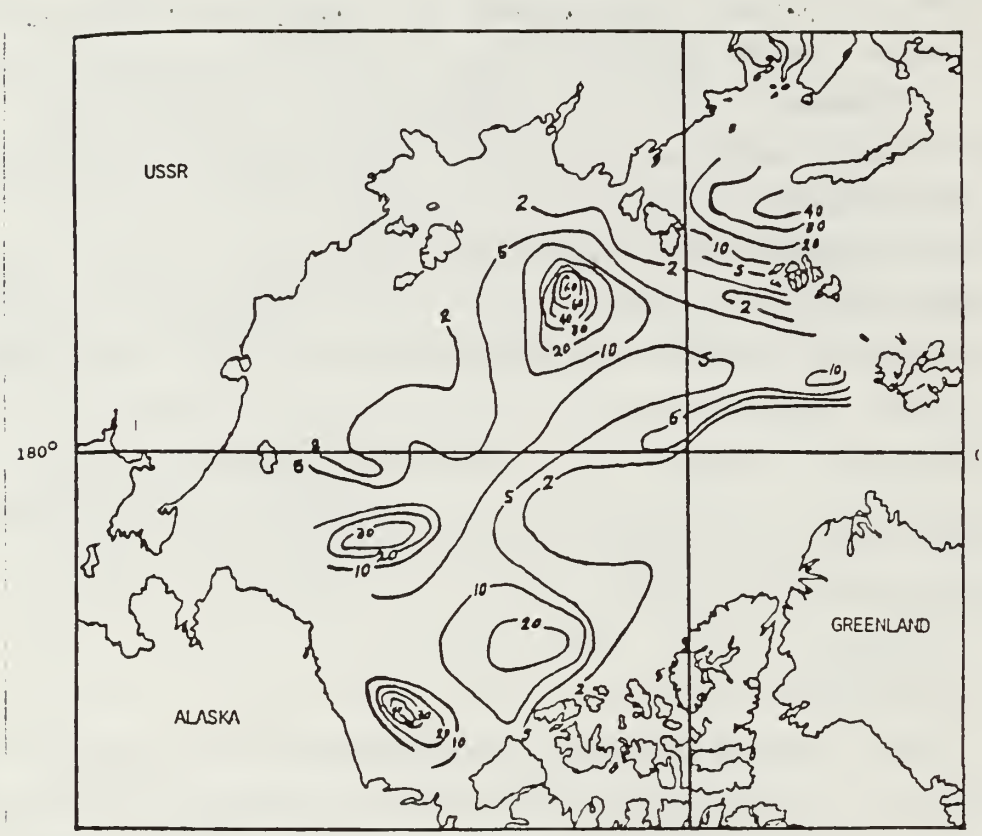

Figure 2.4 Contours (percent) of the area containing open water in the Arctic Ocean (after LeSchack, 1983).

III. DISCUSSION AND RESULTS

This chapter is divided into two sections: the first is a discussion of ice conditions and distributions for the entire Arctic Basin; the second is a regional discussion of the different areas of the Arctic and the ice conditions and distributions associated with each. Maps and histograms as well as mean ice thickness values are provided on a seasonal and regional basis to aid in the discussion of temporal and spatial sea ice distributions within the Arctic.

A. ARCTIC BASIN

The Arctic Basin, for the purposes of this study, represents the entire oceanic regime north of 65°N. A general discussion follows with regard to the mean ice thickness distribution on a seasonal basis for the Arctic Basin. Pressure ridge distributions as well as the mechanisms influencing the observed distributions are also discussed.

1. Mean Annual Ice Thickness

The mean annual ice thickness for the entire Arctic Basin was calculated from the combined submarine underice data set given in Appendices A-B. The resulting mean annual ice thickness is 2.9 m with a standard deviation of 1.8 m. This value, which incorporates both seasonal and spatial fluctuations, compares closely to the 3.0 m thickness value frequently quoted throughout the literature (Zubov, 1943; Hibler, 1979; Weeks, 1984; Weeks and Ackley, 1982). This latter value is also representative of measurements taken throughout the year and spanning many different geographic

regions of the Arctic Ocean. It was comprised from the BIRDSEYE reconnaisance data or from a collection of many individual measurements, i.e. ice corings.

Figure 3.1 is a histogram which shows the variability of the mean annual ice thickness (averaged over all seasons) over the entire Arctic region. A peak is present in the 0-1 m range, indicative of the first-year ice which is present during part of the year. A second peak, between 2-4 meters , is a manifestation of the large amount of multi-year and ridged ice present throughout the year. This is the same type of distribution observed in Figure 1.2. The tail visible in Figure 3.1 is indicative of the ridging which occurs in the thin weak floes of first-year ice and shows that extremely high sails are rare. Very high sails (> 6m) are seldom seen in the Arctic due to ice ablation in the summer (ridges melt from the top downward) and from the effects of wind erosion on the ice surface.

The standard deviation of the mean annual ice thickness is indicative of the degree of uncertainty. In this case it is quite large, approximately 70% of the mean value. Mean ice thickness values vary widely throughout the Arctic Ocean being dependent upon local geographical and mechanical effects. A standard deviation of ±1.8 m was calculated for the entire Arctic Ocean and represents the magnitude of error when the mean ice thickness of 2.9 m is quoted as the representative value of the Arctic Ocean. Axiomatically, when mean ice thickness is averaged over the entire Arctic Basin and over all seasons, the mean value is expected to vary ±1.8 m as determined from the combined submarine underice data set. However, as will be demonstrated in the section on regional ice thickness, the variance changes dramatically from region to region as does the regional mean ice thickness values.

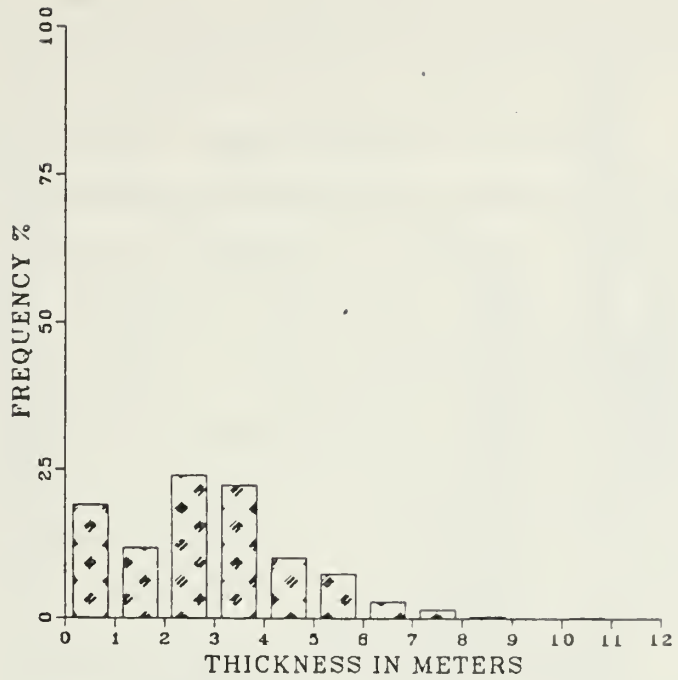

Figure 3.1 Arctic mean ice thickness distribution.

2. Mean Annual Pressure Ridging

Pressure ridging data are not suitable for the calculation of a mean ridge height representative of the entire Arctic Ocean due to the extreme variability of this parameter over the different regions of the Arctic Ocean. A mean annual pressure ridge thickness value was, therefore, not calculated.

A histogram showing the distribution of observed keel depths, as obtained from the combined submarine underice transits, is displayed in Figure 3.2. This histogram, based on a 5 m cutoff, indicates the vast majority of the observed pressure ridge keels fall in the 5 to 10 m range of keel drafts rapidly tailing off towards 20 m. Although individual keels have been recorded with drafts greater than 40 m, the histogram demonstrates that keels with depths greater than 20 m are not a common occurrence.

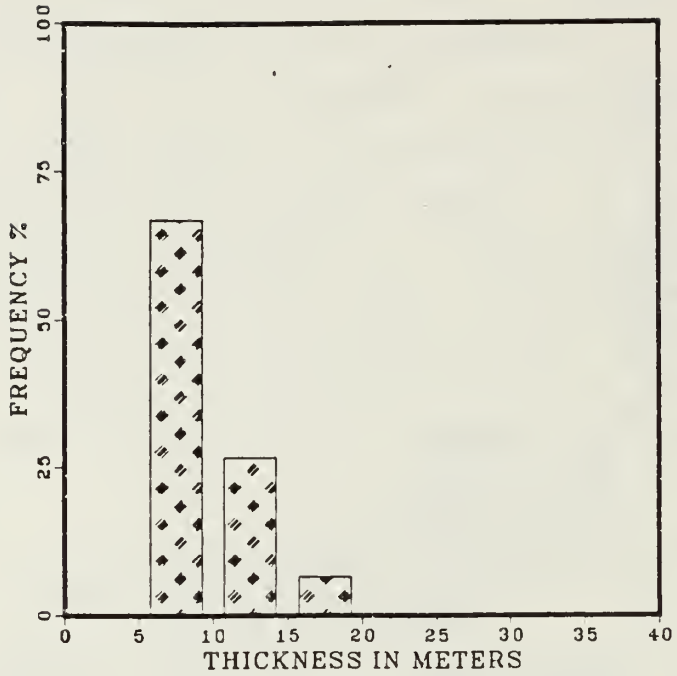

Figure 3.2 Pressure ridge keel depth distribution in the Arctic Ocean.

3. Seasonal Ice Thickness Distribution

a. Contour Maps of Mean Ice Thickness

The distribution of pressure ridges, as well as mean ice thickness statistics, are dependent upon both seasonal and geographical factors. In this section the seasonal distribution of these features in the Central Arctic Basin are explored.

As seen by the distribution of mean ice thickness data points shown in Appendix C, the overall paucity of data in the Arctic makes contouring of this parameter difficult. In spite of this relative paucity enough information was present to permit constructing contours of mean ice thickness on a regional and seasonal basis. Figures 3.3 - 3.6 present mean ice thickness maps of the Arctic Ocean for

each of the four seasons. The width of the contour line in these figures are representative of a swath approximately 50 km wide.

The contour maps provide an overall picture of the mean ice thickness conditions present throughout the Arctic. They clearly dilineate areas of thick ice floes (mean thicknesses greater than 5 m), e.g. the west side of the islands which make up the Canadian Archipelago and the area of the Lincoln Sea to the north of Greenland. This is as expected, since the Beaufort Gyre and Transpolar Drift Stream tend to push the ice pack around the Arctic Ocean in a clockwise direction causing the ice to the north to pile up along the natural barriers to this flow. This same flow causes areas of relatively thinner mean ice to be found on the opposite side of the Arctic Ocean towards the Siberian coast. The spring contour map (Figure 3.3) does not show the heavy ridging and ice thickness associated with the west coast of Greenland and the Canadian Archipelago and is probably attributed to inadequate data available for this area during spring. The mean ice thickness is also observed to decrease westward in a direction away from the west coast of the Canadian Archipelago toward the Siberian coast. This overall ice thickness pattern is relatively independent of season, being observed to a large degree throughout the year. Aagaard et al. (1981) explain the distribution of thin ice in the Arctic Ocean by variations in the depth of the observed halocline. The Siberian seas are areas of reduced salinity due to the runoff from coastal rivers and, when coupled with the seasonal melting and freezing of sea ice, allow only a thin (1-2 m) ice cover to occur which is subsequently maintained throughout the freezing season. The ice in the central Arctic Basin is allowed to grow much thicker due to the presence of a much deeper halocline.

Seasonal variations, however, do exist. In the spring (Figure 3.6) the effects of the winter freezing season can be seen, as this season provides the most uniform mean sea ice thickness distribution throughout the Arctic Ocean. The other seasons are more representative of intensive melting or freezing. In summer and autumn the thick multi-year ice persists while the first-year ice experiences melting. With increasing absence of thinner first-year ice, the remaining thicker multi-year ice shifts the mean ice thickness to greater values with a more complex distribution pattern. This condition persists into winter as the accumulation of first-year ice is not yet sufficient to smooth out the distribution pattern.

Of significant note is the similarity of the contours seen in Figures 3.4-3.6 to the contours of mean annual observed ice thickness obtained from sonar data and analyzed by LeSchack (1980) (Figure 3.7). The solid contours of Figure 3.7 are derived from a composite anaysis of both summer (1960, 1962) and winter data (1960). The dashed contours are from April 1977 data and show the pile-up of massive ice blocks along the northeast coast of Greenland as ice exits the Arctic Ocean via the East Greenland Drift Stream. The thickest ice, depicted on all the maps, is found along the western coastlines of the Canadian Archipelago and the northern coast of Greenland; reduced ice thickness is observed toward the Siberian and Eurasian coasts. Also worthy of note in the comparison of these figures are the dissimilarities which occur. LeSchack's map includes seasonal variability which causes the overall pattern of ice thickness distribution to be over simplified as contrasted to the much more complex, seasonal representations of mean ice thickness observed in Figures 3.3-3.6.

Figure 3.3 Mean ice thickness (m) in spring derived from submarine underice profile data.

Figure 3.4 Mean ice thickness(m) in summer derived from submarine underice profile data.

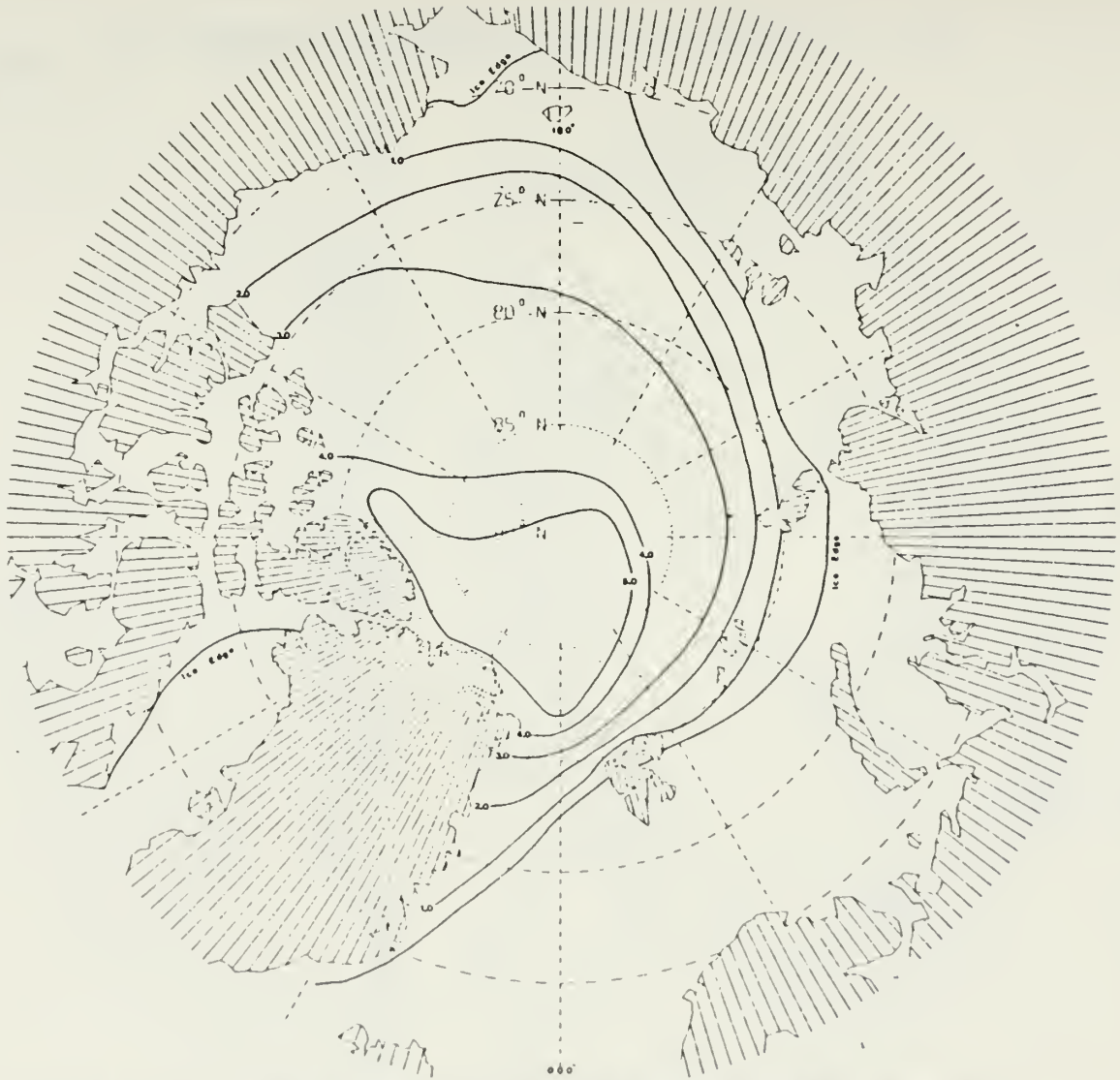

Figure 3.5 Mean ice thickness(m) in autumn derived from submarine underice profile data.

Figure 3.6 Mean ice thickness(m) in winter derived from submarine underice profile data.

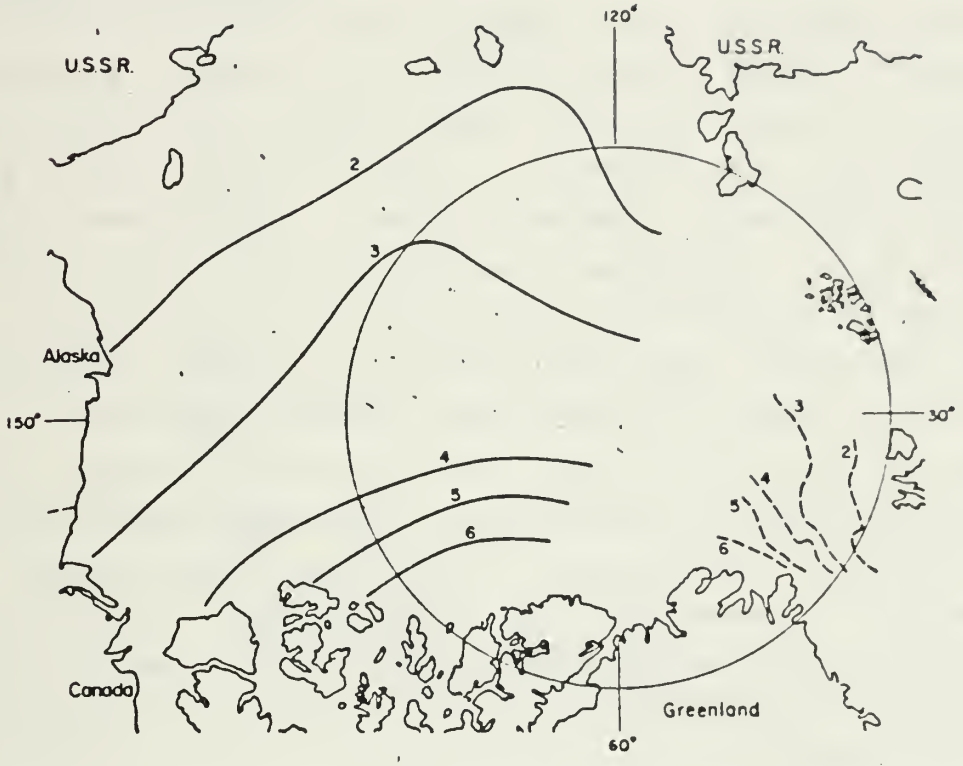

Figure 3.7 Contours(m) of mean annual ice thicknesss. Dashed lines represent conditions in April 1977 (after LeSchack, 1980).

b. Histograms of Mean Ice Thickness

The seascnal histograms of mean ice thickness for the entire Arctic basin are presented in Figures 3.8-3.11. The winter and spring histograms reflect a bimodal distribution with a peak in the 0-1 m range for both seasons and a second peak between 2-4 m during spring and between 3-4 m during winter. This bimodal distribution is attributable to the presence of first-year ice during the months in which most freezing occurs. In winter older, thicker (3-4 m) multi-year ice is slightly more prevalent than the newly formed young, first-year ice. In spring, as freezing continues, even more first-year ice is observed in the 0-2 m and the 2-3 m range than observed in winter. The increase in the 2-3 m band is indicative of more ridge building occurring in this season. The single peak between 2-4 m in summer and autumn reflects the small amount of first-year ice present and the large amount of multi-year ice remaining. In autumn the largest single peak in any of the seasons is observed in the 2-3 m range and is indicative of the predominance of multi-year ice.

Due to the extensive nature of the combined submarine underice data, little of the seasonal differences noted above are due to sampling variability, i.e. virtually all regions of the Arctic are equally represented in each seasonal histogram as is the number of data points. An exception is autumn where the number of measurements in heavily ridged areas were less than those obtained in not so heavily ridged areas. Yet, the autumn contour map (Figure 3.5) still depicts a large area of mean ice thickness, greater than 5 m, along the Greenland and Canadian Archipelago coastlines as expected. Thus, in autumn (Figure 3.10) one would probably expect the observed peak of mean ice thickness to occur in the 3-4 m range vice the 2-3 m

range. In addition, the summer and autumn histograms (Figures 3.9 and 3.10) show the presence of extremely thick ice (>10 m) whereas no ice greater than 7 m is present in spring. This feature is probably due to sampling vice seasonal variations.

Figure 3.8 Arctic spring mean ice thickness distribution.

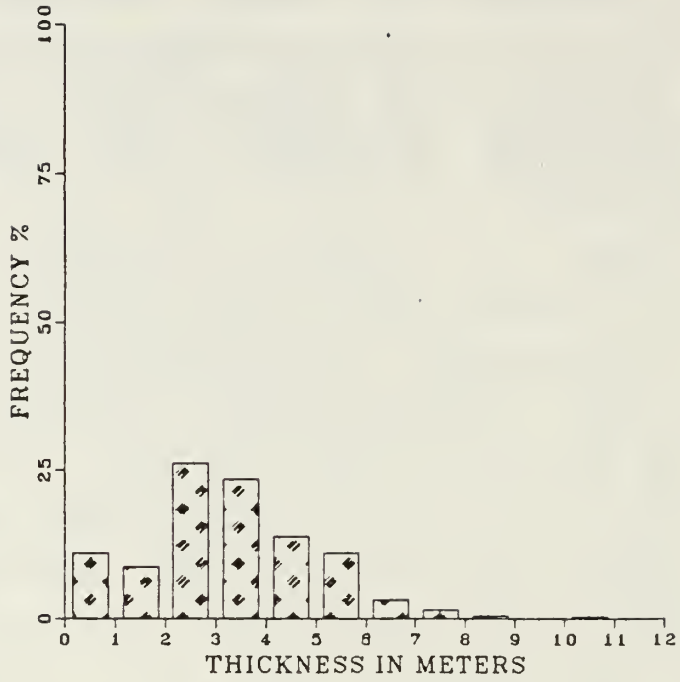

Figure 3.9 Arctic summer mean ice thickness distribution.

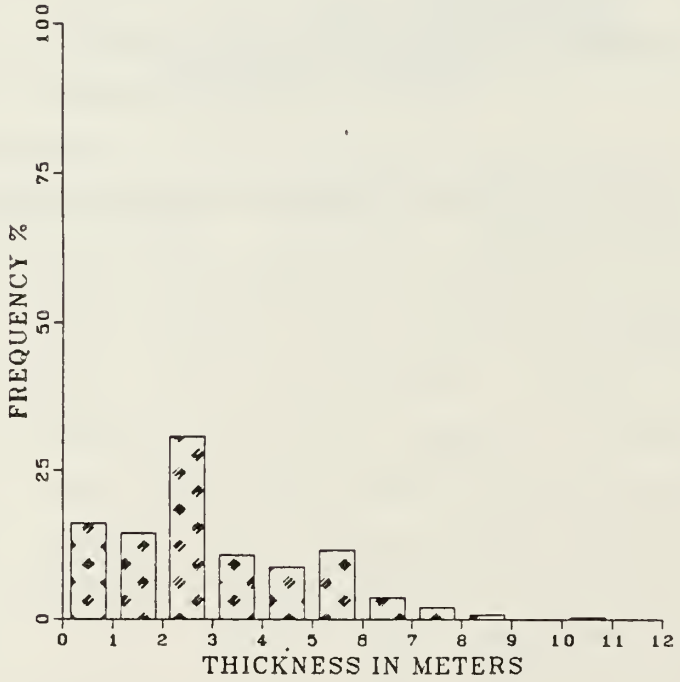

Figure 3.10 Arctic autumn mean ice thickness distribution.

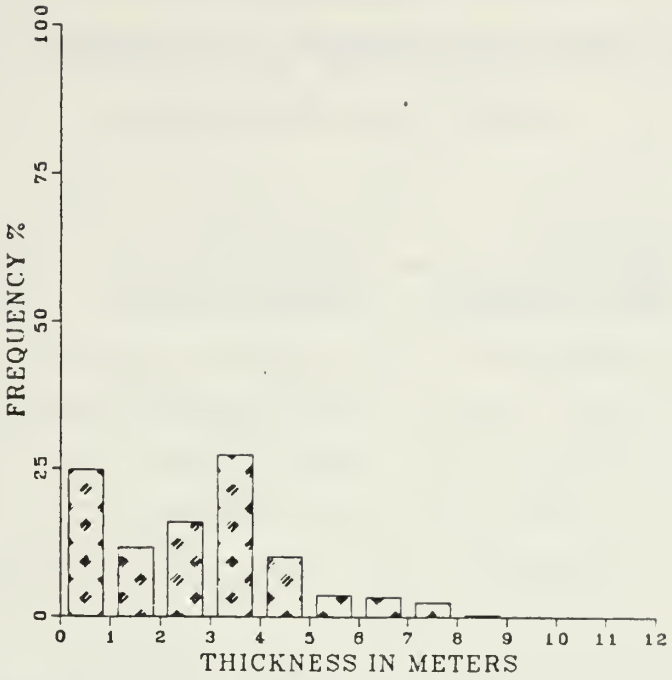

Figure 3.11 Arctic winter mean ice thickness distribution.

c. Mean Ice Thickness and Standard Deviation

The combined submarine underice data were used to produce overall mean values and standard deviations of mean ice thickness measurements for each season over the entire Arctic Ocean. The data are listed in Table IV.

The overall seasonal mean ice thickness values echo the same observations noted in the contoured maps and histograms, i.e. larger mean ice thickness values in summer and autumn when multi-year ice dominates and smaller values in winter and spring when large amounts of first-year ice are present to complement the perennial multi-year ice.

In spring the standard deviation, or degree of uncertainty, is less than that observed in other seasons (1.4 m vice about 1.8 m). This is due, in part, to the formation of first-year ice which experiences growth during the freezing season providing a more uniform distribution of mean ice thickness and thus a more stable mean ice value.

TABLE IV

Seasonal Mean Ice Thickness and Standard Deviation for the Arctic Ocean

Season	Mean ice thickness(m)	Standard deviation(m)	Number of obs.
Spring	2.4	1.4	267
Summer	3.3	1.7	344
Autumn	3.0	1.9	247
Winter	2.8	1.8	340

The other seasons reflect a higher degree of uncertainty in mean ice thickness, in part due to the larger quantities of multi-year ice of variable age and thickness surrounded by thin ice undergoing melting or freezing.

The analyzed submarine data (from digitized underice profiles, Appendix A and B) provide only two points where tracks from different submarine cruises have crossed. One of these points is in M'Clure Strait where the USS SARGO (summer 1960) crossed the track of the USS SEADRAGON (winter 1960). The mean ice thickness measured on both occasions was 3.5 m. In M'Clure Strait only a slight seasonality is expected in mean ice thickness as the strait remains ice choked year-round. The other crossing point occurred in the spring of 1979 when HMS SOVEREIGN crossed her own autumn 1976 track in Fram Strait. There was also no significant difference in mean ice thickness observed in this area either. One might expect little difference in ice thickness to occur in this region, however, as the amount of multi-year ice exiting the Arctic through Fram Strait remains quite constant throughout the year.

d. Contour Maps of Pressure Ridging

Data from the U.S. Navy BIRDSEYE flights provide an estimate of the intensity of ridging over selected regions of the Arctic Ocean. Ridging intensity refers to the number and mean height of ridges observed per nautical mile, i.e., the volume of deformed ice per unit distance. Figures 3.12 and 3.13 are maps of pressure ridge intensity as determined by Weeks et al. (1971) for summer and winter, respectively. These figures show clearly that the areas of intense ridging are located along the west and north coasts of the Canadian Archipelago and along the north and northeast coasts of Greenland. As noted previously, this is the region where the Beaufort Gyre and Transpolar Drift Stream converge on the coastline.

Ridging intensity differs from summer to winter. For example, in the above regions of high ridging intensity, 20-30 ridges are observed per nautical mile during summer. The same area in winter is characterized by ridging intensities between 30-40 ridges per nautical mile. This is attributable to ice melting in summer and ice growth in winter. In addition, summer is a season of less intense wind conditions. Hence, less movement and interaction among the ice floes occur which have a direct impact on the amount of pressure ridging observed. Comparing these figures to the contour maps of mean ice thickness for summer and winter (Figures 3.4 and 3.6), a similar westward shift of maximum ice thickness in winter is observed. Although summer is still the season when maximum mean ice thickness is observed, as illustrated in Figures 3.9 and 3.11, winter (and perhaps spring) is the season of greater pressure ridge intensity.

Insufficient data are available from areas near the Siberian Arctic as they are beyond the limit of coverage

of the BIRDSEYE flights. The limit of observation is shown in Figures 3.12 and 3.13.

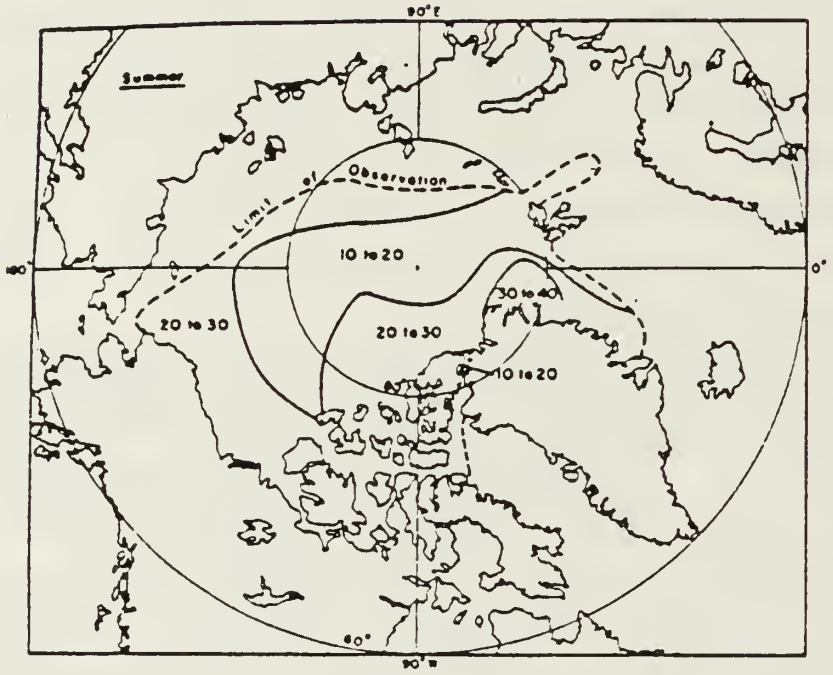

Figure 3.12 Summer pressure ridging intensity from BIRDSEYE data (after Weeks, 1971).

e. Histograms of Pressure Ridge Keel Depths

The submarine underice data provide information regarding the seasonal distribution of pressure ridge keel depths and is shown in Figures 3.14 - 3.17. The dominant peak in all four seascns appears in the band between 5-10 m. Keels with drafts deeper than 20 m are seldom observed, as was also the case for the annual distribution of pressure

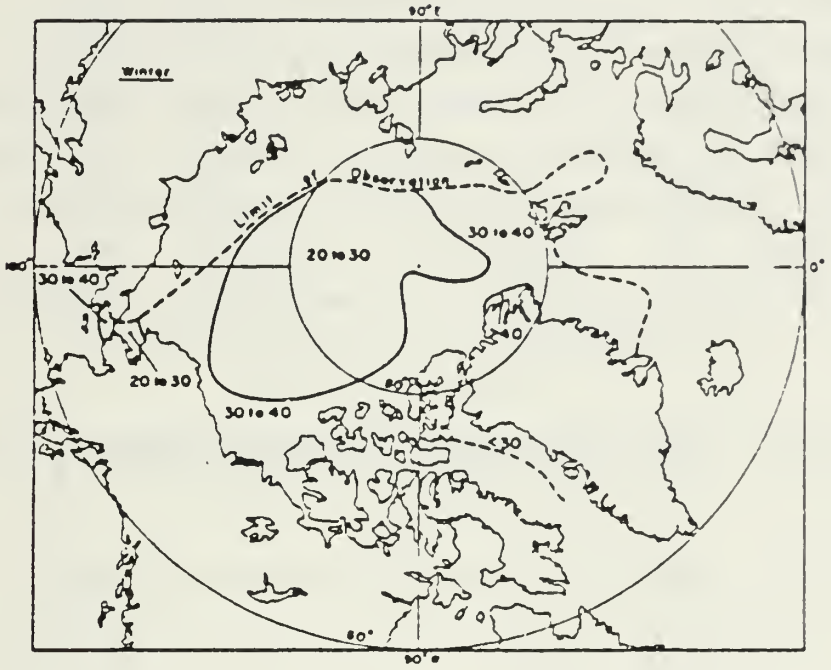

Figure 3.13 Winter pressure ridging intensity from BIRDSEYE data (after Weeks, 1971).

ridge keels. Little seasonal variability in keel depth distribution is observed and any variability which may occur is probably the result of spatial sampling differences. The variation in seasonal pressure ridging occurs mainly from the ablation of the ice surface in warmer months while the underice keel depths remain virtually unchanged from season to season, i.e., their fluctuation time scale is much longer, perhaps annually or longer. The fall season (Figure 3.16) shows an absence of values between 10-15 m, probably due to the general paucity of pressure ridging data available for this season.

Submarine underice profile data may be biased against encountering many deep or extreme keel drafts because they tend to navigate around these hazardous obstacles (personal communication with McLaren, 1985). This is especially true in shallow regions where pressure ridging may be extensive. Therefore, there may be a lack of extreme keel depth data when using submarine profiles. Wright et al. (1978) record measurements of keel depths in excess of 30 m occurring near flaw leads, e.g., the Canadian Beaufort Sea. These measurements are the result of individual pressure ridge thickness measurements as determined by single drill holes vice measurements averaged over 50-150 km segments which are typical of submarine ice profiles.

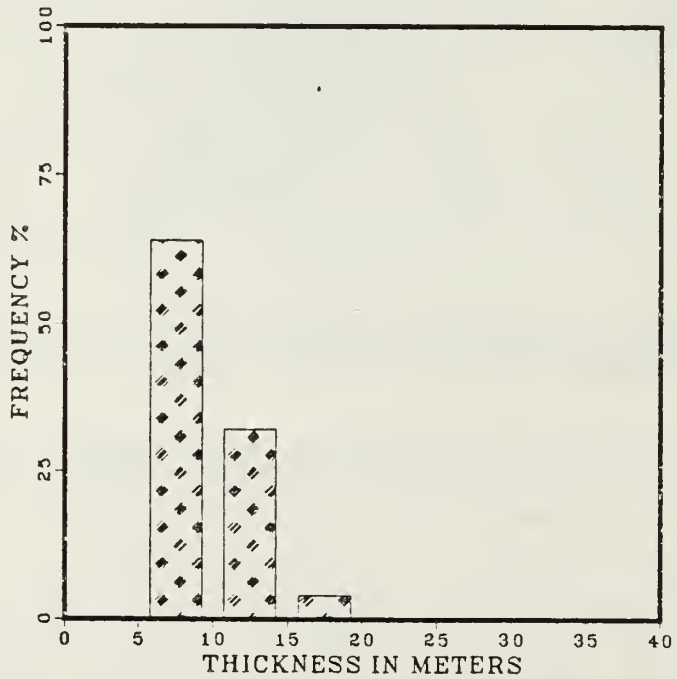

Figure 3.14 Spring pressure ridge keel distribution from submarine underice data.

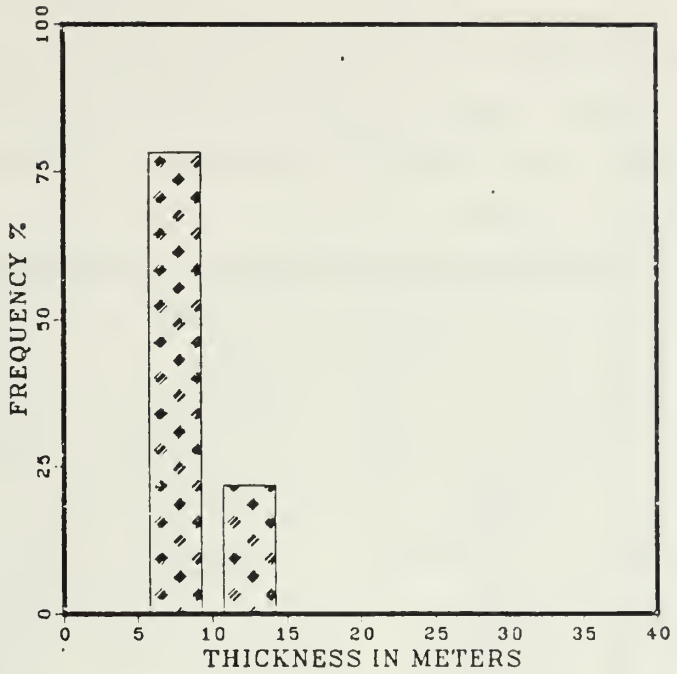

Figure 3.15 Summer pressure ridge keel distribution from submarine underice data.

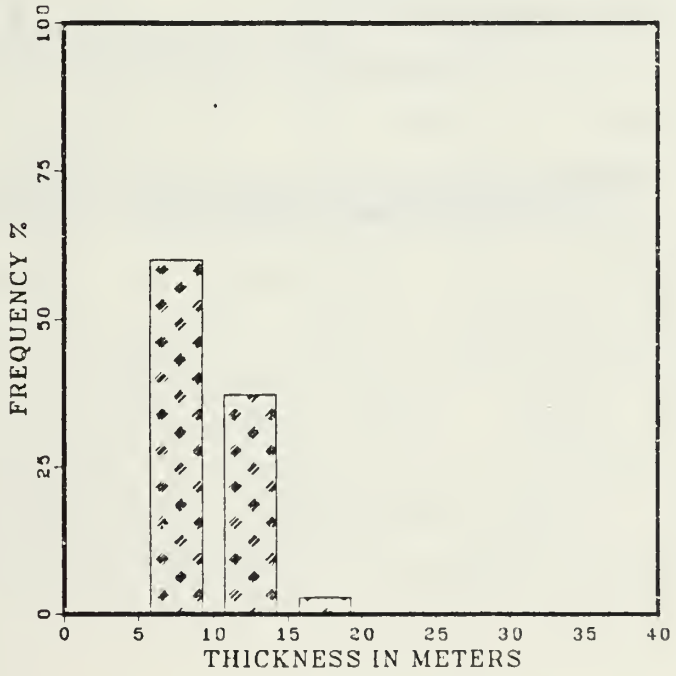

Figure 3.16 Autumn pressure ridge keel distribution from submarine underice data.

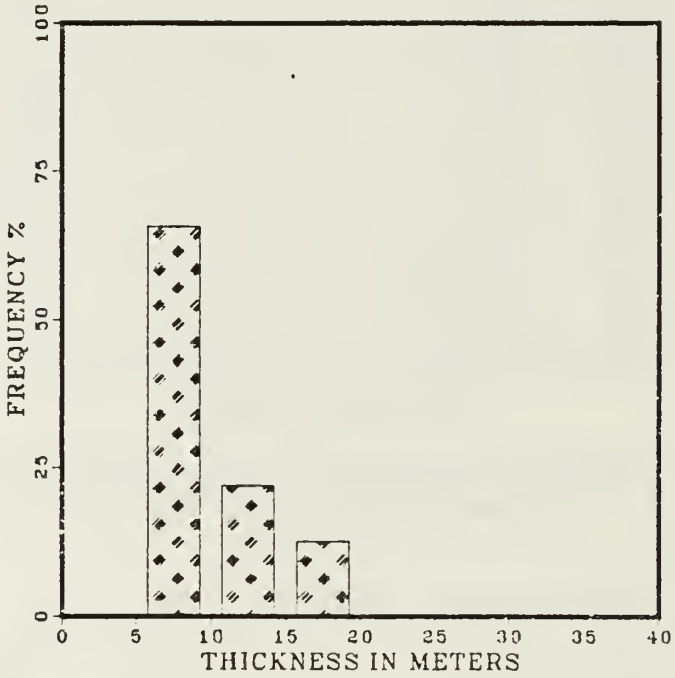

Figure 3.17 Winter pressure ridge keel distribution from submarine underice data.

B. REGIONAL DISCUSSION

This section treats the mean ice thickness and the pressure ridging distributions in the Arctic Ocean on a regional basis. In addition, various ice characteristics, i.e., type and age of the sea ice as well as polynya occurrence, are discussed regionally. From the combined underice data sets mean ice thicknesses and standard deviations were determined on a regional basis. They represent mean annual conditions since the amount of submarine data becomes sparse if partitioned on both a regional and seasonal basis. Table V lists regional mean ice thickness and standard deviation values, omitting the East Siberian , Barents, and Norwegian Seas, for which insufficient data were available to make an estimate of regional ice thickness. As might be expected, the standard deviations, in general, increase as the mean ice thickness values increase. The rate of increase of standard deviation with mean ice thickness is characterized by a slope of approximately 0.52. Regional histograms were constructed for both mean ice thickness and pressure ridge keel draft distributions. The location of pertinent bodies of water discussed in this section are shown in Figure 3.18.

The discussion of each region takes into account the results provided by analysis of the combined submarine underice data set as well as the regional characteristics derived from the current literature and previously evaluated data sets, such as BIRDSEYE data. Where conflicting or supporting findings of regional ice conditions arise from other researchers or ice prediction models, these findings are provided in the analysis for comparison and completeness of the study.

TABLE V

Regional Mean Ice Thickness

Region	Mean Ice Thickness (m)	Standard Deviation (m)
Cent. Arctic	3.4	1.4
Beaufort Sea	3.2	1.0
Chukchi Sea	1.9	1.1
Canadian Arch.	4.0	2.7
Baffin Bay	1.1	0.5
Greenland Sea	2.7	2.1
Laptev Sea	2.5	1.2
Kara Sea	1.0	0.8
Combined overall	2.9	1.8

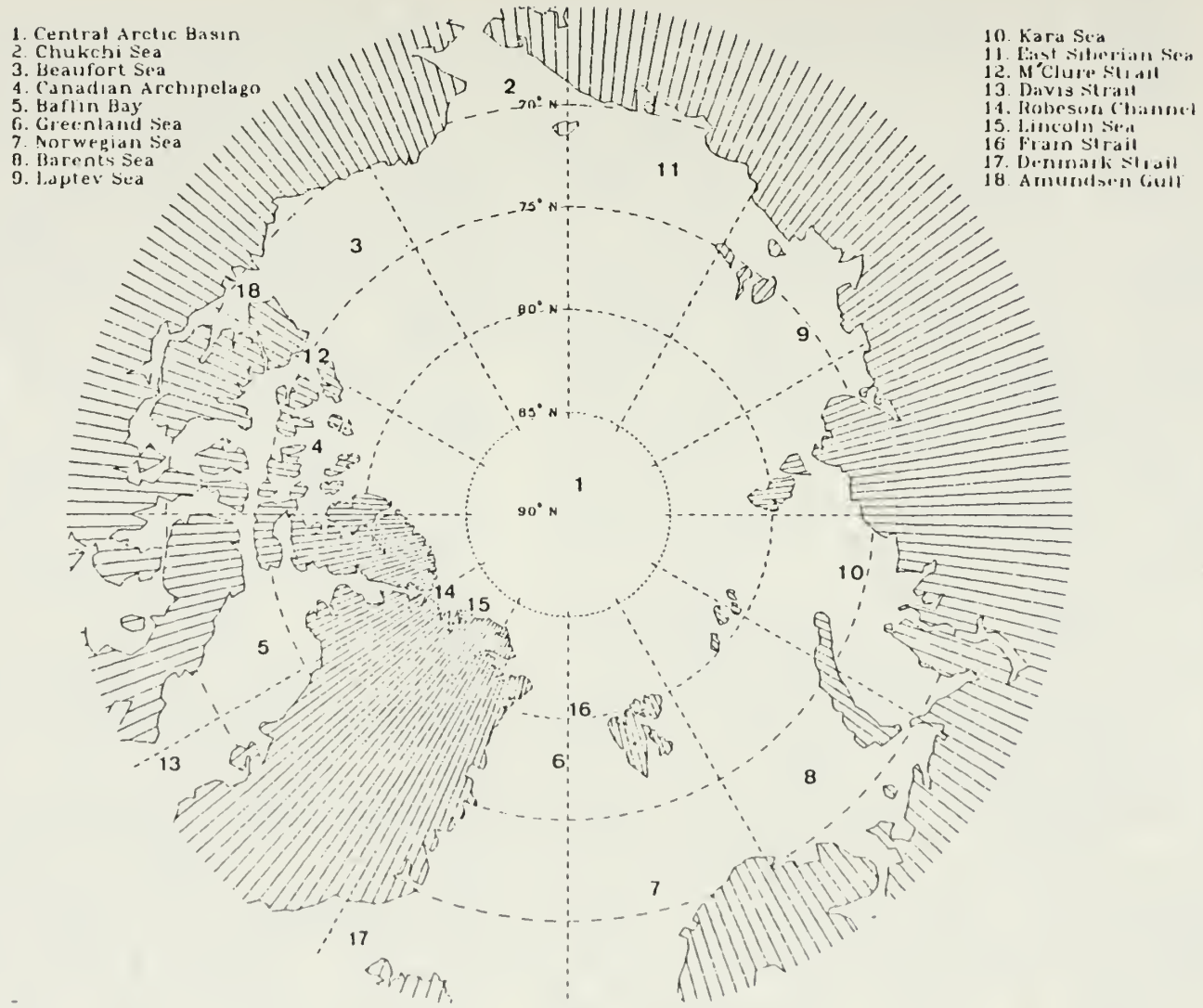

Figure 3.18 Regional locater map for the Arctic Ocean

1. Central Arctic Basin

The Central Arctic Basin is the largest region of the Arctic Ocean and is largely composed of multi-year ice. The mean ice thickness in this region, as calculated from the combined submarine underice data, is 3.4 m with a standard deviation of 1.4 m. The mean ice thickness is the second largest found in the Arctic Ocean and is due to the dominance of multi-year ice in this region.

This region is completely covered by permanent sea ice, kept continually in motion by the Transpolar Drift Stream and the northern portion of the Beaufort Gyre. The average age of ice in the Central Arctic Basin is 10 years (Zubov, 1943). The thickest ice is found north of Greenland and the Canadian Archipelago which provide natural barriers to the movement of the ice and, consequently, the most intense ridging also occurs in this area. The areas towards the Soviet side of the Central Arctic Basin are areas of thinner ice and less intense pressure ridging. First-year ice is also found toward the Soviet side of the region in more abundant quantities.

The histograms shown in Figures 3.20 and 3.21 were derived from the combined underice data sets and are representations of mean ice thickness and pressure ridge keel depth distributions in the Central Arctic Basin, respectively. The mean ice thickness histogram shows a Rayleigh-type distribution with a peak between 3-4 m, tailing off to the right towards even thicker ice. The keel depths can extend to great depths as shown by Figure 3.21 which shows a peak between 10-15 m. The Central Arctic Basin is the only region which has its peak keel depth between 10 and 15 m. This peak shows that greater than 50% of the observed keel depths in this region occur within this range. All other regions in the Arctic Ocean have peak keel

depths of 5-10 m. Although the peak keel depth is less in other Arctic regions, it will be later shown that the frequency of occurrence of pressure ridging is greater in other regions, e.g., along the west coast of the Canadian Archipelago.

Ice conditions in the Central Arctic Basin, as obtained from BIRDSEYE data, are summarized in Table VI (after Weeks et al., 1971). Notable features which can be derived from this table include the dominance of multi-year ice throughout the year while the frequency of pressure ridging remains almost constant throughout the year. The observed pressure ridging shows a dominance of the larger ridges and hummocks in this region which support the findings provided by Figure 3.21. Table VI shows that the percentage of area affected by pressure ridging is moderate, 21-23%, indicating that although pressure ridges have large keel depths, their spatial distribution is not as great as that observed in other regions. Also worthy of note, is the limited seasonal variation of ice conditions observed in this region. The ice conditions remain rather uniform throughout the year.

Histograms of mean ice thickness and pressure ridge keel drafts for the Central Arctic Basin are also provided by Weeks et al. (1971) (Figures 3.22 and 3.23). These figures were obtained from individual submarine cruises into the Arctic Basin by the USS SARGO (winter, 1960) and the USS SEADRAGON (summer, 1960) and provide seasonal insight into the character of the sea ice in this region. The histograms of Figure 3.22 show how the mean ice thickness changes seasonally. The predominant ice thickness varies little between summer and winter remaining approximately 2 m throughout the year. Although the ice thickness tails to the right in both seasons, the summer season shows a larger percentage of ice with drafts greater than 4 m. This may be

TABLE VI

Ice Conditions in the Central Arctic Basin

(after Weeks et al., 1971)

Source	*Subject*		*Season* Winter	Summer
BIRDSEYE	Concentration (areal, %)	average	99	92
		range	98-100	30-100
	Ice types (areal, %)	young	1	4
		winter	17	27
		multi-year	81	61
	Topography (areal, %)	large ridges and hummocks (>3 m high)	21	23
		small ridges and hummocks (<3 m high)	4	4
	Number of water openings	>30 m/100 nm	23	39
		<30 m/100 nm	33	53
Submarine	Topography (linear, %)	openings	1	5
		ice	99	95
		keels	15	15

due to the increase in ice ablation in summer which melts the thinner ice leaving behind a greater fraction of thicker ice in each 50-100 km segment. It may also be due to sampling differences between the two cruises e.g., the SEADRAGON track was longer and more frequently traversed areas of greater deformed ice.

On the left side of the histogram can be seen the effects of winter ice growth and summer ice melt. The summer figure shows a larger amount of ice between 0-1 m than that seen in winter which may be indicative of the melting of ridged first-year ice taking place; in winter the thinner first-year ice is readily fractured and subject to pressure ridging and hence the smaller amount of 0-1 m ice observed.

A comparison with Figure 3.20 contrasts the 1960 mean ice thickness conditions to the longterm mean ice conditions. The histogram given by Figure 3.20 shows that longterm mean ice thickness (which is inclusive of the SEADRAGON and SARGO cruise data) is greater than that observed in the single year of 1960, illustrating the possibility of an anomalously warmer year in 1960 which produced overall thinner mean ice conditions.

The histogram given in Figure 3.23 shows little difference in the percentage of keel drafts in the Central Arctic Basin on a seasonal basis. When compared with Figure 3.21, it is apparent that the peaks do not exactly correspond. The peaks in Figure 3.23, at about 8-10 m, are more than that observed from the longterm mean which may be indicative of 1960 being a year of greater wind stress and more intense ridging. These collective histograms illustrate the great variability of ice conditions that may be observed at any one time in the Central Arctic Basin.

Hibler et al. (1974) report the results of a one-parameter model to predict ridging intensity in the Arctic. The model was compared to the AIDJEX laser profilometer data used by Tucker and Westhall (1973) with good results. This procedure illustrates that to a degree pressure ridging may be predicted with some degree of accuracy. The relative accuracy of the model is mainly due to the fact that in this region the distribution of pressure ridging is fairly stable. The chartlets shown in Figure 3.24 provide a seasonal sampling of pressure ridge intensity as determined by the model. The contours are centered along discontinuities in pressure ridge intensity and provide a good delineation of actual observed pressure ridging conditions for this area. The samples in Figure 3.24 correspond to the 26 geographical sites catalogued by Tucker and Westhall (1973) using the AIDJEX data given in Figure 2.3. The seasonal

samples encompass the seasons of fall and winter and include interannual variations by producing samples for the years 1970 to 1973. The sample maps indicate that, although the ridging intensity may vary from month to month, the contours delineating the separation of pressure ridging intensity by geographic area remain quite constant. The position of the contours illustrate the increase in ridge intensity as one proceeds towards the coasts of Greenland and the Canadian Archipelago. Although the contours of October, 1971 do not reflect the degree of pressure ridging one would expect, (they appear to be too low) the separation of ridging intensity is still seen and the inconsistency may be attributed to some problem internal to the model itself.

Leads are generally temporary and small in this region, refreezing almost immediately after formation (Zubov, 1943). The motion of the ice pack causes continual and rapid changes to occur adding to the unpredictability of ice conditions in the Central Arctic Basin. Consequently, as the ice pack diverges and a lead forms and then refreezes, this feature may only remain in this condition or location for a short period of time (Sater et al., 1971). The area directly to the north of the Lincoln Sea and south of the North Pole, between 20°W-60°W, is an area of frequent lead occurrence. Leads in this area are due to the divergence of the Transpolar Drift Stream and the Beaufort Gyre which produce cracking and opening of the ice pack. No current information exists on the width or frequency of polynyas which occur in this area.

Wadhams (1983b) found the distribution of level ice in the Central Arctic to be between 45-55% of the total ice. This domain of level ice was found to exist north of Greenland where the mean ice thickness was found to be 4.5 m from data obtained by HMS SOVEREIGN, 1976 (Refer to Figure 1.3).

In summary, the Central Arctic Basin contains the oldest, thickest and most dense sea ice found within the areas of the Arctic Ocean, which includes the area encompassed by the center of the Beaufort Gyre. These old ice floes have been recorded to attain ages of more than 20 years although the average age is about 10 years. These floes, which consitute the predominant ice type in the Central Arctic Basin, are covered with large smooth hummocks which have been worn down by several summers of melting. The relatively smooth upper surface often deceptively masks the deep keels on the underside of the ice. The overall keel depth distribution observed throughout this region remains quite constant from season to season but may change gradually over longer time scales. Mean ice thickness does change, however, on a seasonal basis as varying seasons of ice growth and melt effect the amount of first-year ice present.

2. Chukchi Sea

The Chukchi Sea provides a gateway into the Arctic Ocean from the Pacific Ocean through the Bering Strait. The sea ice cover in this region varies greatly over the annual cycle. In winter this area is composed mostly of first-year ice which extends southward through Bering Strait covering most of the shallow Bering Sea. In summer the sea ice recedes northward leaving large areas of open water and detached floating ice floes. The ice pack reaches its minimum extent in August or September at which time most of this region is ice free (Sater et al., 1971).

The mean ice thickness for this region, determined from five submarine cruises, (Table V) is 1.9 m with a degree of uncertainty of ±1.1 m. This is in close agreement with the 2 m mean ice thickness value determined by LeSchack et al. (1970) using data from one submarine underice cruise

(USS SARGO, 1960). Most of the submarine data are during the freezing season; hence the mean is more indicative of winter conditions. The thickest ice as well as most of the pressure ridging occurring in this region is found along the north Alaskan coast and the far northeast coast of the Soviet Union, a result of the compression of the ice pack against land barriers by the westward flowing Beaufort Gyre. Additional thick ice is found along the northern peripheries of the Chukchi Sea as the transition is made to the Central Arctic Basin and the permanent Arctic ice pack. The variability of ice conditions in the Chukchi Sea depends upon the amount of multi-year pack ice being transported to the southeast by the Beaufort Gyre (Sater et al., 1971).

The distribution of mean ice thickness in the Chukchi Sea is given in Figure 3.25. This histogram depicts a peak of mean ice thickness at 2-3 m, but is exceeded in total volume by the amount of ice in the 0 to 2 m regime. This distribution is indicative of the large amount of first-year ice observed in winter which surrounds broken fragments of thicker multi-year ice that have been transported from the north.

The histogram given in Figure 3.26 shows the percentage of keel depths associated with the pressure ridging inherent to the Chukchi Sea. The majority of keel depths in this region occur in the 5-10 m range. Keels in excess of 10 m are quite rare. The peak observed at 5-10 m is indicative of the moderate pressure ridging occurring from the compression of first-year ice in the coastal areas.

BIRDSEYE data provide additional information on sea ice conditions in the Chukchi Sea. Table VII (after Weeks et al., 1971) summarizes the observations obtained from the Chukchi and Beaufort Seas in summer and winter. The seasonal variation is self-evident. During summer there is a large variation among ice types somewhat dependent upon

location within the region. In summer, ice openings are much larger with more occurrences in the >30 m/100 nm range than observed in winter due to the melting and ablation of the ice pack experienced in summer. In winter, openings in the ice tend to be smaller and are due mainly to the cracking and fracturing of the moving ice floes. Additionally, there is twice as much multi-year ice present in winter than in summer as the Arctic ice pack extends further southward in winter and then is subsequently melted in the summer. The greater ice concentrations noticed in Table VII are a reflection of the inclusion of the Beaufort Sea into this table. The higher ice concentrations in summer are associated with the Beaufort Sea and are not generally observed in the Chukchi Sea.

TABLE VII

Ice Conditions in the Chukchi and Beaufort Seas

(after Weeks et al., 1971)

Source	Subject		Season Winter	Summer
BIRDS EYE	Concentration (areal, %)	average	99	78
		range	70-100	8-100
	Ice types (areal, %)	young	7	5
		winter	46	46
		multiyear	46	27
	Topography (areal, %)	large ridges and hummocks (>3 m high)	21	15
		small ridges and hummocks (<3 m high)	5	8
	Number of water openings	>30 m/100 nm	34	76
		<30 m/100 nm	134	73
Submarine	Topography (linear, %)	openings	2	9
		ice	98	91
		keels	12	7

The histograms shown in Figures 3.27 and 3.28, obtained from BIRDSEYE data, compare the summer and winter frequency distributions of ridge heights and the number of ridges observed per nautical mile in the Chukchi and Beaufort Seas and the Central Arctic Basin (Canadian Basin). Since the BIRDSEYE flights measured the topside ice features, by applying a keel/sail ratio of 3.3/1 to the sail height measurements, a comparison of keel depths with Figure 3.26 can be made. Both summer and winter pressure ridge height histograms show peaks at 2-4 m, which gives a mean thickness of about 9.9 m when the 3.3/1 keel/sail height ratio is applied. This compares favorably to that given by the combined submarine underice data shown in Figure 3.26. In both the Chukchi and Beaufort Seas the predominant ridge frequency in summer is in the 0-10 per nautical mile band which reflects the reduced ice concentration in these seas at this time of year. In the winter the peak shifts to the right and is not so concentrated in a single band. Greater ridging is experienced in winter due to the more extensive ice cover, mostly first-year which buckles easily when forced against land barriers.

The area to the north-northwest of Barrow, Alaska is always highly ridged in winter. This is correlated to an area of compression in the Beaufort Gyre and strong northerly and easterly winds which drive the pack ice back along the Alaskan coast near Point Barrow (Sater et al., 1971). Since the ice pack is predominately first-year ice surrounding chunks of multi-year ice, fracturing readily occurs. The result is an area of pressure ridge keels of 5-10 m with occasional keels of >10 m observed.

Studies of the Chukchi Sea ice pack have not presently produced information concerning any locations of recurring leads or polynyas other than a recurring flaw lead

located in the fast ice along the Alaskan coast (Sater et al., 1971). Because of ice melt in the summer, this entire region is characteristic of many leads, polynyas, and areas of open water. Winter also produces many leads and polynyas as the young first-year ice remains in motion throughout the season, but information is still lacking in being able to predict their occurrence in the Chukchi Sea.

3. Beaufort Sea

The Beaufort Sea is a region of greater mean ice thickness and more intense pressure ridging than experienced throughout most of the Arctic Ocean. The mean ice thickness of this region, as obtained from the combined submarine underice data, is 3.2 m with a standard deviation of 1.0 m. LeSchack et al. (1970) support this finding by describing mean ice thickness in the Beaufort Sea as between 3-4 m. This mean ice value reflects the large amount of multi-year ice being transported into this region by the Beaufort Gyre and the large amount of pressure ridging occurring in first-year ice along the Alaskan coast. There are, however, in the western and central Beaufort Sea vast areas of several hundreds to several thousands of square km of dense pack ice located in the center of the Beaufort Gyre that migrate very slowly and are not subject to great stresses (Sater et al., 1971). This ice tends to be thick, relatively smooth multi-year pack ice. It rotates about the axis of the Beaufort Gyre eventually working its way to the periphery of the gyre where it is melted or subjected to shearing motions and forms pressure ridges.

In the summer the ice pack melts and recedes northward, between 20-30 nm, leaving the Alaskan coastline and large areas to seaward ice-free (Sater et al., 1971). In the winter the Beaufort Sea is nearly completely covered with an ice pack consisting of first-year and multi-year

ice. Rubbled fast ice is a common occurrence along the Alaskan coast in winter.

The distribution of mean ice thickness in the Beaufort Sea (Figure 3.29) shows a large peak, approaching 45% of the total, between 3 and 4 m indicative of large quantities of multi-year ice. The relatively small amount of ice with mean thickness between 0 and 2 m (compare with the Chukchi Sea, Figure 3.25) illustrates the extent of pressure ridging in the Beaufort Sea. As first-year ice is compressed and ridging results, much of the first-year ice is found in the ≥3 m range bin. As in the Chukchi Sea, keel depths in the Beaufort Sea (Figure 3.30) are predominately in the 5-10 m band. However, fewer keels exceeding 10 m are found in the Beaufort compared to the Chukchi Sea. Shallower keels are found because this region is located in an area where the Beaufort Gyre diverges and expands and the sea ice is subjected to smaller compression and shearing forces which produce the larger keels (Sater et al., 1971).

In their analysis of BIRDSEYE data, Wittman and Schule (1966) joined the Beaufort Sea with the Chukchi Sea to comprise the Offshore Province because of the large amount of unstable first-year ice present in both of these seas. Although ice conditions in these two seas are similar in the summer due to the ablation of the ice pack and, in particular, the presence of large amounts of first-year ice which dominates these two regions, the similarities cease in winter. The Beaufort Sea is much more variable and ice conditions change rapidly. The ice is in winter thicker and pressure ridging is more intense than that observed in the Chukchi Sea. As seen in Figures 3.27 and 3.28, the summer pressure ridging statistics are similar between the two seas, but the winter values show clearly that there are many more pressure ridges present in the Beaufort than the Chukchi Sea (217 vs. 109 observations) but their

distribution per nautical mile is about the same. The distribution of pressure ridging is dependent, however, upon the amount of ablation occurring on the surface which masks many of the keels which would be detected on the bottom side of the ice. Since Figures 3.27 and 3.28 are derived from BIRDSEYE data, the character of the underside of the ice is unknown at the time these observations are made.

In April 1976 the USS GURNARD traversed 1400 km under the ice of the Beaufort Sea. The cruise track is shown in Figure 3.31. Along the coastal leg of the cruise a mean ice thickness value of 3.7 m was observed. This rapidly reduced to 2.7 to 2.9 m once deep water was encountered. Heavily ridged ice along the coast of Alaska was observed with a mean draft of 5.1 m. A maximum draft of 31.12 m was recorded (Wadhams and Horne, 1980). These mean thickness values are similar to those derived through analysis of the combined submarine underice data set.

The motion of ice in the Beaufort Sea, dominated by the Beaufort Gyre, not only results in pressure ridging but also causes the formation of leads and polynyas due to the same motion. Wadhams and Horne (1980), through analysis of the GURNARD track data, reported that leads occur in the Beaufort Sea approximately every 200 m, but tend to be very narrow, seldom exceeding 50 m in width. A lead or polynya approximately 200 m wide can be expected to be encountered every 68 km. In the southern Beaufort Sea, however, they found that 50 m wide leads occur every 10 km due to the divergence associated with the Beaufort Gyre.

Wadhams and Horne (1980) found that in winter level ice in the Beaufort Sea, from GURNARD data, constitutes between 35-60% of the total ice cover with a mean ice thickness of 3.0 m. The mean level ice was found to comprise 54.3% of this ice cover. The reader is cautioned that this figure was obtained from observations made during one

particular cruise and does not include temporal or spatial variations and may not be representative of long-term ice conditions in the Beaufort Sea.

4. Canadian Archipelago

The Canadian Archipelago is considered to be entirely a coastal region (Weeks et al., 1971). The many islands, straits, and channels have not been fully explored and many details concerning ice conditions in this region are generally unknown. An exception to this is the M'Clure Strait which was transited by two different submarines in 1960 in two different seasons, USS SARGO (winter) and USS SEADRAGON (summer). In addition, the entire western coastline of the Canadian Archipelago was skirted by the USS SARGO. With the inclusion of data points obtained by other submarines which have transited through this region bound for other Arctic locations, a reasonably good picture of sea ice conditions in this region is now available. Because it has similar ice characteristics, the Lincoln Sea, located at the northwestern edge of the Greenland land mass, has been included in this region.

The mean ice thickness for this region is 4.0 m (Table V), the largest mean ice thickness value found in any region of the Arctic. The standard deviation (2.7 m) is also the largest obtained for any of the Arctic regions. The large mean ice thickness and standard deviation values are representative of the large amounts of first-year and multi-year sea ice which have been piled up along the west coast of the Canadian Archipelago and the northern coast of Greenland producing extensive and highly variable rubbled ice fields. A histogram of mean ice thickness indicates that this region exhibits the most unique distribution of mean ice thickness found in the Arctic (Fig. 3.32). Two distinct peaks are noticed. The first is at 0-1 m which is

indicative of the large amounts of first-year ice which form seasonally in the straits and waterways of the southern islands. The second peak (6-7 m) illustrates the extensive amount of ridging and piling up of first-year and multi-year ice along the coastlines by the Beaufort Gyre and the Transpolar Drift Stream.

The histogram of pressure ridge keel depths (Figure 3.33) shows a distribution similar to that found elsewhere in the periphery of the Arctic basin with a dominant peak at 5-10 m which rapidly tails off to higher values. The unique feature of this region, however, arises in the pressure ridge frequency per unit distance which is the most dense of any of the Arctic subregions (Sater et al., 1971). This feature is illustrated in Figure 3.28 which was obtained from BIRDSEYE data. Weeks et al. (1971) referred to the Canadian Archipelago as the Canadian Basin in their study, from which Figure 3.28 was taken, and found that pressure ridges attained greater heights (>4 m) and a greater frequency of occurrence (>20 per nm) than observed in the Chukchi and Beaufort Seas.

The northern channels and waterways of the Canadian Archipelago remain ice-covered throughout the year. The mean ice thickness, determined in these areas by actual physical measurements, is 2.4 m (Sater et al., 1971). Within these channels and waterways the effects from the Arctic drift streams are not felt as strongly and pressure ridging is not as severe as that directly along the western Archipelago coast.

In the southern islands near the Canadian mainland, higher air temperatures and rivers which drain relatively warmer water into the waterways permit early melting in June and remain relatively ice free until October. Freezing begins again in October and by November the entire coast is effectively sealed with first-year ice cover (Sater et al.,

1971). Ice freezes rapidly in this portion of the Archipelago due to the inherent low tidal range which discourages mixing and encourages the rapid growth of fast ice (Sater et al., 1971). Leads occur frequently in the southern channels adjacent to river mouths and may persist for several days in the presence of a favorable offshore wind (Sater et al., 1971).

M'Clure Strait, a principal northwest passage sea route in the Canadian Archipelago, is a waterway in which submarine underice profiles have been made. These profiles were obtained by the USS SARGO in February 1960 and by the USS SEADRAGON in August 1960. Analysis of these profiles were made by McLaren et al. (1984) and provide a detailed description of ice conditions within this strait and the seasonal variations which occur. They found that the mean ice thickness changes dramatically from the western entrance to the strait (7.8 m, the highest recorded from submarine tracks in the Arctic) to the interior of the strait (4-5 m). Pressure ridging changed in a like manner with the heaviest, thickest ridging occurring at the Beaufort Sea entrance to the strait. This ice distribution pattern is probably due to the reduced effects of the Beaufort Gyre felt within the channel as compared to the extensive compression taking place on the west coast of the Canadian Archipelago as ice movement first becomes inhibited by the islands of the Archipelago (personal communication with McLaren, 1985). The ice in the strait is mostly first-year ice which is evidenced by the large amounts of open water observed in the summer and the increased number of pressure ridges observed in the winter. Polynyas were also more frequent in summer. The ranges of mean ice thickness and the depth of keel drafts observed from these two submarine cruises were similar to those determined from the combined underice data set.

Level ice statistics were also obtained from the SARGO and SEADRAGON data. An analysis by McLaren et al. (1984) gave percentages of level ice observed in the M'Clure Strait as 55.2% and 57.5% for winter and summer, respectively. Both of these values are indicative of the dominance of smooth first-year ice found within the confines of M'Clure Strait at the particular times of the two cruises. Wadhams (1980a) reports 27-40% of the ice in the heavily ridged areas of the Canadian Archipelago as level ice (mean ice thickness of 5 m). This illustrates the reduced amount of level ice that may observed in heavily ridged areas.

Polynyas and leads in the Canadian Archipelago are rarely observed in the heavily ridged fringes of the northwestern coastlines of the Archipelago and northern Greenland in both summer and winter. In the southern islands, polynyas are more frequent with large open water areas visible throughout the summer season.

5. Baffin Bay and Davis Strait

In the Baffin Bay/Davis Strait region sea ice conditions vary greatly from season to season. The warm water influx of the West Greenland Current generally keeps the shores of the southern half of western Greenland ice-free all year except in fjords (Wadhams et al., 1985). In contrast, the eastern coastlines of this region are characteristic of fast ice coupled with extensive floes of first-year ice throughout much of the winter (Sater et al., 1971). Virtually all of Baffin Bay and Davis Strait are free of pack ice in the summer. There are, however, icebergs present in the summer which are calved from the Greenland glaciers. In the winter this region experiences rapid growth of Arctic first-year ice which entirely covers the northern portion of Baffin Bay and covers major portions of Davis Strait along the eastern Canadian Archipelago. Strong

northerly currents create compacting forces in the ice pack and result in significant pressure ridging in the northern areas of Baffin Bay. Ridging occurring in Robeson Channel is so extensive that it remains ice covered through the summer. Although many leads and polynyas occur in this region during the winter, there is much fast ice and most harbors and inlets are covered with ice throughout the winter.

Most of the sea ice data available for this region are from a single submarine cruise to Davis Strait. In the winter of 1967 the USS QUEENFISH gathered 669 km of underice profile data from the Davis Strait. These data have been augmented with several other measurements from various submarines (SEADRAGON, BLUEFISH, PINTADO, and SILVERSIDES) which have transited this region. The mean sea ice thickness is 1.1 m with a standard deviation of 0.5 m (Table V). The QUEENFISH data alone yield a mean ice thickness of 1.0 m for Davis Strait (Wadhams et al., 1985). The distribution of mean ice thickness indicates that 75% of the ice is between 1-2 m (Fig. 3.34) although a review of the data points indicate that few segments are greater than 1.5 m in thickness. The analyzed Queenfish underice profile data indicate a level ice percentage of 83% (Wadhams et al., 1985). This distribution plainly shows the predominance of undeformed first-year ice in this region.

Pressure ridging is a common occurrence along the coasts of Baffin Bay and Davis Strait. However, ridges rarely build to exceptional heights (maximum is approximately 20 m) as keel drafts seldom exceed 10m (Figure 3.35). Larger keels may be present on a sporadic basis which result from icebergs surrounded by first-year ice in the winter (Wadhams et al., 1985).

Level ice in Davis Strait, as determined from SOVEREIGN data (Figure 3.36), constitutes 83% of the total

ice cover in those areas where the mean ice thickness is about 1.5 m (Wadhams et al., 1985). In the marginal ice zone where the mean ice thickness is 0.5 m, level ice accounts for 93-100% of the total ice cover.

Leads are common in Baffin Bay and Davis Strait, although many are small (about 5 m in width). Polynyas with 1 km widths are observed approximately every 5 km and occur throughout the region (Wadhams et al., 1985). Open water may occur, on an infrequent basis, in the extreme north of Baffin Bay due to shearing between the moving ice pack and the fast shore ice in winter (Sater et al., 1971). There is, however, no other recurring pattern (as yet discovered) to lead distribution and frequency indigenous to any particular area within this region.

6. Greenland Sea

This region includes the Greenland Sea, Denmark Strait, and Fram Strait. Due to the accessibility of this region many measurements and observations have been made of local ice conditions. Predominant among these are the underice profiles obtained by HMS SOVEREIGN during fall 1976 and spring 1979 (Wadhams 1981b, 1983a, 1983b; LeSchack, 1983). The track of the SOVEREIGN in October 1976 is shown in Figure 3.37. The location of mean ice thickness measurements in Figure 3.38 indicates the route taken by Sovereign in the spring of 1979.

Ice in the Greenland Sea exhibits greatly varying conditions from year to year and season to season. Because of the East Greenland Drift Stream which runs down the entire East Greenland coast, this region acts as the exit point for the heavy, thick multi-year pack ice of the central Arctic Basin. Intense ridging with large keels of multi-year ice occurs in the northern Greenland Sea and Fram Strait. Most areas in the northern Greenland Sea remain ice

covered throughout the year while areas to the south of Svalbard Island are generally ice free in the summer and fall. In milder years, the limit of pack ice in August may be as far north as 85°N (Sater et al., 1971). Fast ice is common throughout the year along the east coast of Greenland. Because of warmer conditions in the vicinity of Denmark Strait, keel depths decrease, mean ice thickness decreases, and first-year ice begins to dominate. The mean ice thickness in Denmark Strait varies from 0.8 m at the ice edge to 2.9 m towards the Greenland coast (Wadhams, 1981b). This represents a marked reduction in mean ice thickness from those values observed in Fram Strait where large amounts of thick multi-year ice exit the Arctic Basin. As the ice proceeds southward into Denmark Strait, it experiences melting and divergence which results in thinner mean ice in this area.

The peak at 0-1 m in the mean ice thickness distribution (Figure 3.39) is indicative of the large amounts of first-year ice present throughout this region which also includes the large marginal ice zone. The peak at 5-6 m is representative of the thick multi-year ice which exits from the central Arctic Basin through this region. The mean ice thickness of the Greenland Sea region is 2.7 m with a relatively large standard deviation (2.1 m) a result of the rather broad spectrum in Figure 3.39. The distribution of pressure ridge keel depths (Figure 3.40) for this region is representative of the general distribution of keel depths observed throughout much of the Arctic Ocean, i.e., most keels are of 5-10 m draft, but a substantial number do exceed 10 m.

The most interesting feature of this region is the general decrease in sea ice thickness and pressure ridge intensity from the northern and eastern coasts of Greenland towards the marginal ice zone which seasonally fluctuates to

the north and south of Svalbard. The ice distribution in the vicinity of Fram Strait (Figure 3.38) is derived from the cruise of HMS SOVEREIGN in the spring of 1979. Comparing Figure 3.38 to that of the Arctic Ocean spring mean ice thickness map (Figure 3.3) shows considerable consistency between that from an individual cruise and that based on many different spring cruises. The decrease in sea ice thickness is due to the ice cover in Fram Strait and Denmark Strait being greatly influenced by the influx of warm water from the south with subsequent melting of the ice pack. Similar features are also present in the fall (Wadhams, 1981b). In addition, Wadhams (1983b) concluded that the ice distribution pattern in Fram Strait is the result of ice originating from two sources. The ice exiting from the Arctic basin on the east side of Fram Strait is not related to that on the west side. The east side is characterized by young ice from the Siberian shelf while to the west the ice is older and more fragmented having originated in the central Arctic Basin.

Level ice observed in the Greenland Sea constitutes about 60% of the total ice cover as determined from analysis of the SOVEREIGN 1976 data (Figure 1.3). The mean ice thickness for this observation was 3.5 m (Wadhams, 1983a).

Polynyas and leads occur frequently in the Greenland Sea to the east of the fast ice located along the Greenland coast. Polynyas persist for days in this region and may open and close repeatedly. Wadhams (1981b) suggests that there are four areas in the Greenland Sea where polynyas occur on a frequent basis. These four areas are (Figure 3.19):

a.) the largest and widest polynya is found from just south of Nordostrundingen (81° 30' N) extending southward to Holms Land (80° 30' N) off the east Greenland coast, occurring frequently in winter and spring;

b.) the second polynya, not found in winter, is located off the southern part of Store Koldeway and extends to the north of Ile de France, 76-78° N;

c.) another polynya is found from Bass Rock southward to Jackson O, 73°30'-75° N; and

d.) a frequently occurring polynya in the mouth of Scoresby Sound.

7. Eurasian Seas

This region incorporates the areas of the Norwegian, Barents, Kara, Laptev, and East Siberian Seas. Analysis of these individual seas was done collectively due to the data sparse nature of these areas. Proximity to the Soviet Union has influenced this data paucity. The Norwegian Sea, although not included in this category, is mostly beyond the southern limits of observed sea ice. The ice which does occur in the northern portion of the Norwegian Sea is composed almost entirely of first-year ice and is limited to the winter season.

The Barents Sea is almost entirely ice-free during the summer. In the winter, because the Transpolar Drift Stream transports large quantities of muti-year pack ice to the east of Svalbard and into the Barents Sea, it is an area of highly variable ice conditions and ice thickness. Overall the Barents Sea is exceptionally ice-free when compared with the other peripheral seas of northern Siberia (Sater et al., 1971). This is a consequence of the warm Atlantic water which enters this area from the south. Wittman and Schule (1966), using BIRDSEYE data, estimated the winter composition of Barents Sea ice to be 58% multi-year ice, 23% thick winter ice (>1 m), and 18% new ice (<1 m). During the summer the composition was 40% multi-year ice, 22% thick winter ice, and 38% new ice. BIRDSEYE data

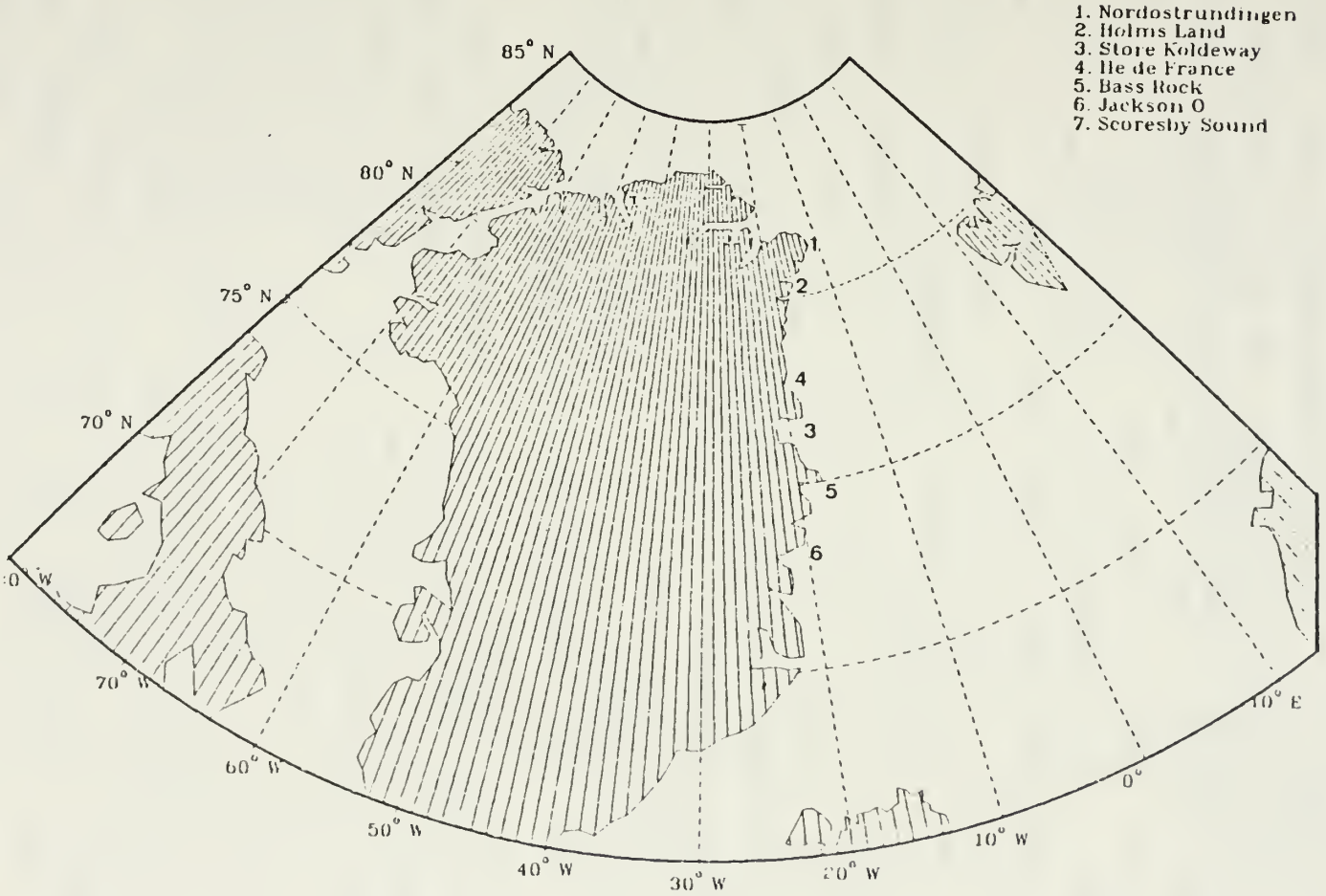

Figure 3.19 Location of regions of frequently occurring polynyas.

also provide an estimate of the pressure ridge frequency, 18 ridges per km (Wadhams, 1981b).

In the Kara, Laptev, and East Siberian Seas submarine underice profiles are limited to the outer portions of these seas. Although mean ice thickness values were calculated for the Laptev and Kara Seas as 2.5 m and 1.0 m, respectively (Table V), the number of observations for these areas was very small and as such may not provide a true depiction of mean ice values for the northern fringes of these seas. Ice conditions in the Laptev and East Siberian Seas are generally more severe than in any of the other peripheral seas off the north Asian coast (Sater et al., 1971). Sea ice forms rapidly in autumn due to rapidly falling water temperatures. A zone of pressure ridging, often exceeding 10 m in keel depth, is common along the periphery of the fast ice in these seas. A shear zone exists to the north of the New Siberian Islands, as a result of the movement between the Beaufort Gyre and the fast ice. Here the largest keel depths in the entire Arctic Ocean are found with keel depths of up to 42 m having been observed in this area (personal communication with McLaren, 1985).

Zubov (1943) provides a general discussion of the sea ice conditions within these three seas. In summer these areas are generally free of permanent ice cover. Sporadic occurrences of floating or drifting ice, having broken away from the Arctic ice pack to the north are, however, frequently seen. In the winter and spring seasons, young, thin, first-year ice (<1 m) typically covers the entire area of these essentially enclosed seas. In addition, the coastal harbors and channels are choked throughout much of the freezing season with fast ice which extends well southward into the coastal rivers and waterways. Infrequent

pressure ridging is also generally the rule thr ughout the Arctic winter as this newly formed ice becomes t e rejuvenating source of ridging and pack ice found in he central Arctic Basin. The ice is eventually carried ut by the Transpolar Drift Stream and the Beaufort Gyre a d incorporated into the Arctic Basin ice pack. Insuff cient data were available to make any judgements concerning he distribution and possibilities of reoccurrence of lea is in this region.

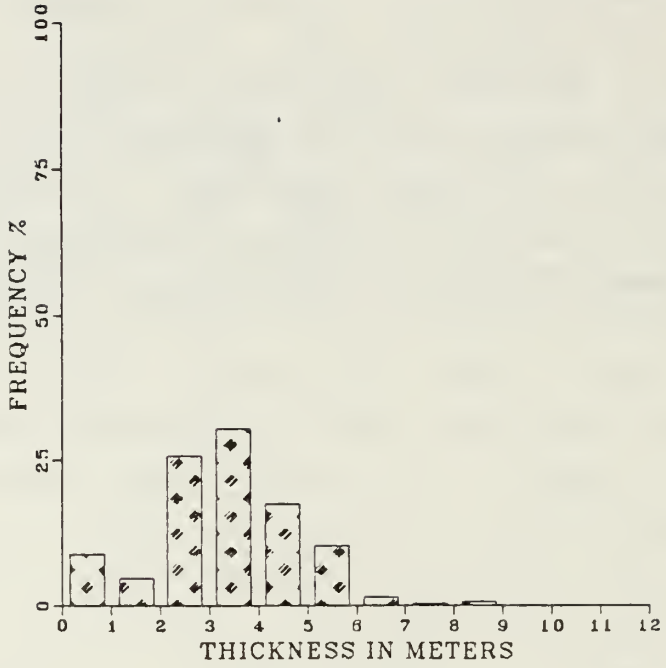

Figure 3.20 Frequency distribution of mean ice thickness in the Central Arctic Basin.

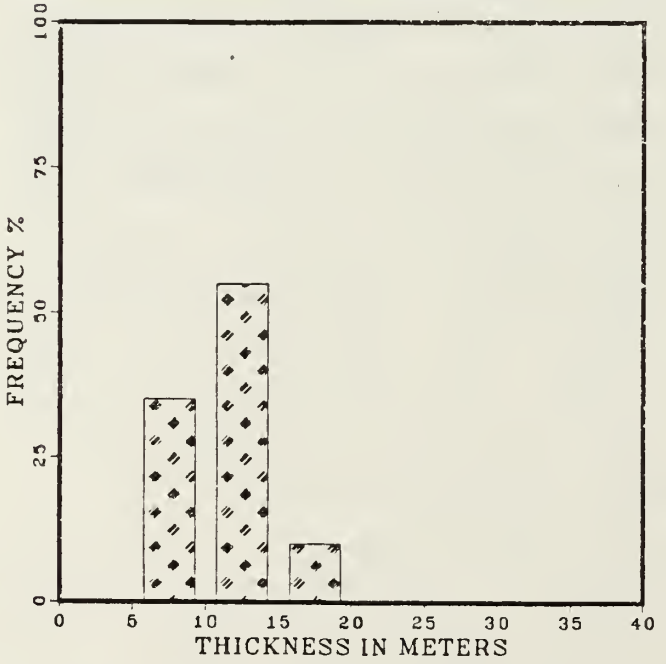

Figure 3.21 Percentage of keels of different drafts in the Central Arctic Basin.

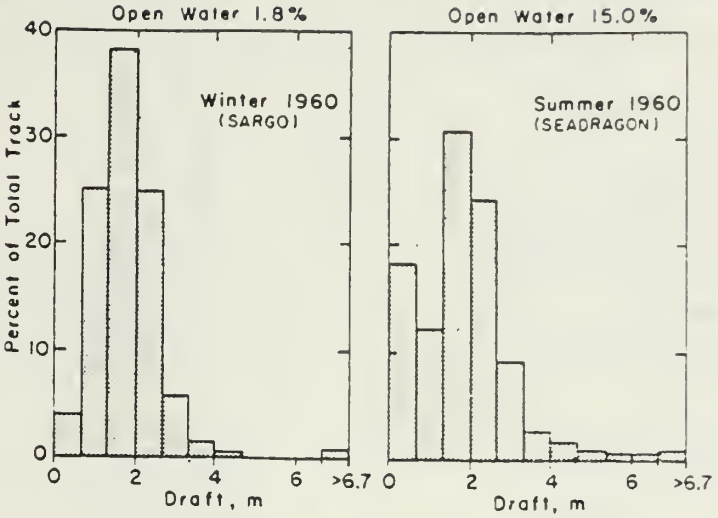

Figure 3.22 Histograms of sea ice drafts in the Central Arctic Basin (after Weeks et al., 1981).

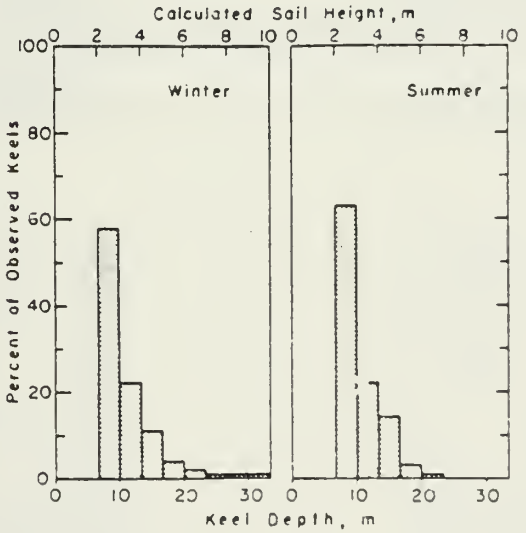

Figure 3.23 Percentage of keels of different drafts in the Central Arctic from 2 submarine cruises (after Weeks et al., 1981).

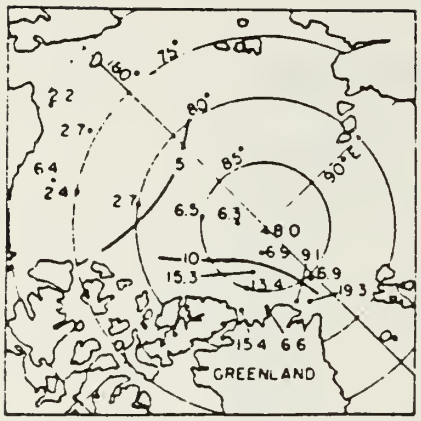

Nov. 1970

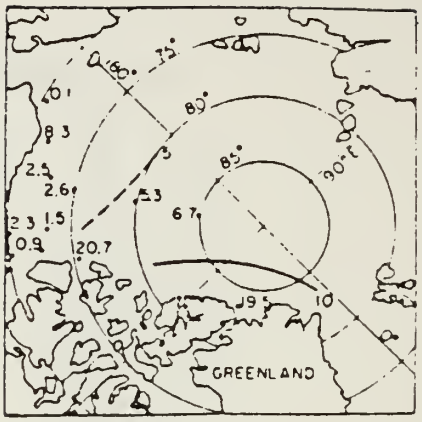

Jan. 1971

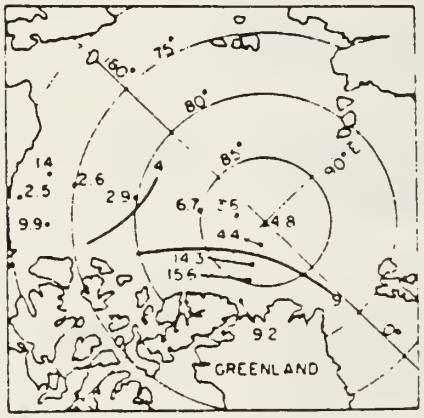

Mar. 1971

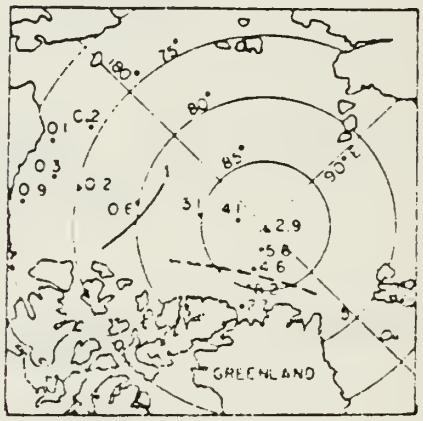

Oct. 1971

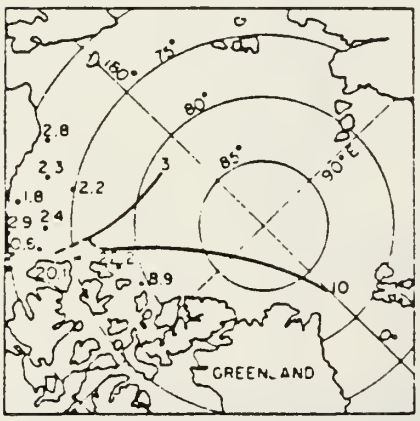

Mar. 1972

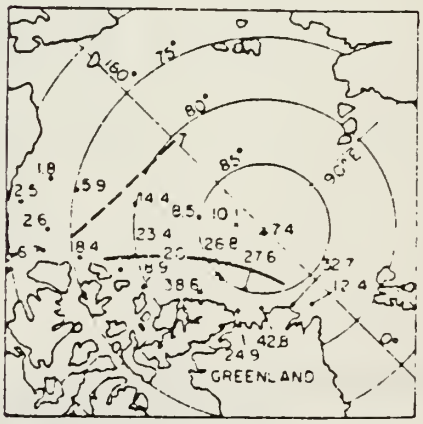

Feb. 1973

Figure 3.24 Regional variation in ridging intensity from the one-parameter model (after Hibler et al., 1974).

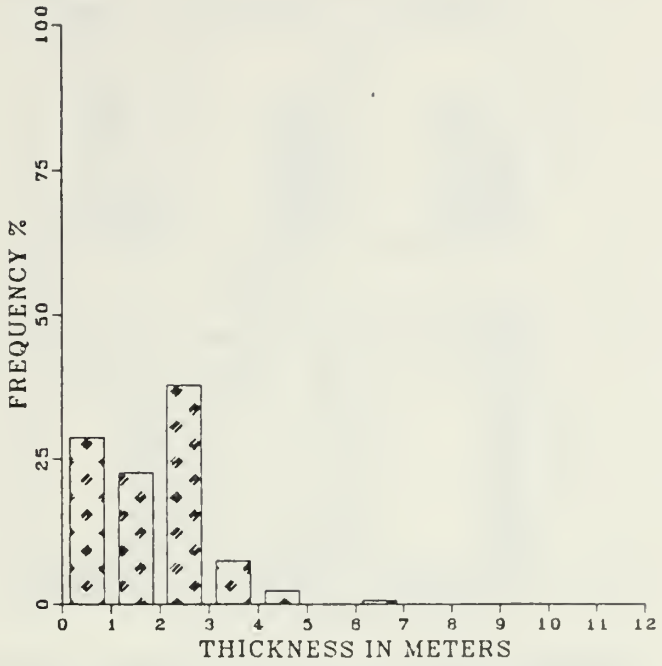

Figure 3.25 Frequency distribution of mean ice thickness in the Chukchi Sea.

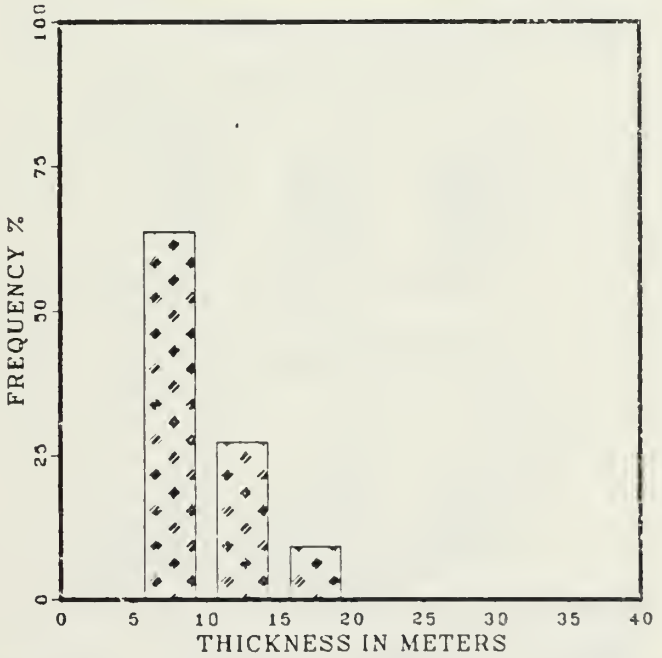

Figure 3.26 Percentage of keels of different drafts in the Chukchi Sea.

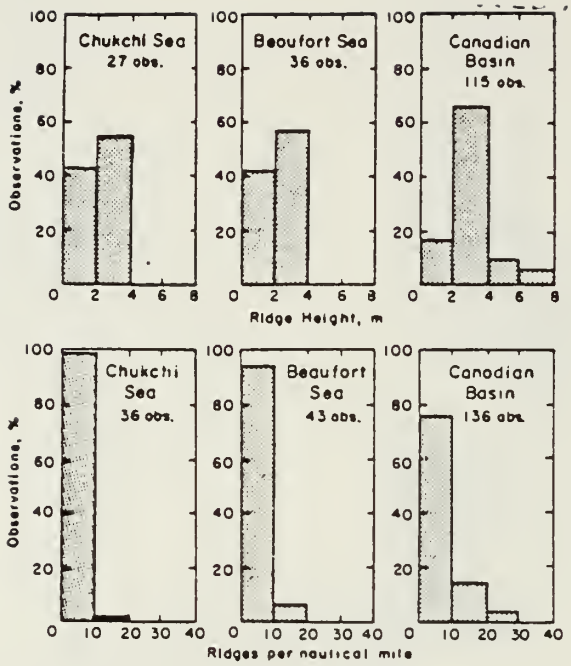

Figure 3.27 Summer frequencies of ridge heights and number of ridges per nautical mile (after Weeks et al., 1981).

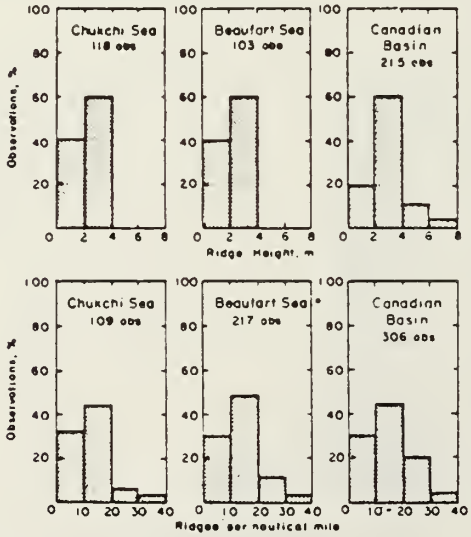

Figure 3.28 Winter frequencies of ridge heights and number of ridges per nautical mile (after Weeks et al., 1981).

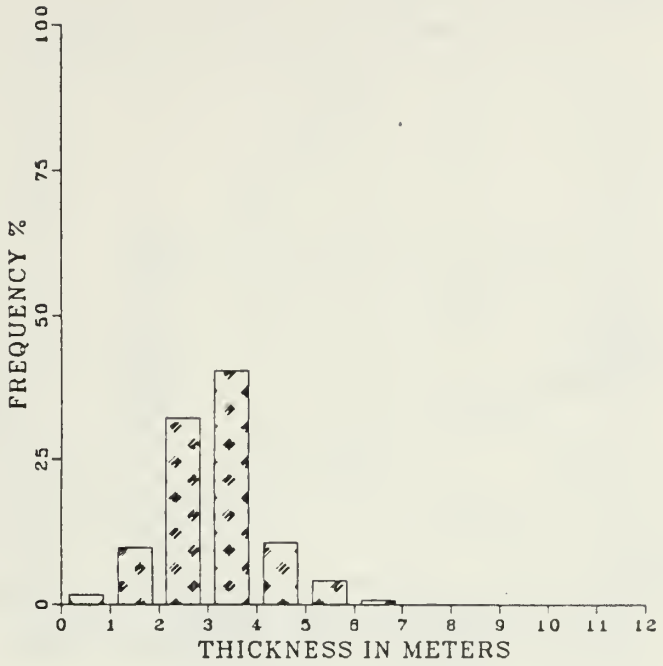

Figure 3.29 Frequency distribution of mean ice thickness in the Beaufort Sea.

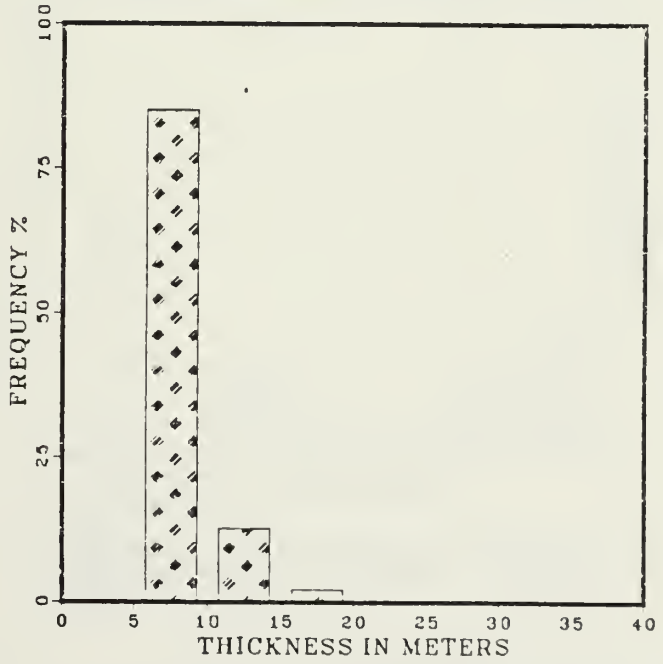

Figure 3.30 Percentage of keels of different drafts in the Beaufort Sea.

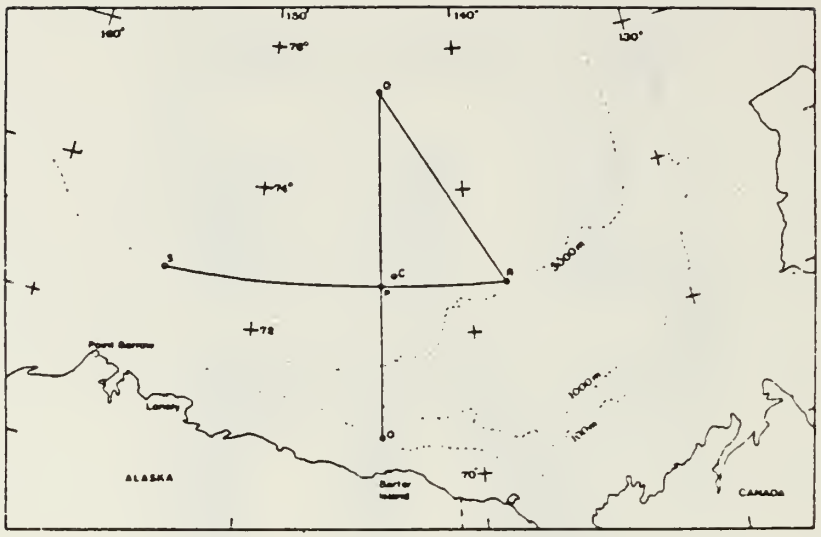

Figure 3.31 Route of the USS GURNARD, 7-10 April 1976 (after Wadhams and Horne, 1980).

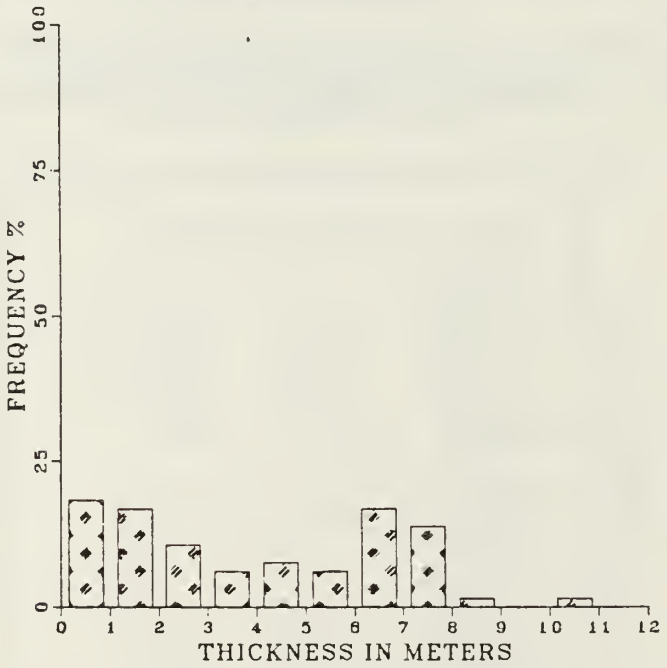

Figure 3.32 Frequency distribution of mean ice thickness in the Canadian Archipelago.

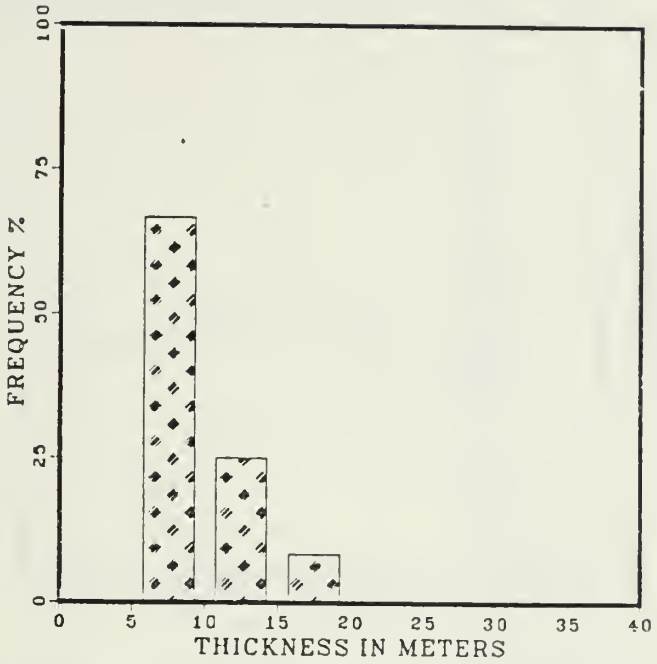

Figure 3.33 Percentage of keels of different drafts in the Canadian Archipelago.

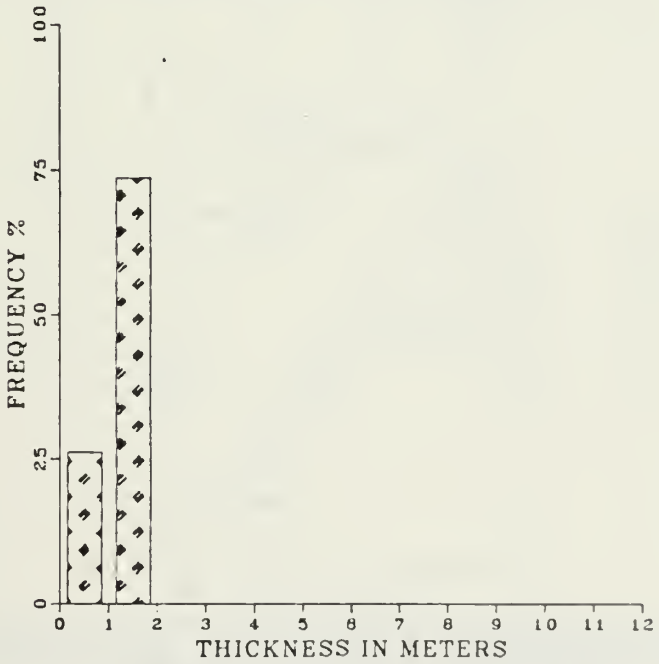

Figure 3.34 Frequency distribution of mean ice thickness in Baffin Bay and Davis Strait.

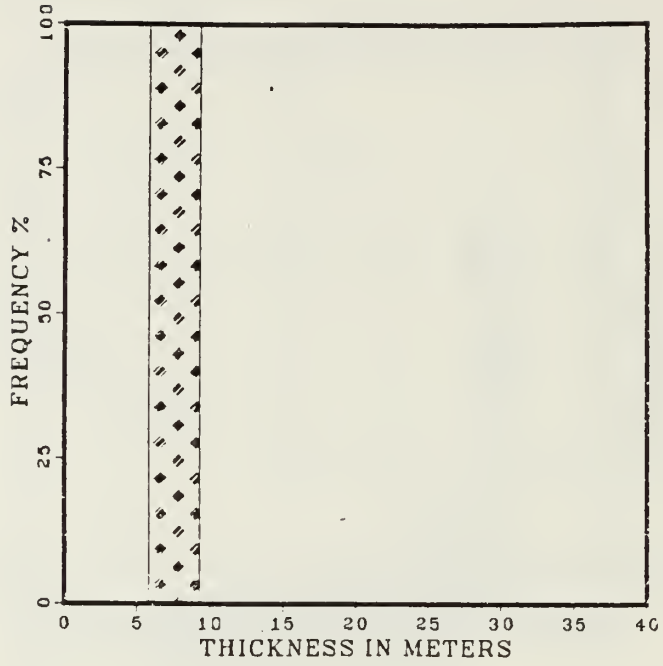

Figure 3.35 Percentage of keels of different drafts in Baffin Bay and Davis Strait.

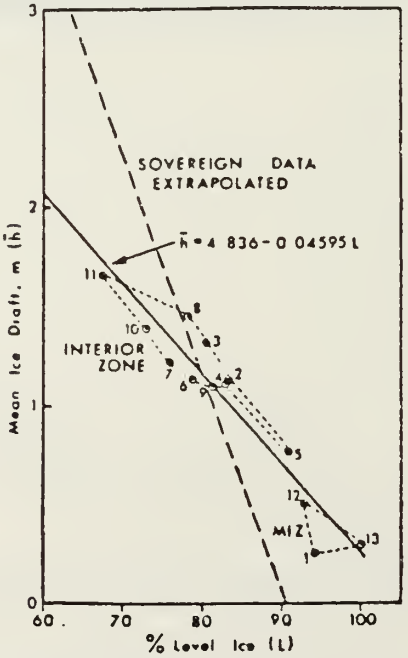

Figure 3.36 Percentage of level ice in Davis St. with respect to mean ice draft with linear regression (after Wadhams, 1985).

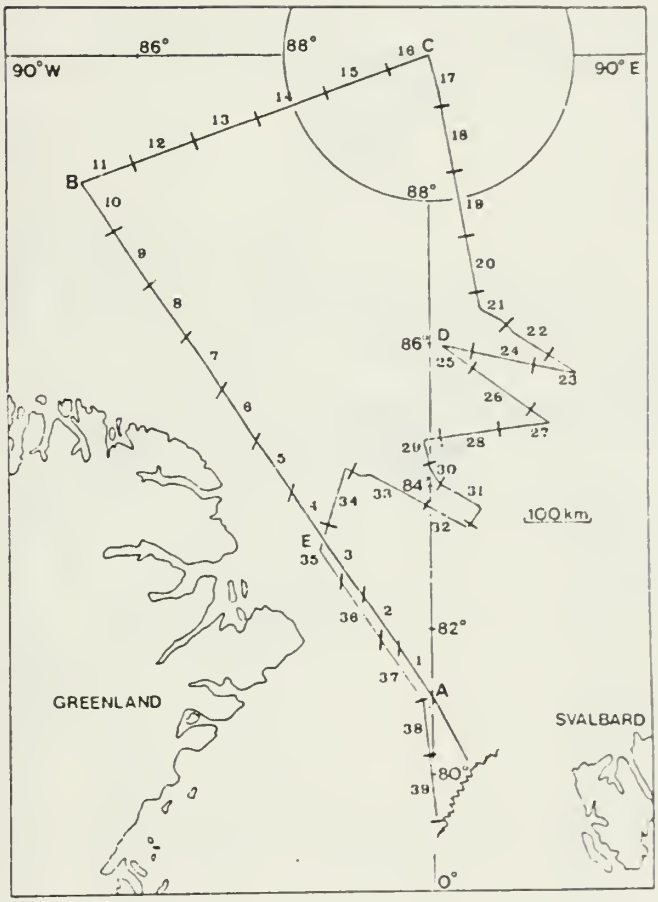

Figure 3.37 Track of HMS SOVEREIGN, October 1976. The numbers refer to the 100 km sections used by Wadhams (1981b).

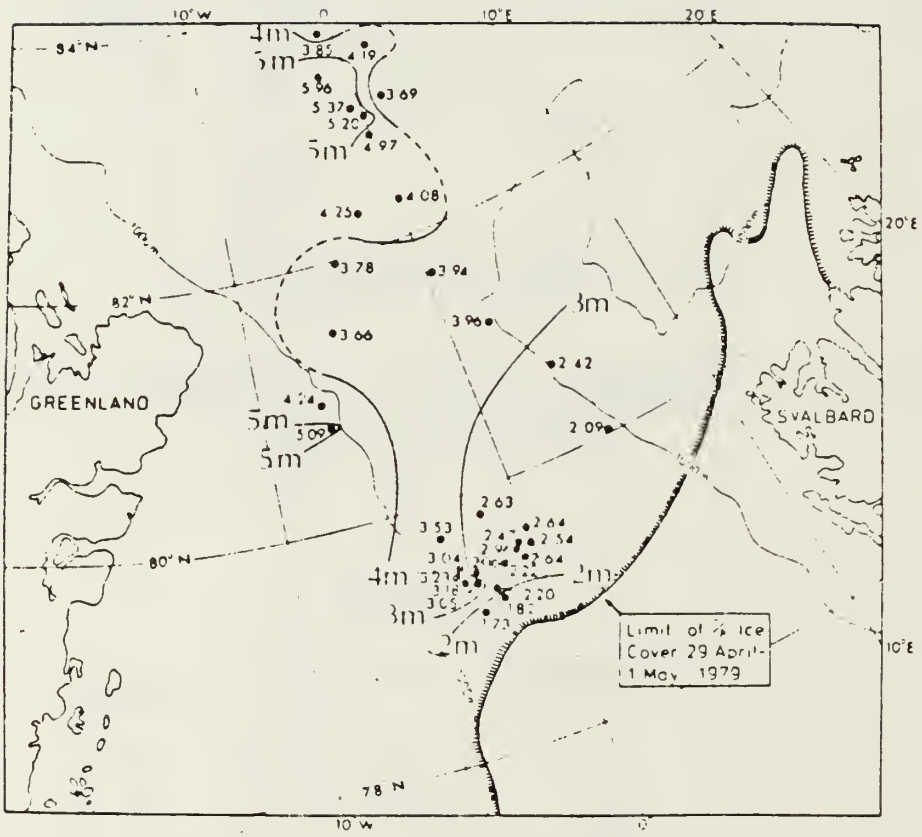

Figure 3.38 Contours of mean ice draft in Fram Strait in April-May 1979 (after Wadhams, 1981b).

Figure 3.39 Frequency distribution of mean ice thickness in the Greenland Sea.

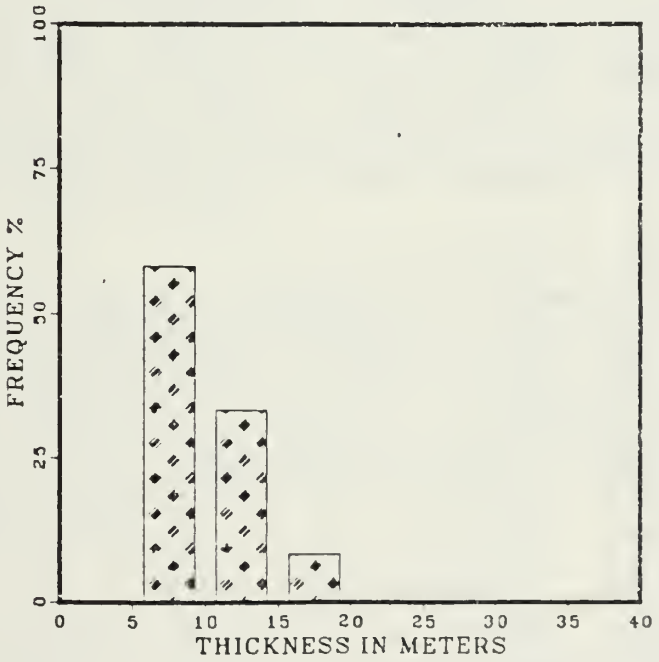

Figure 3.40 Percentage of keels of different drafts in the Greenland Sea.

IV. CONCLUSIONS

The results of this study permit insight concerning the temporal and spatial variability of mean sea ice thickness, pressure ridging, and polynya distribution in the Arctic Ocean and its peripheral seas. Caution should be taken, however, when using the values and observations determined from this study because sea ice conditions in the Arctic are highly variable. Because of the ever continuous motion of the ice, even an observation made by a submarine cruising under the ice may be substantially different from an observation made the previous day upon returning to the exact geographic location.

A summary of the findings of this study are:

1. The mean ice thickness of the entire Arctic Ocean, independent of season, and derived from all the analyzed submarine underice data sets, is 2.9 m. The overall mean ice thickness of the Arctic Ocean fluctuates from 2.4 m in spring to 3.3 m in summer illustrating the seasonal growth and ablation of first-year ice.

2. The regional mean ice thickness ranges from 1.0 m in the Kara Sea to 4.0 m in the Canadian Archipelago and north of Greenland. The mean ice thickness is generally thinner (<2.5 m) in the Siberian seas, Norwegian Sea, Denmark Strait, and Baffin and Davis Straits. Thicker mean ice (>2.5 m) is found in the Central Arctic Basin, Chukchi Sea, Beaufort Sea, Canadian Archipelago, and to the north of Greenland including Fram Strait. These regions containing thicker mean ice are where the Arctic drift streams and currents have

greater influence upon the movement of the ice. This type of distribution is visible throughout the year independent of season.

3. In winter and spring the mean sea ice thickness demonstrates a bimodal distribution depicting the presence of first-year and multi-year ice. A single peak occurs in summer and fall characteristic of the dominance of multi-year ice during the melt season.

4. The local mean ice thickness (based upon 50 to 100 km track lengths) varies from less than 1 m in the marginal ice zones to greater than 7 m along the west coast of the Canadian Archipelago and the north coast of Greenland.

5. Pressure ridging also varies between seasons and regions. Maximum pressure ridging occurs where the motion of the ice pack is influenced by the Arctic drift streams and piles up against land masses, e.g., the Canadian Archipelago. Minimum pressure ridging occurs in the Eurasian Seas where the Arctic drift streams move the ice away from the coasts and into the Central Arctic Basin.

6. Keel drafts do not vary substantially between seasons. They are generally protected from the smoothing and melting effects that pressure ridge sails experience on the surface of the ice. Large keels are, however, found in the same areas where extensive pressure ridging occurs.

APPENDIX A

SUBMARINE TRANSECT DATA FROM LESCHACK (1983)

LATITUDE	LONGITUDE	THICKNESS (M)	RIDGING (M)	MONTH	YEAR	COMMENT
		SARGO				
73.20N	174.60W	2.1	--	FEB	60	11.9% WATER
73.10N	174.60W	2.8	--	FEB	60	13.5% WATER
73.40N	176.20W	4.3	--	FEB	60	4.4% WATER
73.80N	176.40W	3.8	--	FEB	60	2.8% WATER
74.30N	177.30W	2.5	--	FEB	60	2.7% WATER
74.50N	178.90W	2.3	--	FEB	60	1.6% WATER
74.70N	179.50E	3.1	--	FEB	60	1.8% WATER
74.80N	177.80E	3.2	--	FEB	60	2.5% WATER
75.00N	176.20E	2.9	--	FEB	60	2.6% WATER
75.20N	174.80E	2.3	--	FEB	60	1.2% WATER
75.40N	172.90E	2.9	--	FEB	60	3.2% WATER
75.70N	174.00E	2.8	--	FEB	60	14.9% WATER
76.10N	175.40E	2.4	--	FEB	60	2.2% WATER
76.50N	176.50E	3.1	--	FEB	60	8.7% WATER
76.80N	179.30E	3.1	--	FEB	60	1.2% WATER
77.30N	179.30E	2.9	--	FEB	60	2.6% WATER
77.60N	179.00W	3.1	--	FEB	60	2.7% WATER
77.80N	177.00W	3.0	--	FEB	60	0.7% WATER
78.10N	174.90W	3.6	--	FEB	60	1.7% WATER
78.30N	175.50W	4.1	--	FEB	60	0.3% WATER
78.50N	176.30W	3.3	--	FEB	60	0.3% WATER
78.70N	177.30W	3.1	--	FEB	60	2.8% WATER
79.00N	179.00W	2.9	--	FEB	60	1.4% WATER
79.40N	179.00E	2.7	--	FEB	60	1.5% WATER
79.70N	176.80E	1.6	--	FEB	60	0.5% WATER
79.90N	174.10E	2.5	--	FEB	60	9.2% WATER
80.20N	172.00E	2.9	--	FEB	60	1.4% WATER
80.50N	169.60E	3.3	--	FEB	60	1.3% WATER
80.60N	166.50E	3.8	--	FEB	60	1.0% WATER
80.80N	163.50E	3.8	--	FEB	60	1.8% WATER
81.10N	160.60E	3.7	--	FEB	60	6.1% WATER
81.50N	163.00E	4.0	--	FEB	60	0.8% WATER
81.80N	166.50E	3.2	--	FEB	60	1.8% WATER
82.00N	170.00E	4.1	--	FEB	60	1.4% WATER
82.20N	174.00E	3.4	--	FEB	60	2.3% WATER
82.50N	177.00E	3.3	--	FEB	60	0.2% WATER
82.60N	179.00W	3.5	--	FEB	60	0.8% WATER
82.70N	175.00W	3.4	--	FEB	60	0.7% WATER
82.80N	171.00W	4.0	--	FEB	60	1.1% WATER
82.90N	167.00W	4.1	--	FEB	60	0.0% WATER
83.00N	162.50W	3.2	--	FEB	60	1.4% WATER
83.20N	159.00W	4.6	--	FEB	60	0.2% WATER
83.30N	156.00W	4.3	--	FEB	60	0.2% WATER
83.60N	158.00W	4.0	--	FEB	60	1.7% WATER
84.00N	161.00W	5.2	--	FEB	60	0.0% WATER
84.50N	164.00W	4.5	--	FEB	60	1.7% WATER
84.80N	166.00W	4.2	--	FEB	60	0.7% WATER
85.30N	168.00W	3.7	--	FEB	60	3.7% WATER
85.70N	171.00W	4.5	--	FEB	60	0.6% WATER
86.20N	170.00W	3.9	--	FEB	60	1.9% WATER
87.20N	170.00W	3.9	--	FEB	60	1.2% WATER
88.00N	170.00W	3.9	--	FEB	60	1.9% WATER
88.80N	170.00W	3.4	--	FEB	60	5.0% WATER
88.50N	105.00W	3.5	--	FEB	60	2.4% WATER
88.10N	107.00W	3.4	--	FEB	60	1.4% WATER

87.50N	103.00W	3.8	--	FEB	60	2.9% WATER
86.80N	102.00W	2.9	--	FEB	60	6.5% WATER
86.30N	100.00W	3.3	--	FEB	60	1.1% WATER
85.80N	099.00W	4.5	--	FEB	60	0.0% WATER
85.30N	098.00W	4.7	--	FEB	60	0.4% WATER
84.80N	097.00W	4.7	--	FEB	60	0.1% WATER
84.20N	097.00W	4.6	--	FEB	60	1.2% WATER
83.60N	096.00W	6.1	--	FEB	60	0.3% WATER
82.90N	095.00W	6.8	--	FEB	60	1.0% WATER
82.40N	095.00W	6.1	--	FEB	60	1.3% WATER
81.80N	095.00W	6.6	--	FEB	60	0.8% WATER
81.30N	096.00W	7.1	--	FEB	60	0.2% WATER
80.90N	098.00W	7.4	--	FEB	60	0.8% WATER
80.50N	100.00W	7.5	--	FEB	60	0.2% WATER
80.20N	105.50W	7.7	--	FEB	60	1.9% WATER
79.80N	105.50W	8.9	--	FEB	60	0.3% WATER
79.50N	108.10W	6.6	--	FEB	60	1.0% WATER
79.20N	110.50W	7.3	--	FEB	60	3.2% WATER
78.80N	111.70W	7.3	--	FEB	60	1.1% WATER
78.50N	114.70W	7.8	--	FEB	60	0.6% WATER
78.20N	116.70W	6.9	--	FEB	60	0.4% WATER
77.70N	118.50W	6.3	--	FEB	60	0.3% WATER
77.40N	120.30W	6.2	--	FEB	60	0.2% WATER
77.00N	122.00W	7.7	--	FEB	60	7.6% WATER
76.50N	123.70W	6.8	--	FEB	60	2.3% WATER
76.00N	125.70W	5.4	--	FEB	60	11.3% WATER
75.60N	124.40W	6.0	--	FEB	60	23.9% WATER
75.30N	122.90W	5.3	--	FEB	60	5.2% WATER
75.30N	122.20W	5.1	--	FEB	60	3.3% WATER
75.30N	125.00W	4.9	--	FEB	60	0.4% WATER
75.30N	126.50W	3.9	--	FEB	60	1.7% WATER
75.30N	128.20W	3.7	--	FEB	60	0.0% WATER
75.30N	130.00W	4.0	--	FEB	60	6.3% WATER
75.30N	131.60W	6.4	--	FEB	60	3.9% WATER
75.30N	133.30W	5.8	--	FEB	60	0.4% WATER
75.30N	135.00W	6.0	--	FEB	60	1.5% WATER
75.20N	136.50W	5.4	--	FEB	60	3.3% WATER
74.90N	137.70W	5.1	--	FEB	60	0.0% WATER
74.70N	139.00W	4.7	--	FEB	60	5.6% WATER
74.30N	140.20W	5.0	--	FEB	60	0.5% WATER
74.00N	141.40W	3.3	--	FEB	60	0.1% WATER
73.70N	142.50W	3.2	--	FEB	60	6.4% WATER
73.50N	143.60W	3.1	--	FEB	60	5.9% WATER
73.20N	144.60W	3.3	--	FEB	60	7.5% WATER
72.80N	145.50W	3.0	--	FEB	60	5.8% WATER
72.60N	146.40W	3.3	--	FEB	60	0.3% WATER
72.30N	147.40W	3.3	--	FEB	60	4.0% WATER
72.80N	165.60W	2.1	--	FEB	60	1.8% WATER
72.50N	166.00W	2.4	--	FEB	60	8.1% WATER
72.20N	166.30W	3.2	--	FEB	60	4.2% WATER

SEADRAGON

75.20N	127.50W	5.0	--	AUG	60	31.5% WATER
75.50N	129.00W	4.5	--	AUG	60	29.8% WATER
75.60N	130.60W	4.3	--	AUG	60	38.2% WATER
75.80N	132.00W	4.0	--	AUG	60	26.9% WATER
76.20N	133.00W	3.3	--	AUG	60	27.1% WATER
76.60N	133.50W	3.1	--	AUG	60	28.1% WATER
77.00N	134.00W	2.7	--	AUG	60	9.7% WATER
77.50N	134.70W	3.4	--	AUG	60	15.7% WATER
77.90N	135.40W	3.0	--	AUG	60	20.7% WATER
78.40N	134.60W	3.2	--	AUG	60	23.2% WATER
78.80N	133.00W	4.5	--	AUG	60	61.0% WATER
79.40N	131.00W	4.1	--	AUG	60	41.0% WATER
79.70N	129.00W	4.9	--	AUG	60	26.0% WATER
80.10N	126.00W	4.9	--	AUG	60	9.7% WATER
80.60N	127.00W	5.6	--	AUG	60	6.5% WATER
81.20N	130.50W	4.6	--	AUG	60	4.6% WATER

81.70N	134.00W	4.3	--	AUG	60	3.2%	WATER
82.20N	137.00W	3.8	--	AUG	60	3.3%	WATER
82.70N	138.00W	5.1	--	AUG	60	2.3%	WATER
83.20N	138.00W	5.1	--	AUG	60	3.4%	WATER
83.70N	134.00W	5.1	--	AUG	60	0.5%	WATER
84.10N	131.00W	4.8	--	AUG	60	1.6%	WATER
84.60N	128.00W	4.9	--	AUG	60	0.8%	WATER
85.00N	125.00W	4.2	--	AUG	60	1.1%	WATER
85.60N	125.00W	4.9	--	AUG	60	0.2%	WATER
86.50N	125.00W	4.5	--	AUG	60	1.3%	WATER
87.10N	125.00W	5.2	--	AUG	60	1.4%	WATER
87.70N	125.00W	4.4	--	AUG	60	0.7%	WATER
88.10N	125.00W	4.1	--	AUG	60	0.6%	WATER
88.80N	125.00W	4.3	--	AUG	60	0.6%	WATER
89.30N	125.00W	4.2	--	AUG	60	0.4%	WATER
90.00N	125.00W	3.8	--	AUG	60	2.5%	WATER
89.70N	000.00E	3.8	--	AUG	60	1.5%	WATER
89.40N	000.00E	3.5	--	AUG	60	0.1%	WATER
89.00N	000.00E	4.3	--	AUG	60	0.1%	WATER
89.00N	000.00E	4.2	--	AUG	60	0.7%	WATER
87.20N	090.00E	4.3	--	AUG	60	0.7%	WATER
86.50N	090.00E	4.6	--	AUG	60	0.5%	WATER
86.10N	090.00E	3.4	--	AUG	60	2.2%	WATER
85.30N	090.00E	2.6	--	AUG	60	1.7%	WATER
84.80N	095.00E	2.9	--	AUG	60	3.4%	WATER
84.50N	100.00E	2.9	--	AUG	60	10.3%	WATER
84.20N	104.00E	3.0	--	AUG	60	3.6%	WATER
83.70N	108.00E	2.9	--	AUG	60	24.2%	WATER
83.30N	112.00E	2.6	--	AUG	60	16.6%	WATER
82.90N	115.00E	2.5	--	AUG	60	7.5%	WATER
82.40N	118.00E	1.7	--	AUG	60	13.9%	WATER
81.70N	120.00E	1.4	--	AUG	60	42.8%	WATER
80.20N	126.50E	1.9	--	AUG	60	65.7%	WATER
80.00N	140.50E	3.9	--	AUG	60	27.1%	WATER
79.80N	143.50E	2.7	--	AUG	60	2.5%	WATER
79.70N	146.50E	3.1	--	AUG	60	2.4%	WATER
79.40N	149.50E	2.5	--	AUG	60	0.8%	WATER
79.10N	152.50E	2.9	--	AUG	60	1.9%	WATER
78.80N	155.00E	3.3	--	AUG	60	1.2%	WATER
78.40N	157.50E	2.3	--	AUG	60	3.4%	WATER
78.20N	159.50E	2.7	--	AUG	60	0.9%	WATER
77.80N	162.80E	3.5	--	AUG	60	0.3%	WATER
77.40N	165.50E	2.5	--	AUG	60	0.3%	WATER
77.10N	167.80E	2.9	--	AUG	60	2.7%	WATER
76.90N	170.00E	3.2	--	AUG	60	2.9%	WATER
76.70N	173.00E	2.6	--	AUG	60	1.6%	WATER
76.50N	179.80E	2.2	--	AUG	60	8.7%	WATER
76.30N	177.00E	3.1	--	AUG	60	1.1%	WATER
76.10N	178.60E	3.2	--	AUG	60	2.5%	WATER
75.90N	179.50W	3.4	--	AUG	60	0.5%	WATER
75.60N	177.50W	3.0	--	AUG	60	3.7%	WATER
75.30N	175.00W	4.2	--	SEP	60	0.7%	WATER

SEADRAGON

72.10N	167.00W	2.9	--	JUL	62	70.9%	WATER
73.40N	167.00W	3.1	--	JUL	62	18.5%	WATER
74.00N	167.00W	3.2	--	JUL	62	27.9%	WATER
74.70N	167.00W	2.4	--	JUL	62	74.3%	WATER
75.30N	167.00W	1.8	--	JUL	62	56.2%	WATER
76.00N	167.00W	2.2	--	JUL	62	11.4%	WATER
76.70N	167.00W	2.3	--	JUL	62	32.1%	WATER
77.30N	167.00W	2.3	--	JUL	62	42.7%	WATER
78.20N	169.30W	2.4	--	JUL	62	30.4%	WATER
78.70N	171.00W	2.2	--	JUL	62	13.8%	WATER
79.30N	173.00W	2.3	--	JUL	62	18.1%	WATER
79.70N	175.50W	2.3	--	JUL	62	37.1%	WATER
80.10N	177.60W	3.0	--	JUL	62	8.3%	WATER
80.60N	179.80E	2.9	--	JUL	62	14.7%	WATER

80.80N	176.00E	3.0	--	JUL	62	18.4% WATER
80.90N	171.50E	2.7	--	JUL	62	16.7% WATER
81.20N	167.00E	2.3	--	JUL	62	26.1% WATER
81.30N	162.50E	2.8	--	JUL	62	19.0% WATER
81.40N	159.00E	3.0	--	JUL	62	14.8% WATER
81.40N	155.00E	3.4	--	JUL	62	10.1% WATER
80.90N	150.00E	3.5	--	JUL	62	5.5% WATER
80.40N	146.00E	4.0	--	JUL	62	7.4% WATER
79.80N	142.20E	3.9	--	JUL	62	5.8% WATER
79.40N	139.80E	5.2	--	JUL	62	3.3% WATER
79.00N	137.80E	4.0	--	JUL	62	13.8% WATER
78.70N	135.90E	3.6	--	JUL	62	4.6% WATER
78.40N	133.80E	3.0	--	JUL	62	6.5% WATER
77.90N	132.00E	2.9	--	JUL	62	4.7% WATER
77.70N	129.70E	3.0	--	JUL	62	6.9% WATER
77.50N	127.00E	2.4	--	JUL	62	4.1% WATER
77.50N	127.00E	2.4	--	JUL	62	4.2% WATER
77.50N	127.00E	3.0	--	JUL	62	5.5% WATER
77.50N	127.00E	2.8	--	JUL	62	3.4% WATER
77.50N	127.00E	3.2	--	JUL	62	1.4% WATER
77.20N	125.50E	3.2	--	JUL	62	1.9% WATER
77.40N	124.00E	3.6	--	JUL	62	4.8% WATER
77.70N	121.90E	3.7	--	JUL	62	1.2% WATER
78.00N	119.80E	3.1	--	JUL	62	0.8% WATER
78.30N	117.60E	3.4	--	JUL	62	2.8% WATER
78.30N	114.00E	4.2	--	JUL	62	5.2% WATER
78.20N	111.00E	3.5	--	JUL	62	4.7% WATER
78.70N	109.80E	3.5	--	JUL	62	0.6% WATER
79.30N	108.70E	3.9	--	JUL	62	1.0% WATER
79.90N	107.40E	3.5	--	JUL	62	1.8% WATER
80.30N	107.00E	2.9	--	JUL	62	1.4% WATER
81.00N	106.00E	2.7	--	JUL	62	1.2% WATER
81.80N	105.00E	2.5	--	JUL	62	1.6% WATER
82.60N	105.00E	3.9	--	JUL	62	7.2% WATER
83.40N	105.00E	3.9	--	JUL	62	2.9% WATER
84.20N	105.00E	3.2	--	JUL	62	4.0% WATER
84.70N	105.00E	3.9	--	JUL	62	12.1% WATER
85.40N	105.00E	4.1	--	AUG	62	5.5% WATER
86.00N	106.00E	3.8	--	AUG	62	10.2% WATER
86.80N	106.00E	4.5	--	AUG	62	2.8% WATER
87.70N	107.00E	3.7	--	AUG	62	6.3% WATER
88.30N	107.00E	3.6	--	AUG	62	13.8% WATER
88.90N	105.00E	3.5	--	AUG	62	6.3% WATER
89.80N	105.00E	4.2	--	AUG	62	0.7% WATER
88.70N	165.00E	3.8	--	AUG	62	1.1% WATER
88.30N	168.00W	4.4	--	AUG	62	0.5% WATER
87.60N	152.00W	4.0	--	AUG	62	0.2% WATER
86.70N	144.00W	3.8	--	AUG	62	0.1% WATER
85.70N	139.50W	3.9	--	AUG	62	2.0% WATER
84.90N	137.00W	3.7	--	AUG	62	2.1% WATER
84.10N	137.50W	3.5	--	AUG	62	1.8% WATER
83.10N	138.00W	3.0	--	AUG	62	1.9% WATER
82.30N	138.00W	3.1	--	AUG	62	2.6% WATER
81.70N	139.50W	3.3	--	AUG	62	3.0% WATER
81.10N	141.50W	2.9	--	AUG	62	1.8% WATER
80.50N	142.50W	2.9	--	AUG	62	4.8% WATER
79.90N	142.70W	3.0	--	AUG	62	8.2% WATER
79.30N	143.30W	2.2	--	AUG	62	14.8% WATER
78.50N	144.00W	2.6	--	AUG	62	25.9% WATER
77.70N	144.70W	2.6	--	AUG	62	16.8% WATER
77.00N	145.00W	2.6	--	AUG	62	13.8% WATER
76.40N	145.30W	2.5	--	AUG	62	7.7% WATER
75.30N	143.50W	2.7	--	AUG	62	5.9% WATER
75.70N	141.70W	2.4	--	AUG	62	16.2% WATER
74.20N	140.20W	2.7	--	AUG	62	19.8% WATER
73.60N	139.00W	3.4	--	AUG	62	10.1% WATER
72.90N	137.70W	3.2	--	AUG	62	27.2% WATER
72.30N	136.20W	3.5	--	AUG	62	18.4% WATER
72.00N	136.00W	3.9	--	AUG	62	28.1% WATER

72.00N	136.00W	3.6	--	AUG	62	24.6%	WATER
72.00N	136.00W	3.7	--	AUG	62	22.7%	WATER
72.20N	134.70W	3.6	--	AUG	62	21.8%	WATER
72.00N	138.00W	3.7	--	AUG	62	19.2%	WATER
72.00N	138.00W	3.4	--	AUG	62	26.7%	WATER
72.00N	138.00W	4.7	--	AUG	62	32.9%	WATER
72.00N	138.00W	4.1	--	AUG	62	28.9%	WATER
72.00N	138.00W	3.9	--	AUG	62	30.0%	WATER
72.20N	139.50W	3.3	--	AUG	62	28.8%	WATER
72.00N	142.00W	3.0	--	AUG	62	26.4%	WATER
72.00N	142.00W	3.1	--	AUG	62	27.8%	WATER
72.00N	142.00W	3.1	--	AUG	62	20.3%	WATER
72.00N	142.00W	1.9	--	AUG	62	39.3%	WATER
72.00N	142.00W	2.2	--	AUG	62	27.5%	WATER
72.30N	144.30W	2.0	--	AUG	62	51.0%	WATER
72.20N	145.70W	1.4	--	AUG	62	88.6%	WATER

SKATE

82.70N	057.50W	4.5	--	JUL	62	9.7%	WATER
83.20N	055.50W	4.9	--	JUL	62	7.2%	WATER
83.60N	051.00W	5.7	--	JUL	62	1.8%	WATER
83.80N	047.00W	6.5	--	JUL	62	2.1%	WATER
84.30N	042.50W	6.0	--	JUL	62	1.3%	WATER
84.50N	032.50W	6.0	--	JUL	62	0.3%	WATER
84.70N	032.50W	6.1	--	JUL	62	0.3%	WATER
84.20N	005.00E	3.6	--	JUL	62	6.0%	WATER
84.30N	012.00E	3.7	--	JUL	62	2.3%	WATER
84.30N	019.00E	3.9	--	JUL	62	4.3%	WATER
84.00N	019.00E	3.8	--	JUL	62	1.6%	WATER
83.70N	017.50E	3.4	--	JUL	62	1.6%	WATER
83.50N	017.50E	4.0	--	JUL	62	1.7%	WATER
83.70N	028.00E	2.9	--	JUL	62	10.6%	WATER
83.50N	039.00E	3.2	--	JUL	62	9.2%	WATER
83.20N	049.00E	3.1	--	JUL	62	3.7%	WATER
82.20N	096.00E	3.2	--	JUL	62	9.3%	WATER
82.40N	098.00E	2.6	--	JUL	62	1.5%	WATER

SOVEREIGN

80.20N	070.00W	7.4	--	OCT	76	0.3%	WATER
85.50N	070.00W	7.2	--	OCT	76	0.2%	WATER
86.00N	070.00W	9.0	--	OCT	76	0.3%	WATER
86.50N	070.00W	6.5	--	OCT	76	1.0%	WATER
86.80N	070.00W	8.2	--	OCT	76	2.6%	WATER
87.30N	070.00W	5.6	--	OCT	76	3.5%	WATER
87.80N	070.00W	5.4	--	OCT	76	1.4%	WATER
88.50N	070.00W	5.1	--	OCT	76	0.8%	WATER
89.10N	070.00W	5.0	--	OCT	76	0.2%	WATER
89.50N	070.00W	5.3	--	OCT	76	0.0%	WATER
90.00N	070.00W	4.8	12.9**	OCT	76	0.5%	WATER
90.00N	070.00W	5.4	12.9**	OCT	76	0.1%	WATER
90.00N	010.00E	4.9	12.9**	OCT	76	0.3%	WATER
89.70N	010.00E	4.4	--	OCT	76	2.5%	WATER
89.30N	010.00E	5.1	--	OCT	76	0.5%	WATER
88.90N	010.00E	5.6	--	OCT	76	0.3%	WATER
88.40N	010.00E	5.9	--	OCT	76	0.2%	WATER
87.90N	010.00E	5.1	--	OCT	76	0.2%	WATER
87.50N	010.00E	5.0	--	OCT	76	0.7%	WATER
87.10N	010.00E	5.9	--	OCT	76	0.1%	WATER
86.50N	010.00E	6.0	--	OCT	76	0.0%	WATER
86.30N	013.00E	4.8	--	OCT	76	0.1%	WATER
85.90N	017.00E	5.8	--	OCT	76	0.2%	WATER
85.70N	020.00E	4.9	--	OCT	76	0.7%	WATER
85.50N	022.50E	5.0	--	OCT	76	0.1%	WATER
85.40N	022.00E	5.0	--	OCT	76	0.6%	WATER
85.60N	017.00E	5.2	--	OCT	76	0.4%	WATER
85.70N	011.00E	5.5	--	OCT	76	0.1%	WATER
85.90N	006.00E	6.2	--	OCT	76	0.0%	WATER

85.70N	006.00E	5.4	--	OCT	76	0.9%	WATER
85.50N	009.00E	6.3	--	OCT	76	0.0%	WATER
85.30N	012.00E	5.9	--	OCT	76	0.0%	WATER
84.80N	017.00E	5.3	--	OCT	76	0.2%	WATER
84.70N	016.00E	5.0	--	OCT	76	0.1%	WATER
84.70N	011.00E	5.5	--	OCT	76	0.0%	WATER
84.70N	007.00E	5.6	--	OCT	76	0.0%	WATER
84.70N	002.00E	5.5	--	OCT	76	0.0%	WATER
84.60N	001.00W	5.3	--	OCT	76	0.1%	WATER
84.40N	000.00W	5.5	--	OCT	76	0.1%	WATER
84.40N	000.00E	5.1	--	OCT	76	0.0%	WATER
84.10N	002.00E	5.1	--	OCT	76	0.6%	WATER
83.70N	005.00E	5.7	--	OCT	76	0.0%	WATER
83.40N	004.00E	5.5	--	OCT	76	2.3%	WATER
83.50N	002.00E	6.1	--	OCT	76	0.6%	WATER
84.00N	006.00W	6.3	--	OCT	76	0.0%	WATER
84.10N	009.00W	4.6	--	OCT	76	4.3%	WATER
83.10N	011.00W	7.2	--	OCT	76	0.2%	WATER
83.70N	012.00W	7.0	--	OCT	76	0.1%	WATER
83.20N	012.00W	7.8	--	OCT	76	0.0%	WATER
82.70N	011.00W	7.3	--	OCT	76	0.0%	WATER
82.30N	008.00W	6.3	--	OCT	76	0.3%	WATER
82.00N	006.00W	5.8	--	OCT	76	2.5%	WATER
81.60N	003.00W	5.6	--	OCT	76	0.7%	WATER
81.40N	002.00W	5.4	12.9**	OCT	76	0.0%	WATER
80.90N	001.00W	5.0	12.2**	OCT	76	6.0%	WATER
80.50N	001.00W	3.9	11.9**	OCT	76	4.0%	WATER

** NOTE 1: Keel draft data from Wadhams (1983b)

APPENDIX B

SUBMARINE TRANSECT DATA FROM WADHAMS

LATITUDE	LONGITUDE	THICKNESS (M)	RIDGING (M)	MONTH	YEAR	COMMENT
		SOVEREIGN				
79.00N	002.40W	1.7	--	APRIL	79	
79.10N	001.80W	1.8	--	APRIL	79	Note 1
79.15N	001.90W	2.2	--	APRIL	79	
79.30N	002.25W	3.1	--	APRIL	79	
79.32N	002.90W	3.2	--	APRIL	79	
79.40N	003.00W	3.2	--	APRIL	79	
79.50N	002.95W	3.0	--	APRIL	79	
79.35N	002.20W	2.1	--	APRIL	79	
79.30N	001.10W	2.2	--	APRIL	79	
79.32N	000.45W	2.6	--	APRIL	79	
79.50N	000.75W	3.0	--	APRIL	79	
79.55N	000.65W	2.5	--	APRIL	79	
79.50N	000.10W	2.5	--	APRIL	79	
79.60N	000.10W	2.6	--	APRIL	79	
79.80N	001.50W	2.6	--	APRIL	79	
79.75N	003.10W	3.5	--	APRIL	79	
80.00N	005.00E	2.1	--	MAY	79	EARLY MAY
80.60N	003.00E	2.4	--	MAY	79	
80.80N	006.20W	5.1	--	MAY	79	
80.95N	006.50W	4.2	--	MAY	79	
81.25N	002.00E	4.0	--	MAY	79	
81.70N	000.20E	3.9	--	MAY	79	
81.50N	005.00W	3.7	--	MAY	79	
82.00N	004.00W	3.8	--	MAY	79	
82.25N	002.20W	4.3	--	MAY	79	
82.30N	000.00E	4.1	--	MAY	79	
82.80N	000.00E	5.0	--	MAY	79	
82.95N	000.00E	5.2	--	MAY	79	
83.10N	000.80W	5.4	--	MAY	79	
83.15N	002.00E	3.7	--	MAY	79	
83.35N	002.00W	6.0	--	MAY	79	
83.50N	002.00E	4.2	--	MAY	79	
83.80N	001.00W	3.9	--	MAY	79	
		GURNARD				
71.05N	144.22W	5.1	8.6	APRIL	76	
71.51N	144.23W	4.2	8.3	APRIL	76	Note 2
71.98N	144.24W	3.8	7.7	APRIL	76	
72.42N	144.25W	4.1	7.6	APRIL	76	
72.87N	144.30W	3.9	7.8	APRIL	76	
73.33N	144.30W	3.5	7.6	APRIL	76	
73.80N	144.33W	3.2	7.4	APRIL	76	
74.27N	144.37W	3.4	7.2	APRIL	76	
74.73N	144.37W	3.6	7.4	APRIL	76	
75.13N	144.37W	3.5	7.5	APRIL	76	
75.26N	143.79W	3.4	7.3	APRIL	76	
74.87N	142.80W	3.7	7.6	APRIL	76	
74.26N	141.33W	3.7	7.6	APRIL	76	
73.87N	140.42W	3.8	7.7	APRIL	76	
73.43N	139.54W	3.5	7.3	APRIL	76	
73.07N	138.73W	3.4	7.4	APRIL	76	
72.67N	138.25W	3.9	7.8	APRIL	76	
72.68N	139.83W	3.9	7.6	APRIL	76	
72.69N	141.43W	3.6	7.5	APRIL	76	

72.71N	142.93W	3.7	7.5	APRIL	76	
72.75N	144.44W	3.5	7.5	APRIL	76	
72.72N	146.39W	3.5	7.7	APRIL	76	
72.71N	147.98W	4.1	7.6	APRIL	76	
72.70N	149.53W	3.6	7.5	APRIL	76	
72.69N	151.04W	4.2	7.7	APRIL	76	
72.70N	152.65W	4.5	8.3	APRIL	76	
72.72N	154.24W	4.6	8.4	APRIL	76	

QUEENFISH

63.25N	059.17W	0.3	--	FEB	67	
63.60N	059.50W	1.1	7.5	FEB	67	Note 3
63.95N	059.38W	1.3	6.2	FEB	67	
64.30N	059.03W	1.1	6.9	FEB	67	
64.57N	059.17W	0.7	6.9	FEB	67	
64.15N	059.01W	1.1	7.2	FEB	67	
63.62N	058.87W	1.2	6.4	FEB	67	
63.30N	059.22W	1.5	7.1	FEB	67	
62.98N	060.00W	1.1	7.2	FEB	67	
62.62N	060.58W	1.4	6.8	FEB	67	
62.33N	060.08W	1.7	6.5	FEB	67	
62.08N	059.47W	0.5	5.7	FEB	67	
61.82N	058.52W	0.3	--	FEB	67	

NOTE 1: Submarine data obtained from Wadhams (1983b)
NOTE 2: Submarine data obtained from Wadhams and Horne (1980)
NOTE 3: Submarine data obtained from Wadhams and others (1985)

APPENDIX C

MEAN ICE THICKNESS AND KEEL DRAFT MAPS.

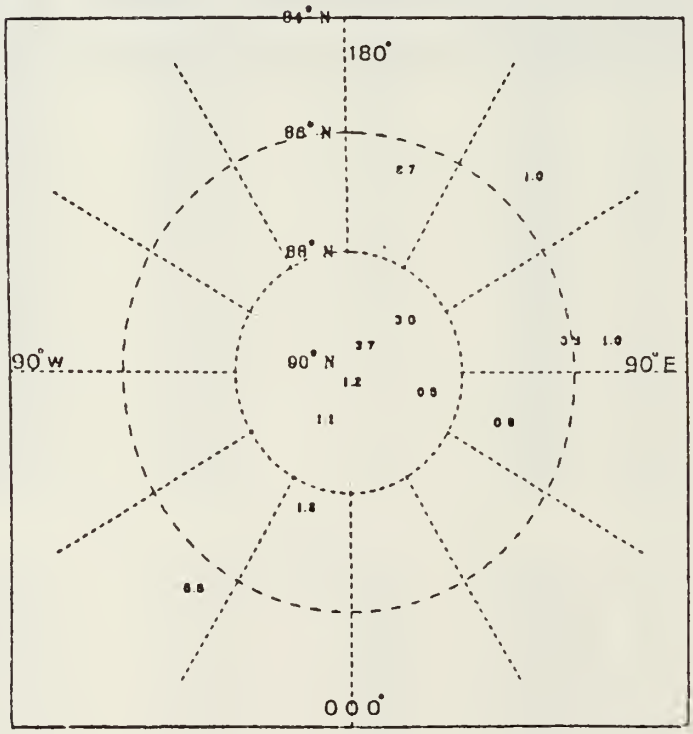

Figure C.1 Mean ice thickness(m) in spring, 84°N-90°N.

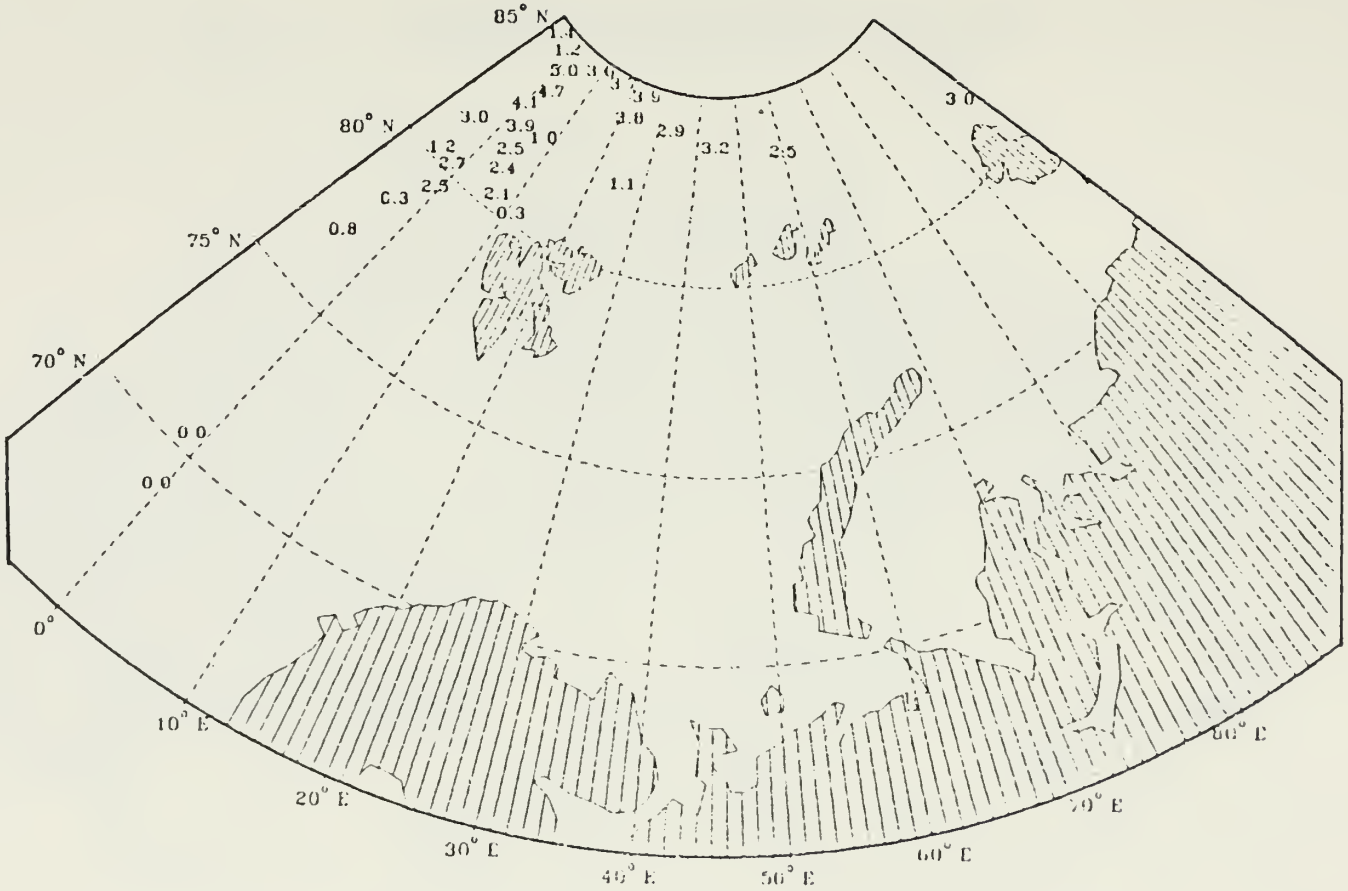

Figure C.2 Mean ice thickness(m) in spring, 65°N-85°N, 010°W-100°E.

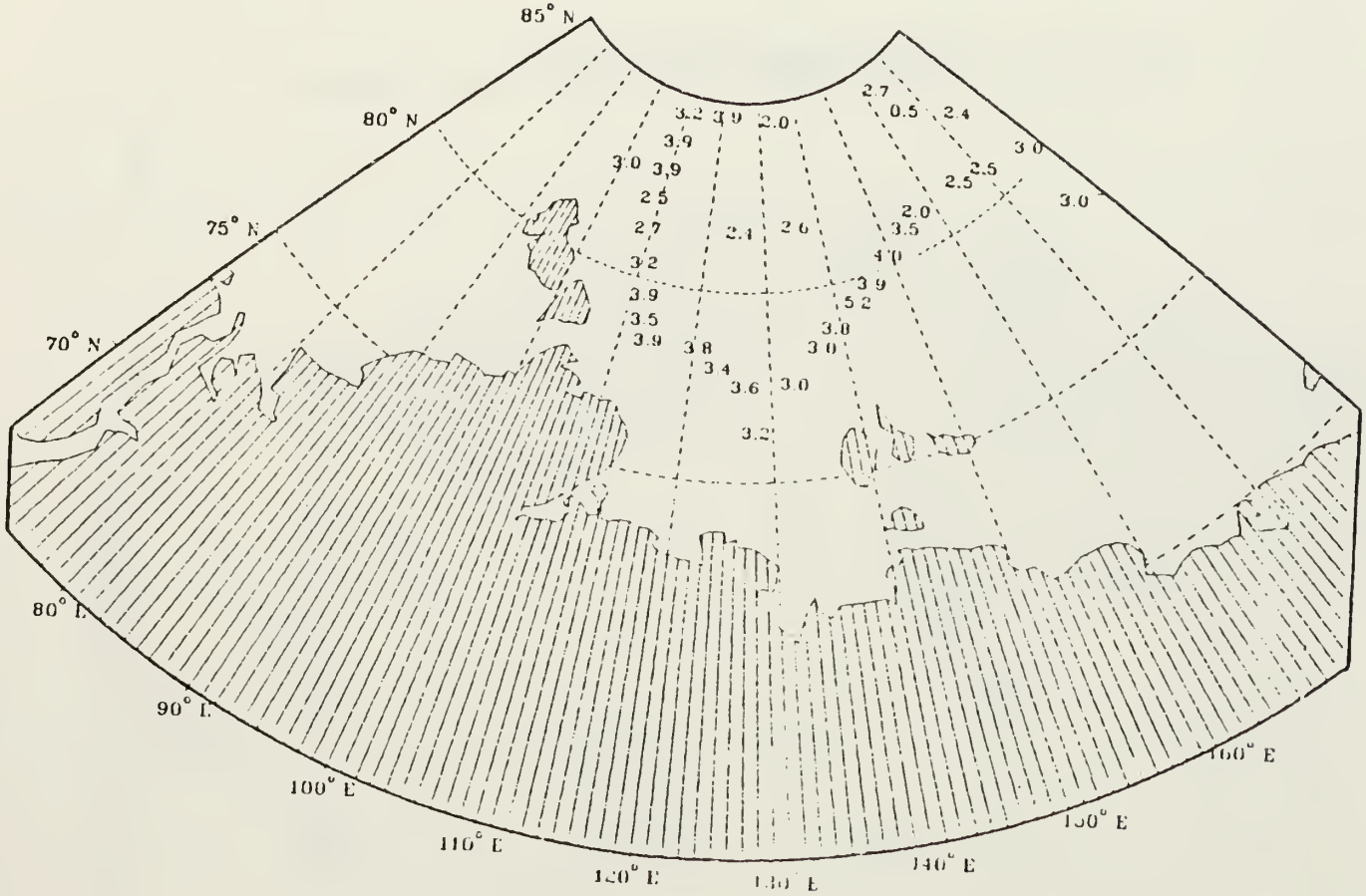

Figure C.3 Mean ice thickness(m) in spring, 65°N-85°N, 070°E-180°E.

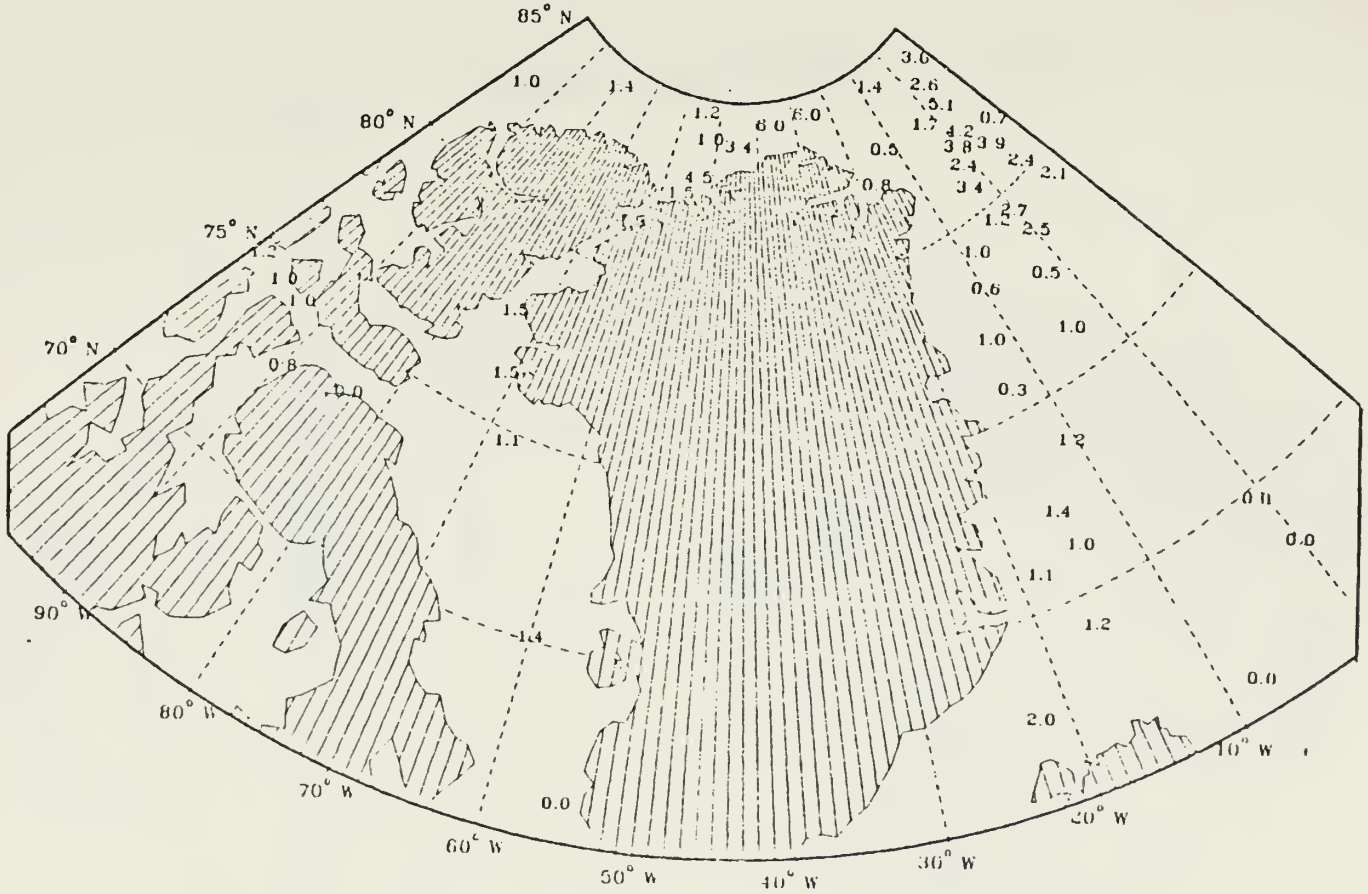

Figure C.4 Mean ice thickness(m) in spring, 65°N-85°N, 100°W-010°E.

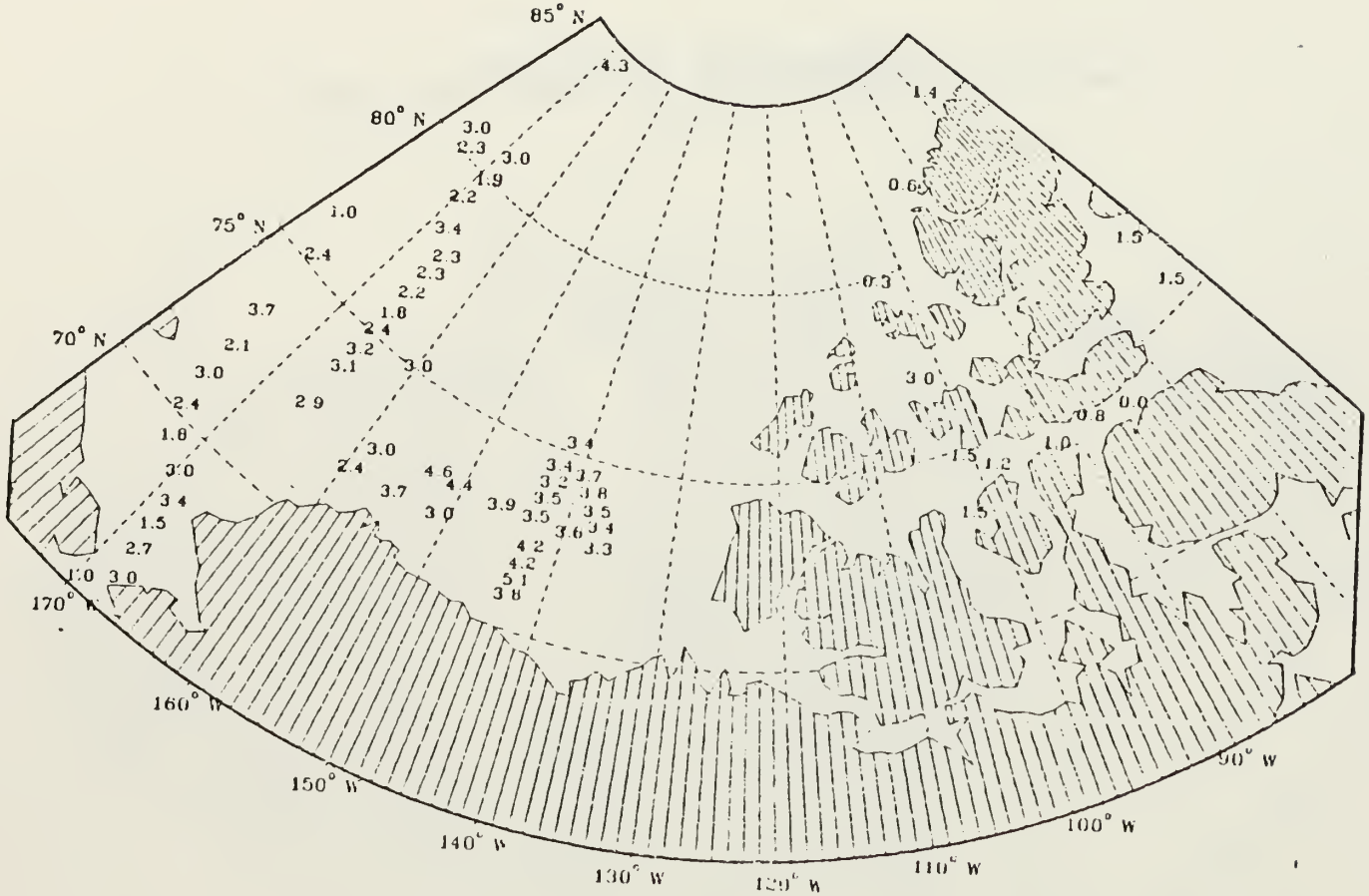

Figure C.5 Mean ice thickness(m) in spring, 65°N-85°N, 180°W-070°W.

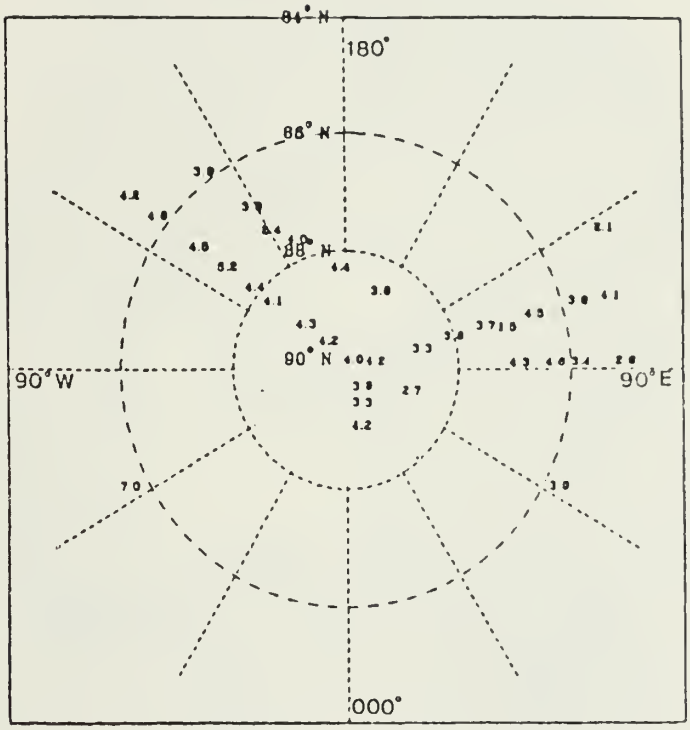

Figure C.6 Mean ice thickness(m) in summer, 84°N-90°N.

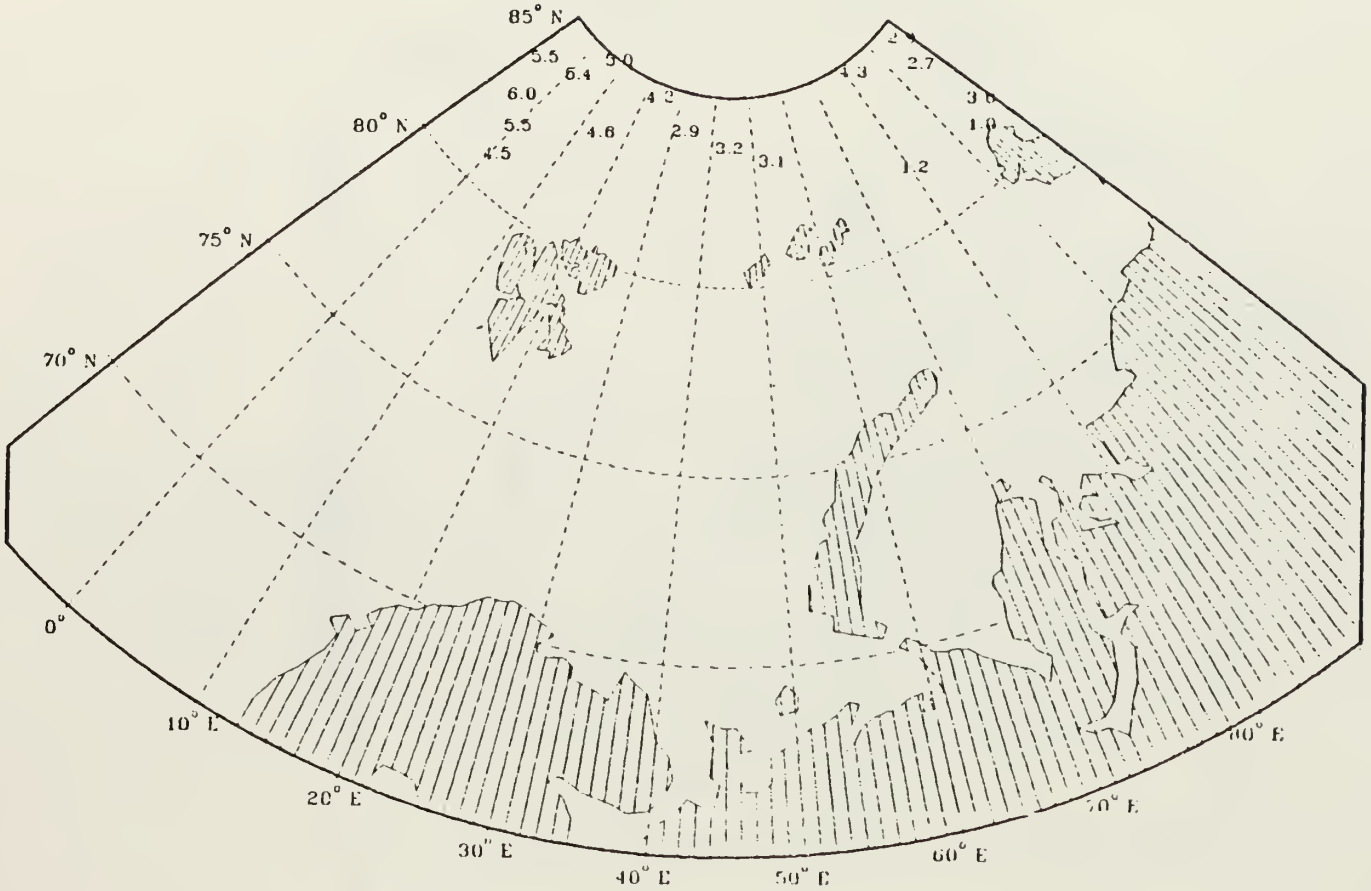

Figure C.7 Mean ice thickness(m) in summer, 65°N-85°N, 010°W-100°E.

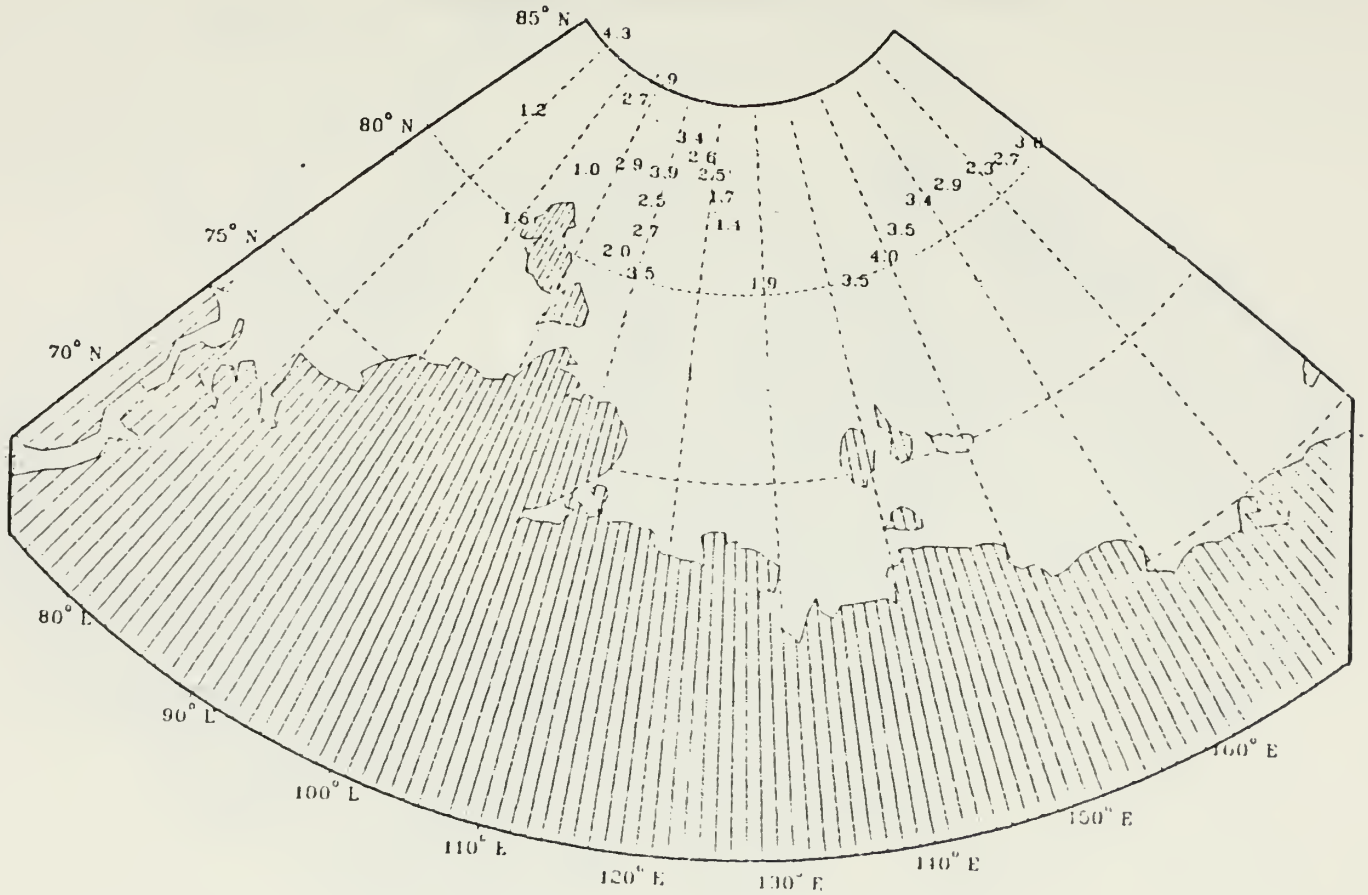

Figure C.8 Mean ice thickness(m) in summer, 65°N-85°N, 070°E-180°E.

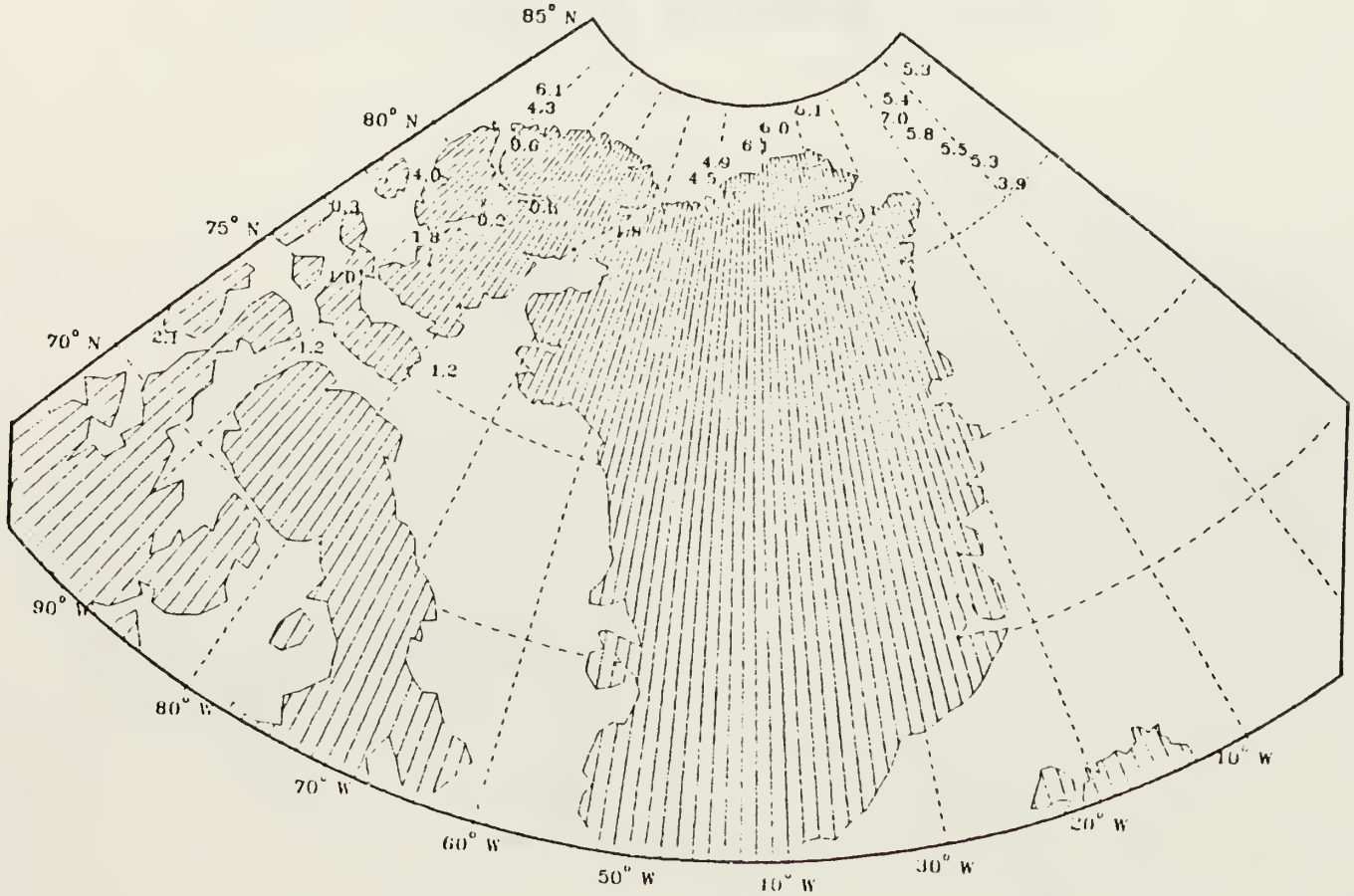

Figure C.9 Mean ice thickness(m) in summer, 65°N-85°N, 100°W-010°E.

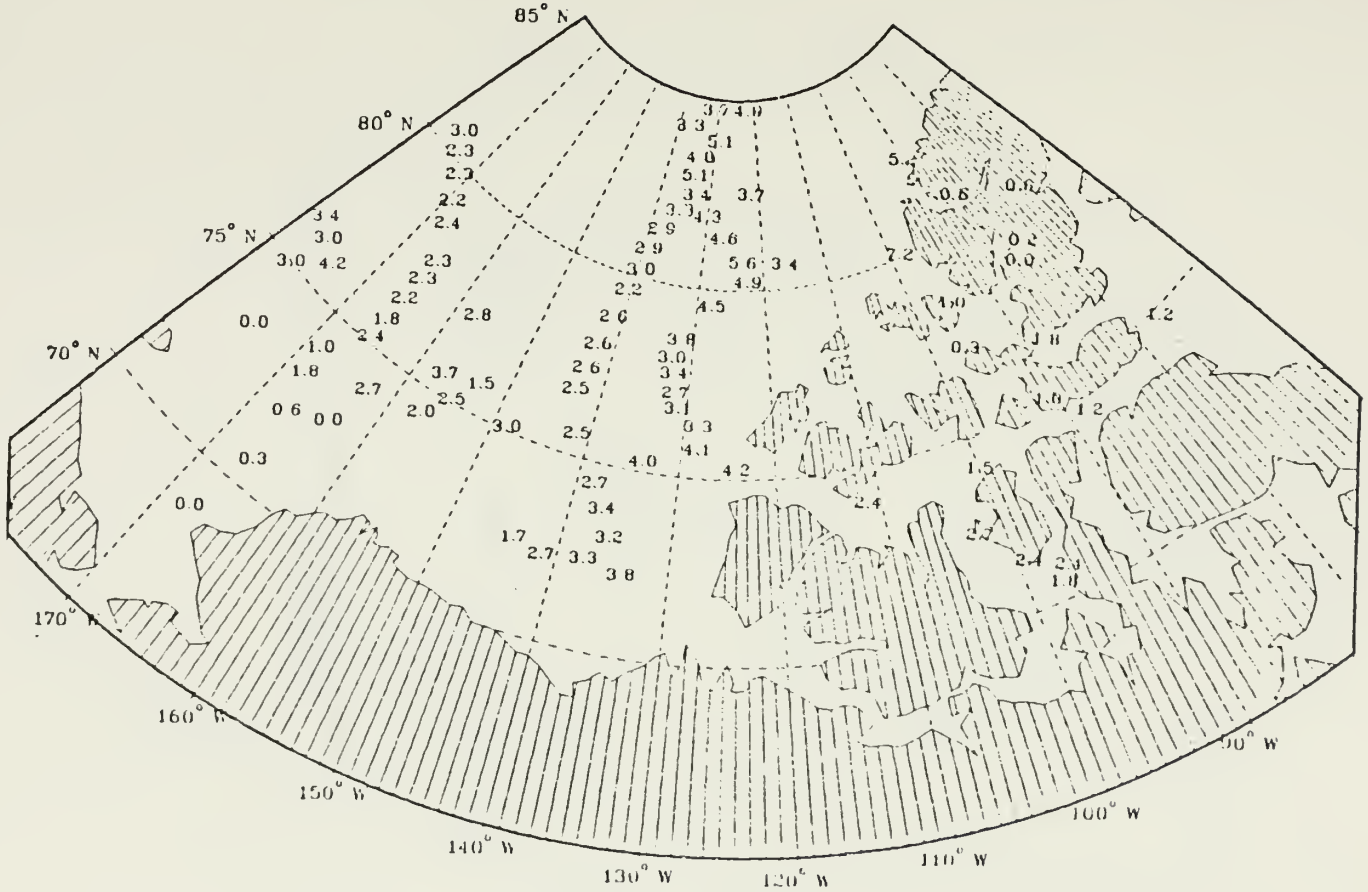

Figure C.10 Mean ice thickness(m) in summer, 65°N-85°N, 180°W-070°W.

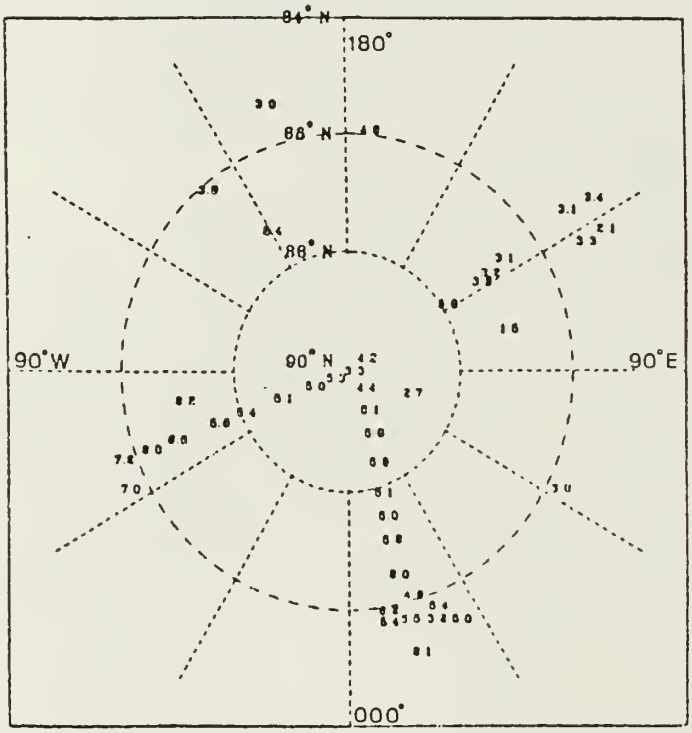

Figure C.11 Mean ice thickness(m) in autumn, $84^{o}N-90^{o}N$.

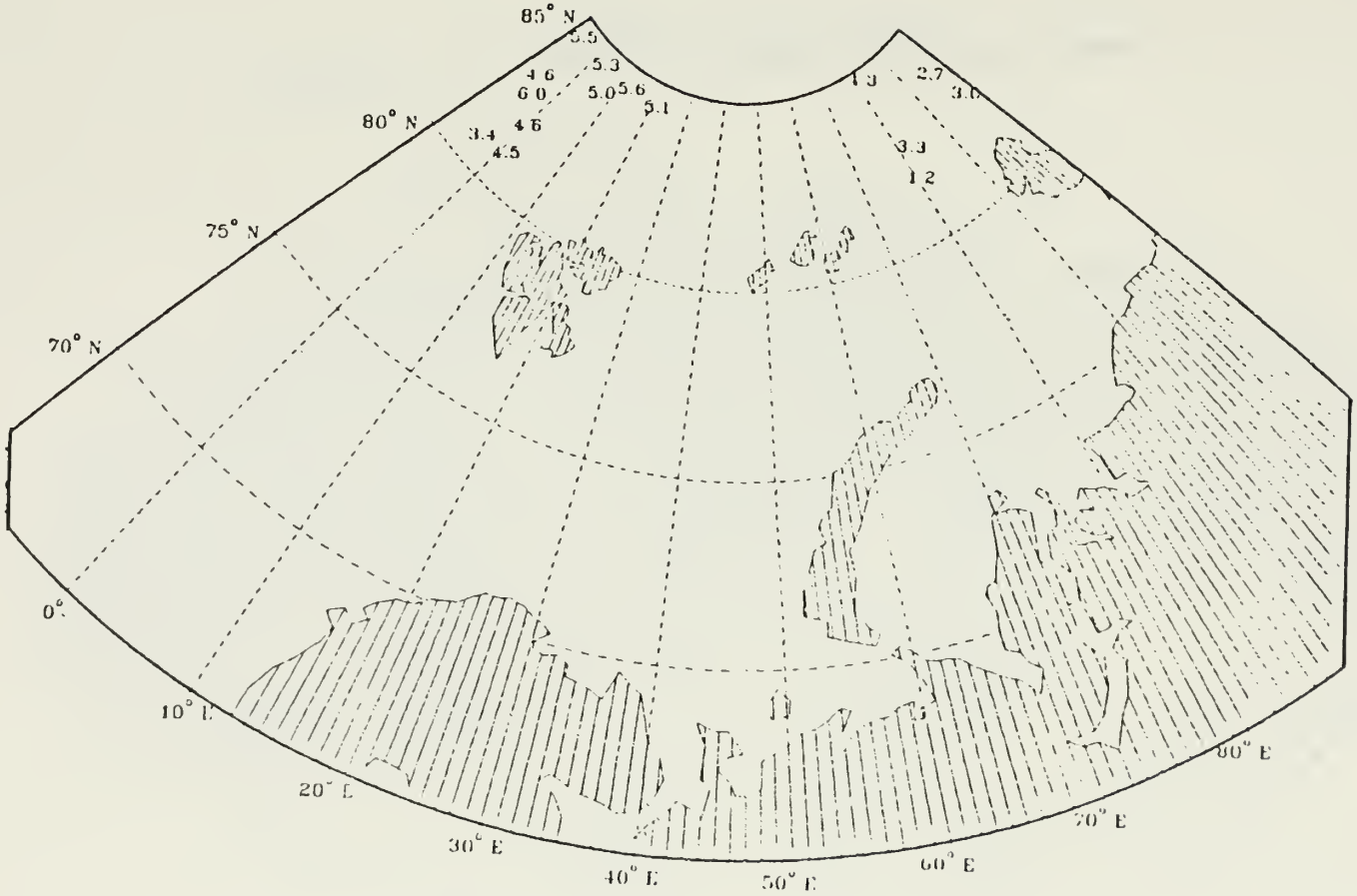

Figure C.12 Mean ice thickness(m) in autumn, 65°N-85°N, 010°E-100°E.

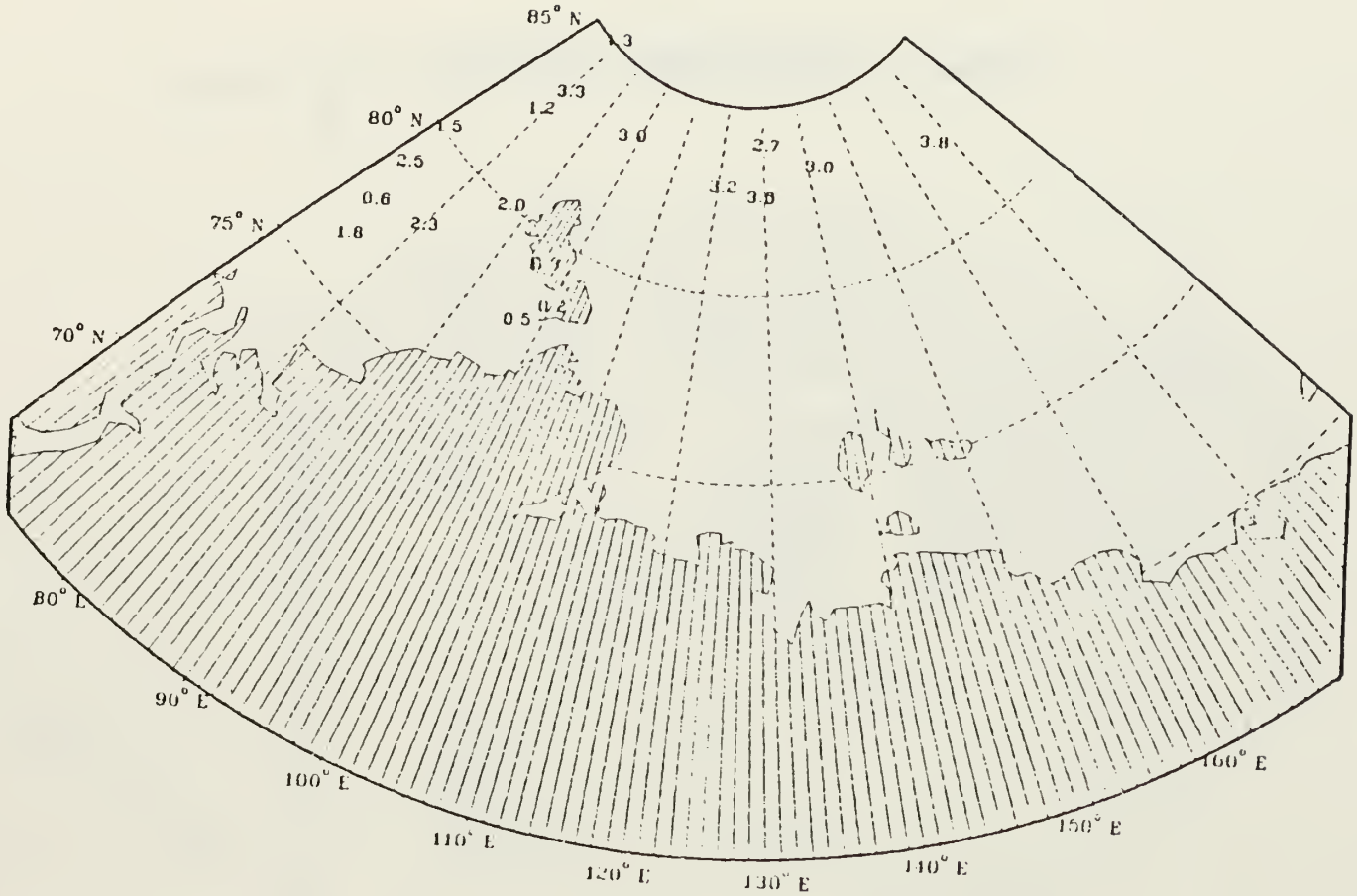

Figure C.13 Mean ice thickness(m) in autumn, 65°N-85°N, 070°E-180°E.

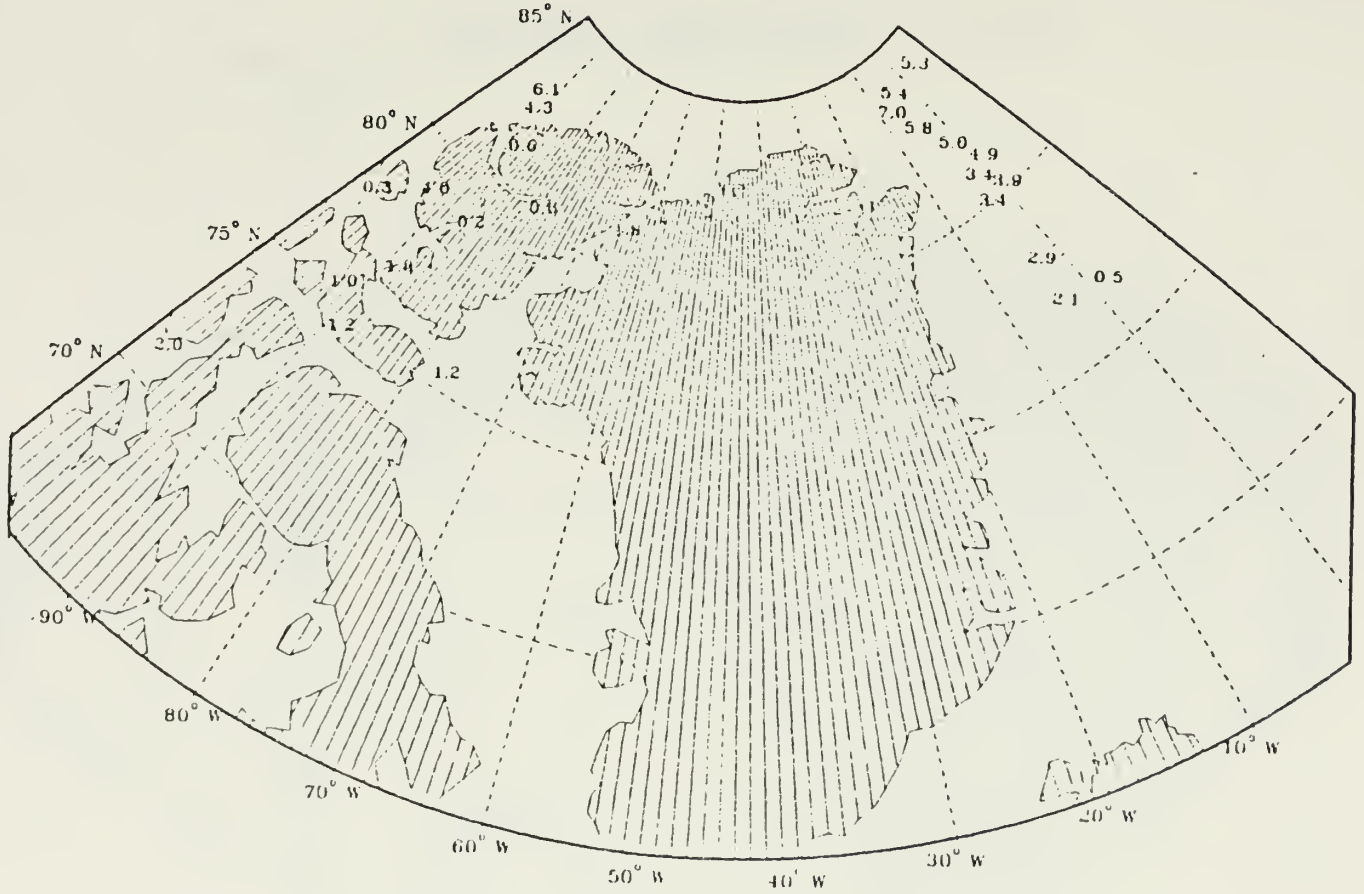

Figure C.14 Mean ice thickness(m) in autumn, 65°N-85°N, 100°W-010°E.

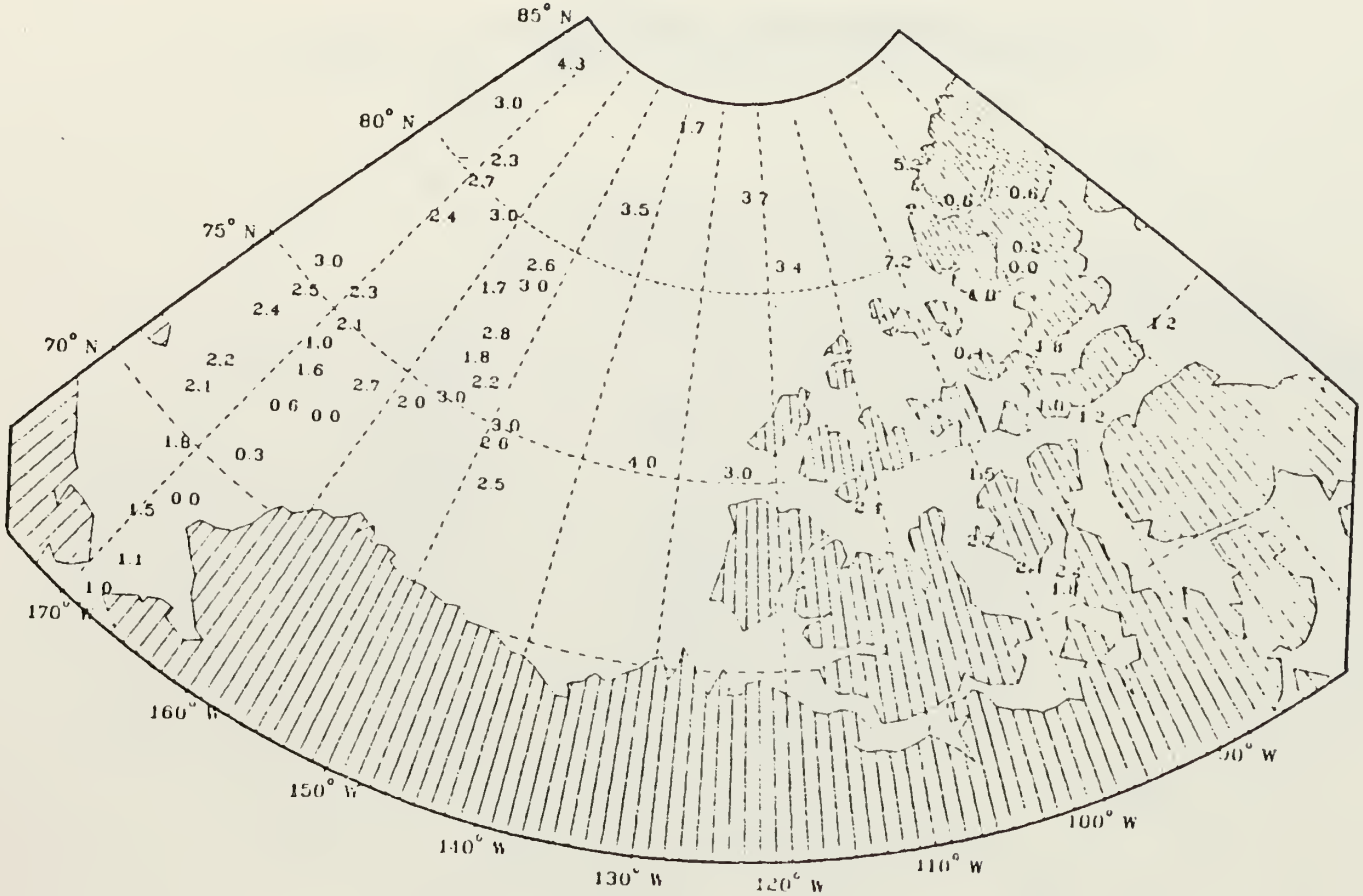

Figure C.15 Mean ice thickness(m) in autumn, 65°N-85°N, 180°W-070°W.

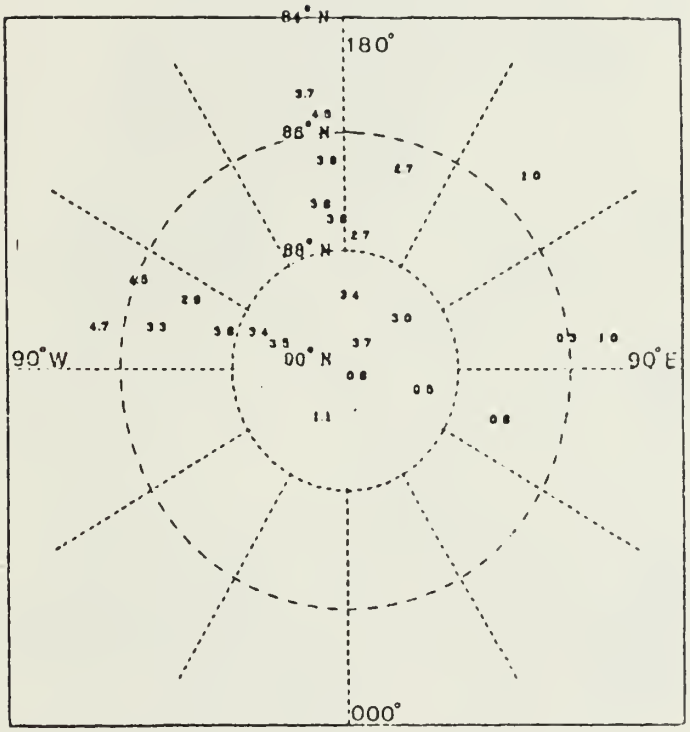

Figure C.16 Mean ice thickness(m) in winter, 84°N-90°N.

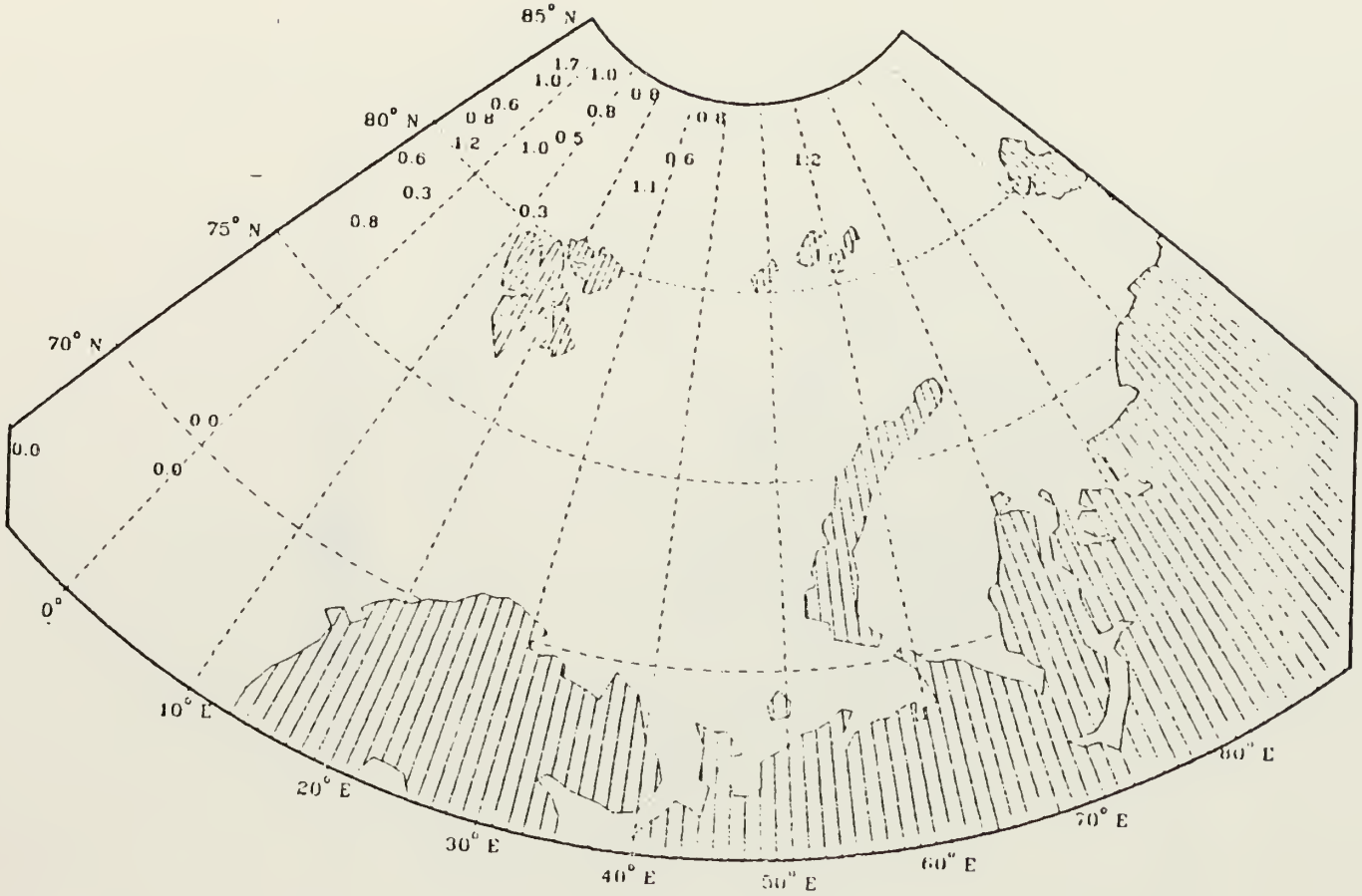

Figure C.17 Mean ice thickness(m) in winter, 65°N-85°N, 010°W-100°E.

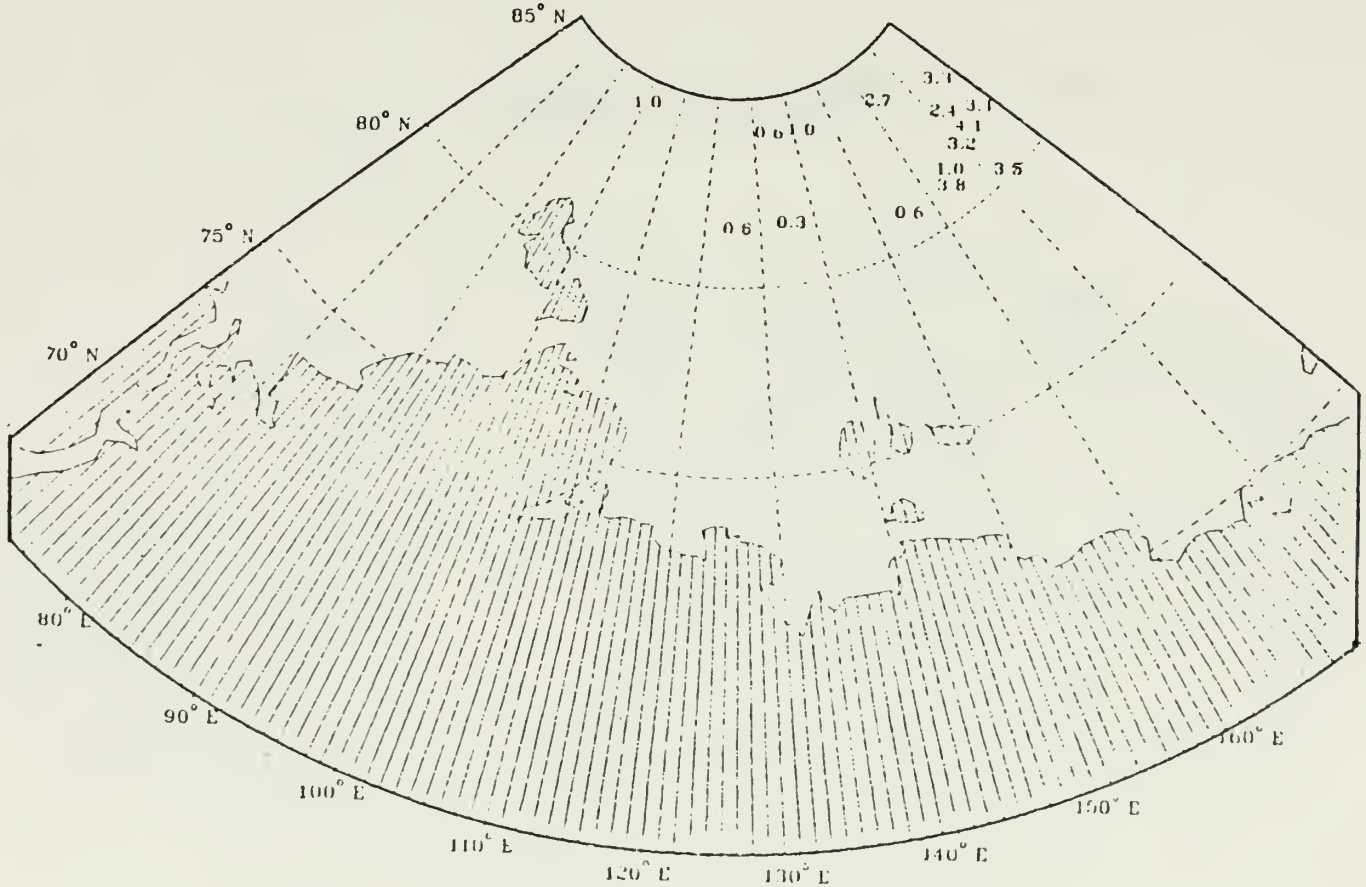

Figure C.18 Mean ice thickness(m) in winter, 65°N-85°N, 070°E-180°E.

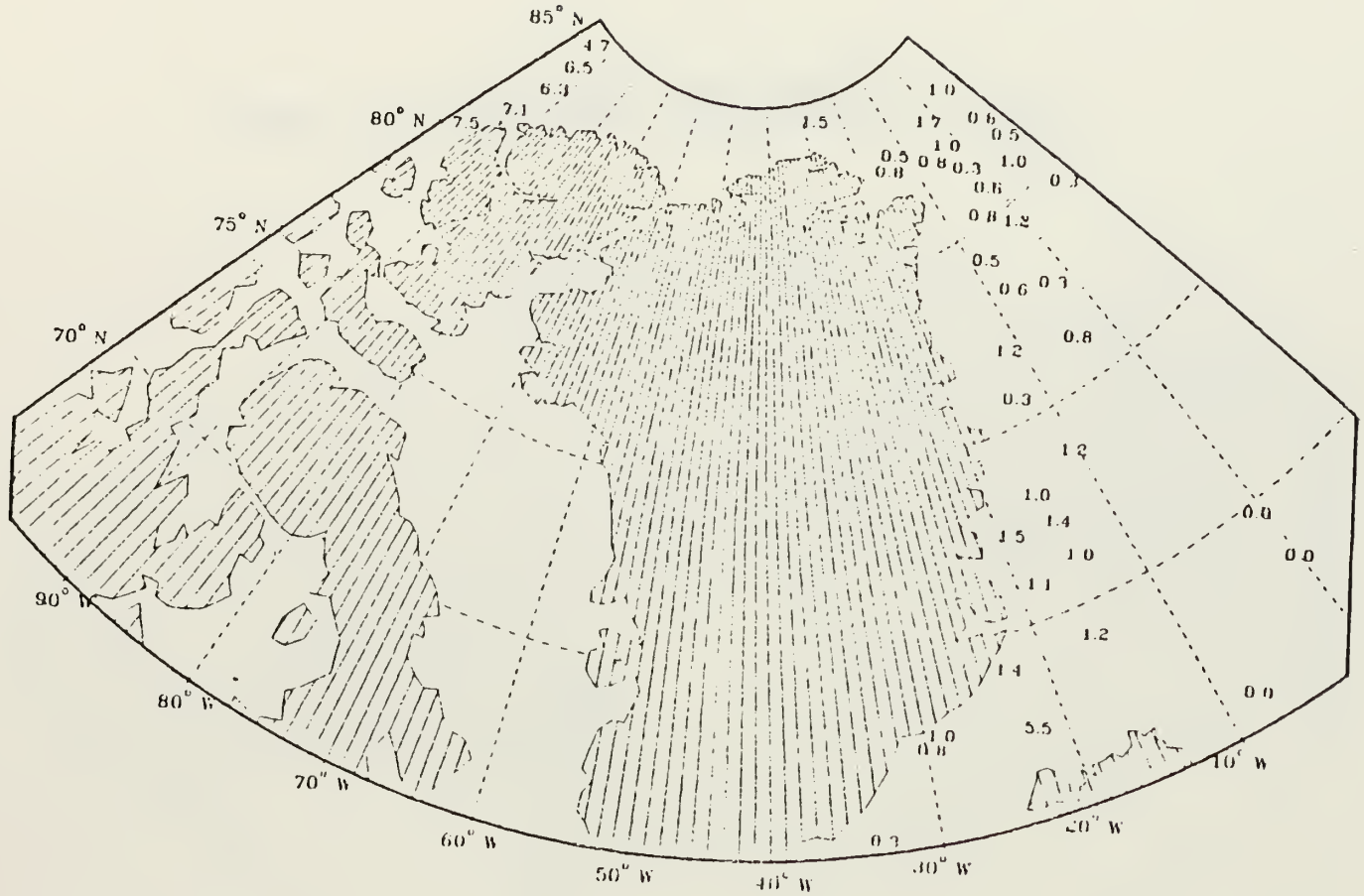

Figure C.19 Mean ice thickness(m) in winter, 65°N-85°N, 100°W-010°E.

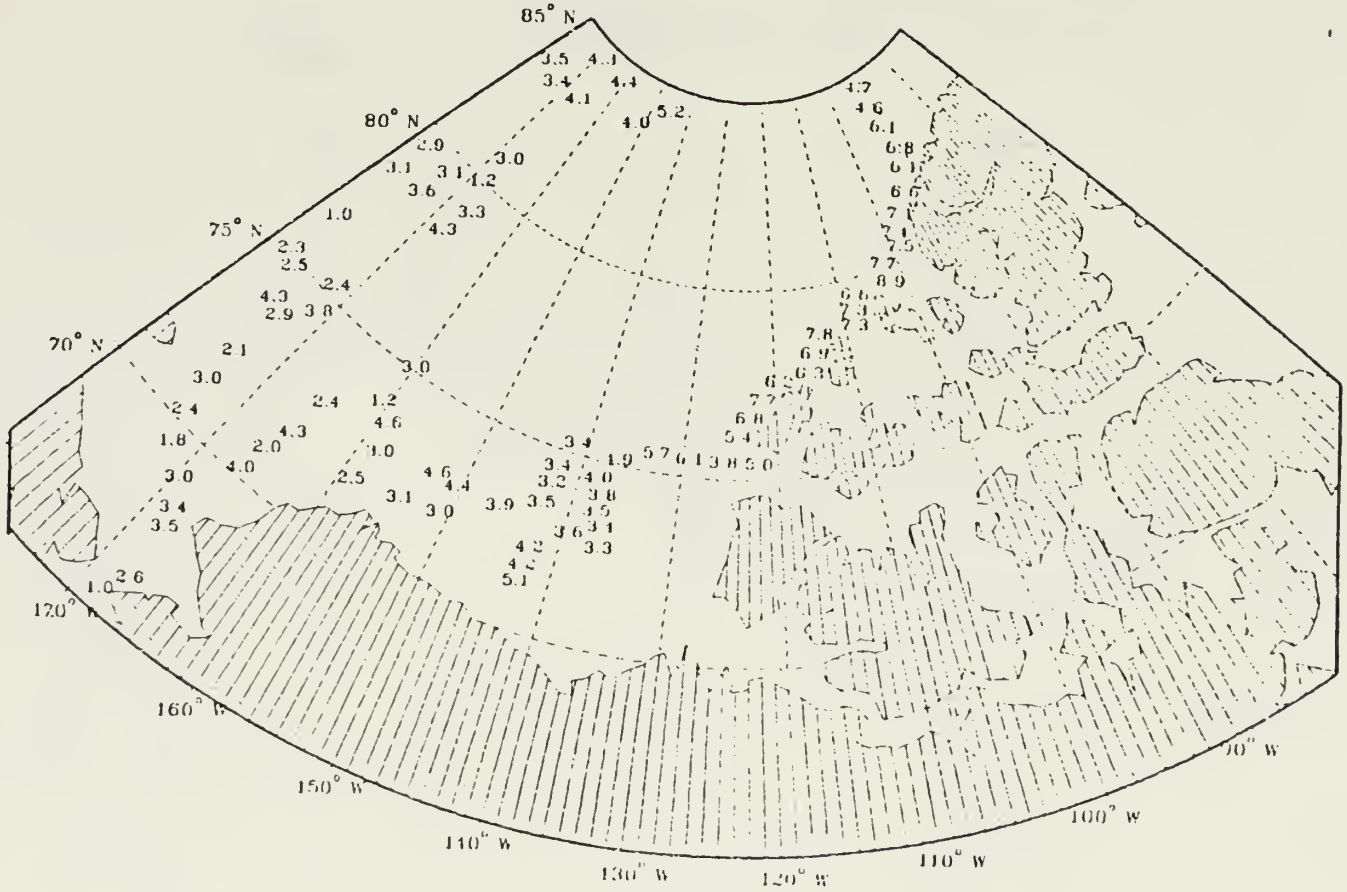

Figure C.20 Mean ice thickness(m) in winter, 65°N-85°N, 180°W-070°W.

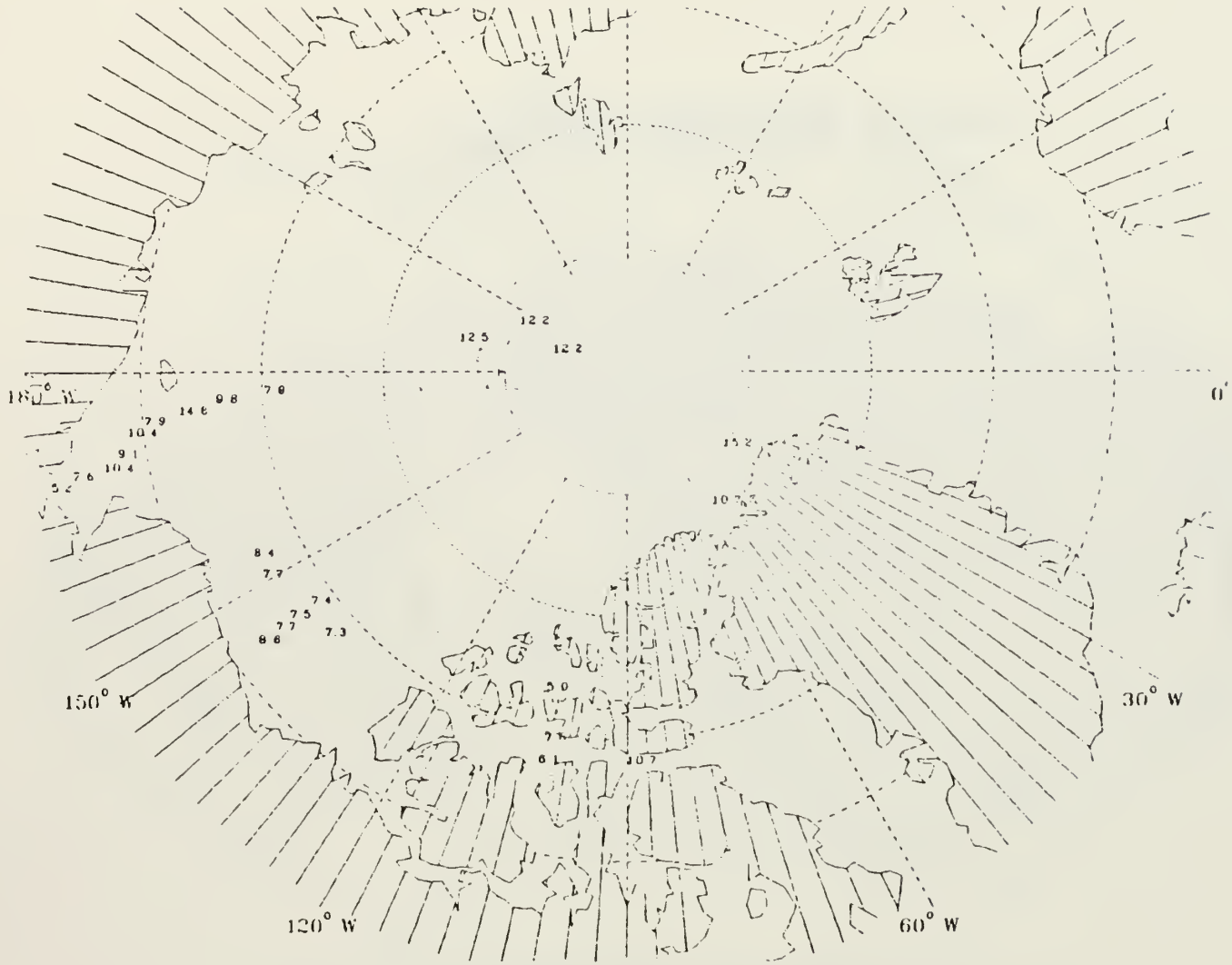

Figure C.21 Mean keel drafts(m) for spring, 65°N-90°N.

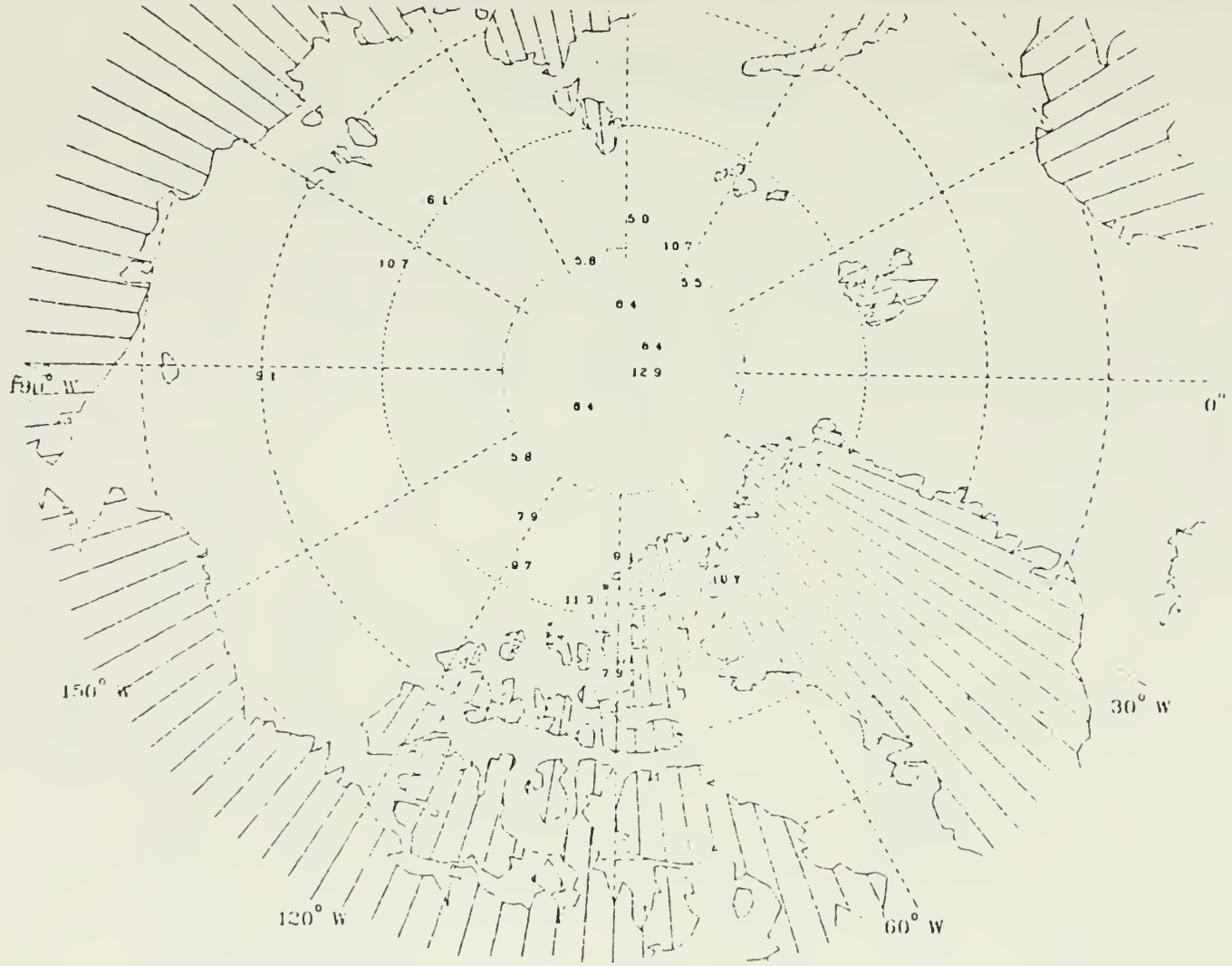

Figure C.22 Mean keel drafts(m) for summer, 65°N-90°N.

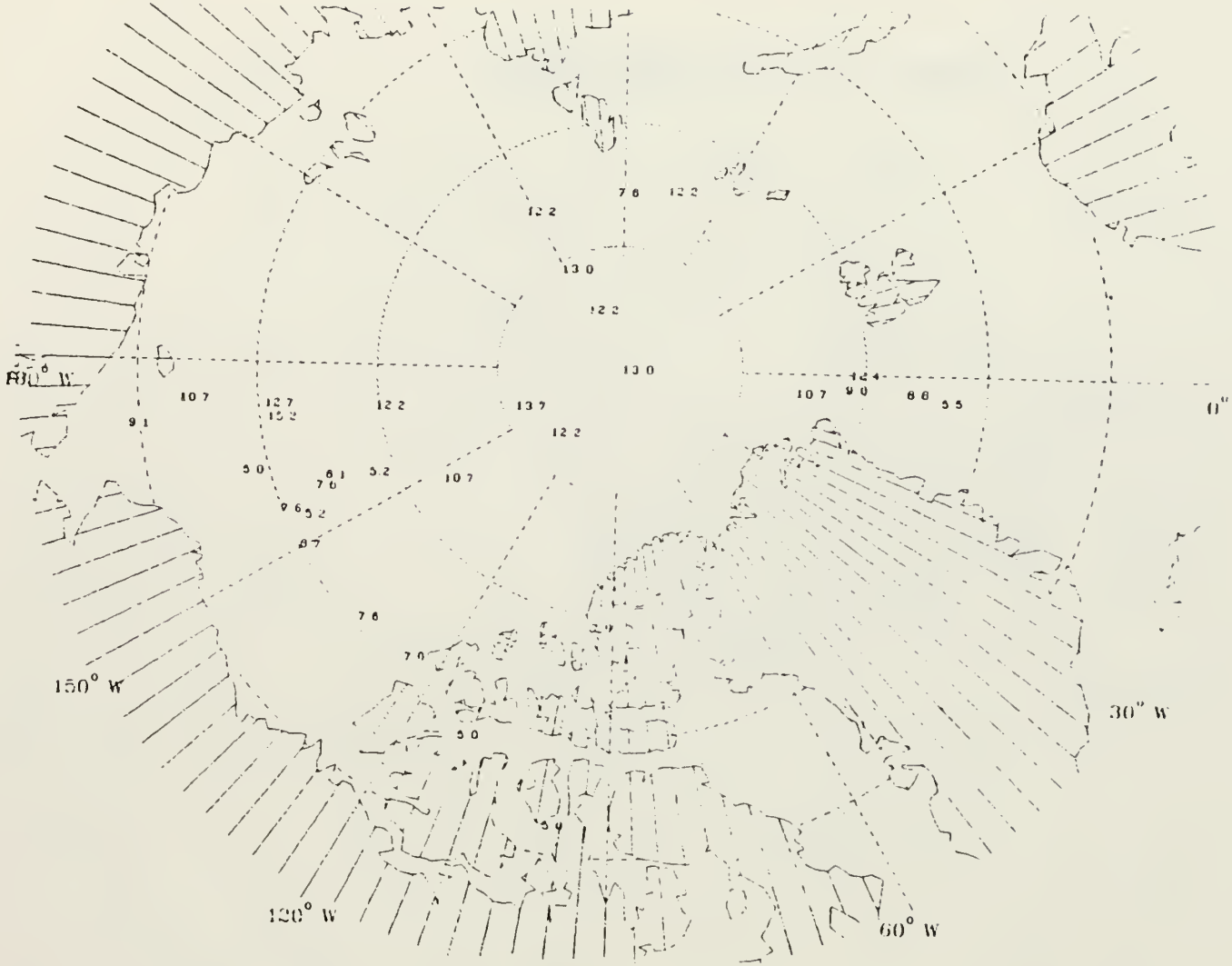

Figure C.23 Mean keel drafts(m) for autumn, 65°N-90°N.

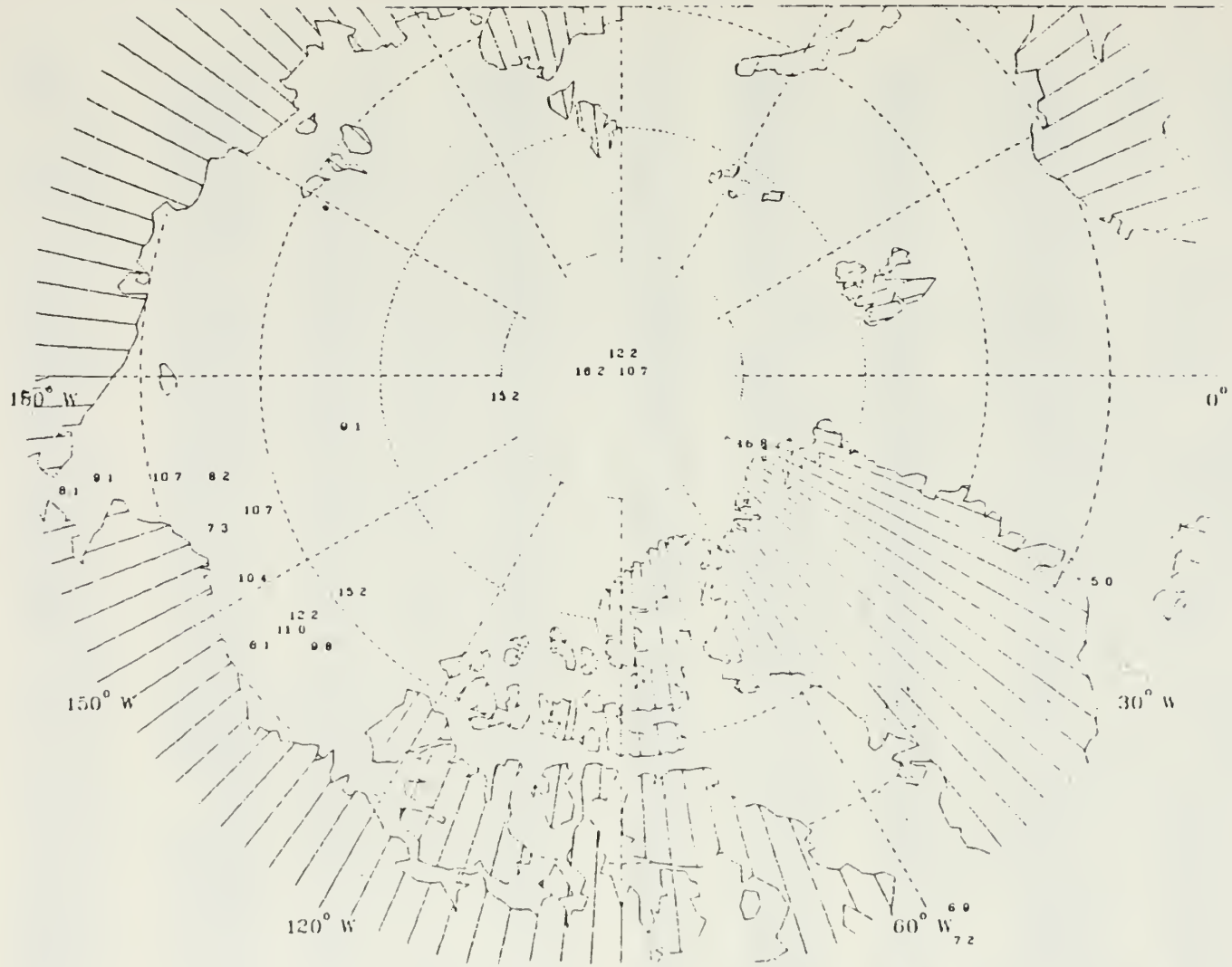

Figure C.24 Mean keel drafts(m) for winter, 65°N-90°N.

LIST OF REFERENCES

Aagaard, K., Coachman, L.K., and Carmack, E., 1981. On the halocline of the Arctic Ocean. Deep Sea Research 28A(6), p. 529-545.

Blidberg, D.R., Corell, R.W., Westneat, A.S., 1981. Probable ice thickness of the Arctic ocean. Coastal Engineering, 5, p. 159-169.

Campbell, W.J., 1984. Aspects of Arctic sea ice observable by sequential passive microwave observations from the NIMBUS-5 satellite. In: Arctic Technology and Policy. Proceedings at the Second Annual MIT Sea Grant College Program Lecture and Seminar and the Third Annual Robert Bruce Wallace Lecture. Hemisphere Publishing Company, New York, p. 197-221.

Campbell, W.J., Weeks, W.F., Ramseier, R.O., and Gloerson, P., 1975. Geophysical studies of floating ice by remote sensing. Journal of Glaciology, 15(73), p. 445-489.

Colony, R. and Thorndike, A., 1985. An estimate of the mean field of Arctic sea ice motion. Journal of Geophysical Research, 90(C1), p. 965-974.

Dunbar, M. and Wittman, W., 1963. Some features of ice movement in the Arctic Basin. In: Proceedings of Arctic Basin Symposium, 1962. Hershey, Pa., Arctic Institute of North America, Montreal, p. 90-108.

Hibler, W.D. III, 1972. Two dimensional statistical analysis of Arctic sea ice ridges. Sea Ice, National Resource Council of Iceland, Reykjavik, 35 p.

Hibler, W.D. III, 1979. A dynamic thermodynamic sea ice model. Journal of Physical Oceanography 9(4), p. 315-846.

Hibler, W.D. III and LeSchack, L.A., 1972. Power spectrum analysis of undersea and surface sea-ice profiles. Journal of Glaciology, 11, p. 345-356.

Hibler, W.D. III, Mock, S.J., and Tucker, W.B., 1974. Classification and variation of sea ice ridging in the Arctic Basin. Journal of Geophysical Research, 79(18), p. 2735-2743.

Hibler, W.D. III and Weeks, W.F., 1983. Modeling of Arctic sea ice characteristics relevant to naval operations. In: Proceedings 23rd Mine Development Conference. U.S. Naval Surface Weapons Center, NSWC, MP-83-146, White Oak, Maryland.

Hibler, W.D. III, Weeks, W.F., and Mock, S.J., 1973. Statistical aspects of sea-ice ridge distribution. United States Army Cold Regions Research and Engineering Laboratory, Hanover, N.H., Research Report 315, 26 p.

Koerner, R.M., 1970. Weather and ice observations of the British Trans-Arctic Expedition 1968-1969. Weather, 25, p. 218-228.

Kozo, T.L. and Tucker, W.B.III, 1974. Sea ice bottomside features in the Denmark Strait. Journal of Geophysical Research, 79(30), p. 4505-4511.

Kovacs, A., Weeks, W.F., Ackley, S., and Hibler, W.D. III, 1972. A study of a multiyear pressure ridge in the Beaufort Sea. AIDJEX Bulletin, 12.

LeSchack, L.A., 1975a. Analysis of Arctic underice profiles. Devlopment and Resources Transportation Co., Silver Spring, Md., 259 p.

LeSchack, L.A., 1980. Arctic Ocean sea ice statistics derived from the upward-looking sonar data recorded during five nuclear submarine cruises. LeSchack Associates Ltd., Silver Spring, Md.

LeSchack, L.A., 1983. Predicting standard deviation about the mean ice depth for the under-ice acoustic equation and charting statistics of open leads from airborne laser profiler data. LeSchack Associates, Ltd., Silver Spring, Md.

LeSchack, L.A. and Chang, D.C., 1977. Arctic under-ice roughness. Development and Resources Transportation Co., Silver Spring, Md.

LeSchack, L.A., Hibler, W.D. III, and Morse, F.H., 1970. Automatic processing of Arctic pack ice data obtained by means of submarine sonar and other remote sensing techniques. A Technical Report for the Office of Naval Research, Washington, D.C., 45 p.

LeSchack, L.A. and Lewis, J.E., 1983. Correlation of airborne laser data gathered contmporaneously with under-ice profile data recorded from a nuclear submarine. LeSchack Associates, Ltd., Silver Spring, Md.

Lowry, R.T. and Wadhams, P., 1979. On the statistical distribution of pressure ridges in sea ice. Journal of Geophysical Research, 84(C5), p. 2487-2494.

McLaren, A.S., Wadhams, P., and Weintraub, R., 1984. The sea ice topography of M'Clure Strait in winter and summer of 1960 from submarine profiles. Arctic, 37(2), p. 110-120.

McLaren, A.S., Wadhams, P., and Weintraub, R., (in press). Winter and summer ice distributions in M'Clure Strait measured by submarine profiling. Arctic.

Naval Polar Oceanography Center, 1983. Eastern-western Arctic sea ice analysis. Suitland, Md.

Sater, J.E., Ronhovde, A.G., and Van Allen, L.C., 1971. Arctic environment and resources. The Arctic Institute of North America, Washington, D.C., 309 p.

Stanford, G., 1984. Microwave radiometric measurement of sea ice salinity. NORDA Technical Report 267, Naval Research and Development Activity, NSTL, Mississippi, 10 p.

Tucker, W.B. III, Weeks, W.F., and Frank, M.D., 1979. Sea ice ridging over the Alaskan continental shelf. United States Army Cold Regions Research and Engineering Laboratory, Hanover, N.H., CRREL Report 79-8, 24 p.

Tucker, W.B. III, and Westhall, V.H., 1973. Arctic sea ice ridge frequency distribution derived from laser profiles. AIDJEX Bulletin 14, p. 171-180.

Wadhams, P., 1977. Characteristics of deep pressure ridges in the Arctic Ocean. In: Proceedings of the fourth International Conference on Port and Ocean Engineering under Arctic Conditions, ed. D.B.Muggeridge, Memorial University of Newfoundland, St. John's, Newfoundland, Canada, Vol. I, p. 544-555.

Wadhams, P., 1980a. A comparison of sonar and laser profiles along corresponding tracks in the Arctic Ocean. In: Sea Ice Processes and Models. ed. R.S. Pritchard, University of Washington Press, Seattle, Wa., p. 283-299.

Wadhams, P., 1980b. The estimation of sea ice thickness from the distribution of pressure ridge heights and depths. In: Proceedings of the International Workshop on Remote Estimation of Sea Ice Thickness. ed. J.R. Rossiter and J.P. Bazely, Memorial Univiversity, St. John's, Newfoundland, Canada, p. 53-76.

Wadhams, P., 1981a. Sea ice topography of the Arctic Ocean in the region 70W to 25E. Philisophical Transactions of the Royal Society of London, A(302), p. 45-85.

Wadhams, P., 1981b. The ice cover in the Greenland and Norwegian Seas. Review of Geophysics and Space Physics, 19(3), p. 345-393.

Wadhams, P., 1983a. Arctic sea ice morphology and its measurement. In: Arctic Technology and Policy. Proceedings at the Second Annual MIT Sea Grant College Program Lecture and Seminar and the Third Annual Robert Bruce Wallace Lecture. Hemisphere Publishing Corporation, New York, p. 179- 195.

Wadhams, P., 1983b. Sea ice thickness distribution in Fram Strait. Macmillan Journals Ltd., Basingstoke, Hampshire, U.K., 14 p.

Wadhams, P., (in press). The prediction of extreme keel depths from sea ice profiles. Cold Regions Science and Technology.

Wadhams, P. and Horne, R.J., 1980. An analysis of ice profiles obtained by submarine sonar in the Beaufort Sea. Journal of Glaciology, 25 (93), p. 401-424.

Wadhams, P., McLaren, A.S., and Weintraub, R., 1985. Ice thickness distribution in Davis Strait in February from submarine sonar profiles. Journal of Geophysical Research, 90(C1), p. 1069-1077.

Weeks, W.F., 1978. Sea ice conditions in the Arctic. United States Army Cold Regions Research and Engineering Laboratory, Hanover, N.H., Report # MP-910, 33 p.

Weeks, W.F., 1982. Physical properties of the ice cover of the Greenland Sea. United States Army Cold Regions Research and Engineering Laboratory, Hanover, N.H., Special Report 82-28, 122 p.

Weeks, W.F., 1984. Sea ice characteristics and ice penetration probabilities in the Arctic Ocean. United States Army Cold Regions Research and Engineering Laboratory, Hanover, N.H., 14 p. (Draft).

Weeks, W.F. and Ackley, S.F., 1982. The growth, structure, and properties of sea ice. United States Army Cold Regions Research and Engineering Laboratory, Hanover, N.H., CRREL Monograph 82-1, 130 p.

Weeks, W.F., Kovacs, A., and Hibler, W.D. III, 1971. Pressure ridge characteristics in the Arctic coastal environment. In: Proceedings from the First International Conference on Port and Ocean Engineering Under Arctic Conditions, Vol. 1, ed. S.S. Wetteland and P. Braun, Trondheim, Norway, p. 152-183.

Williams, W., Swithinbank, C., and Robin, G., 1975. A submarine sonar study of Arctic pack ice. Journal of Glaciology, 15, p. 349-362.

Wittman, W.I. and Schule, J.J., 1966. Comments on the mass budget of Arctic pack ice. In: Proceedings from the Symposium on the Arctic Heat Budget and Atmospheric Circulation, ed. J.O. Fletcher, Lake Arrowhead, Calif. Rand Corporation Research Memorandum RM-5233-NSF, Santa Monica, p. 215-246.

Wright, B.D., Knatiuk, J., and Kovacs, A., 1978. Sea ice pressure ridges in the Beaufort Sea. United States Army Cold Regions Research and Engineering Laboratory, Hanover, N.H., Report # MP-1132, 19 p.

Zubov, N.N., 1943. Arctic Ice. (in Russian), Izdatel'stvo Glavsermorputi, Moscow. Translated by U.S. Naval Oceanographic Office, 1979, Washington, D.C., 490 p.

BIBLIOGRAPHY

Ackley, S.F., 1976. Thickness and roughness variations of Arctic multiyear sea ice. United States Army Cold Regions Research and Engineering Laboratory, Hanover, N.H., Report 76-18.

Ackley, S.F., Hibler, W.D. III, Kovacs, A., Weeks, W.F., Hartwell, A., and Campbell, W.J., 1973. Investigations performed on the Arctic Ice Dynamics Joint Experiment. United States Army Cold Regions Research and Engineering Laboratory, Hanover, N.H., Research Report 315.

Ackley, S.F. and Smith, S.J., 1983. Reports of the U.S.-U.S.S.R. Weddel polynya expedition, October-November 1981, Vol. 5, sea ice observations. United States Army Cold Regions Research and Engineering Laboratory, Hanover, N.H.

Alpinis, J.J. and Peake, W.H., 1976. Passive microwave mapping of ice thickness. National Aeronautics and Space Administration, Lewis Research Center, Cleveland, Ohio. Final Report 3892-2.

Anderson, V.H., 1970. Sea ice pressure ridge study. An airphoto analysis. United States Army Cold Regions Research and Engineering Laboratory, Hanover, N.H. Photogrammetria 26(5-6).

Bajzak, D. and Langford, C.J., 1974. Sea ice mapping of the Labrador pack from satellite imagery. XXI Rassenga Internazioale Elettronica E Nucleare.

Barnes, J.C., Bowley, C.J., Smallwood, S.J., and Willand, J.H., 1977. Use of satellite data to evaluate surface ice conditions for offshore oil and gas exploration. In: Proceedings of the fourth International Conference on Port and Ocean Engineering under Arctic Conditions, ed. D.B. Muggeridge, Memorial University of Newfoundland, St. John's, Newfoundland, Canada, Vol. II.

Berkson, J.M., Clay, C.S., and Kan T., 1973. Mapping the underside of Arctic sea ice by backscattered sound. Journal of the Acoustical Society of America, 53(3).

Biggs, A.W., Fayman, D.L., Matreci, R., Moore, R.K., and Parashar, S.K., 1973. Scatterometry techniques for sensing Arctic sea ice thickness. Kansas University Center for Research Inc., Lawrence, Kansas.

Bilello, M.A., 1961. Ice thickness observations in the North American Arctic and Subarctic for 1958-59, 1959-60. United States Army Cold Regions Research and Engineeering Laboratory, Hanover, N.H., Report No.: CRREL-SR-43.

Bilello, M.A., 1980. Decay patterns of fast sea ice in Canada and Alaska. In: Sea Ice Processes and Models: from the Proceedings of the AIDJEX/ICSI Symposium. Univ of Washington Press., Seattle.

Bogorodskiy, V.V., and Tripol'nikov, V.P., 1972. Radar survey of the thickness of floating ice covers. United States Army Cold Regions Research and Engineering Laboratory, Hanover,

N.H., In: Problems of the Arctic and the Antarctic, 29, Leningrad.

Buck, B.M., (in press). Ice depth and roughness measurements in the Greenland-Svalbard Strait. Polar Research Laboratory, Inc. Santa Barbara.

Campbell, W.J., 1976. Ice lead and polynya dynamics. United States Geological Survey, Professional Paper 929. Washington, D.C.

Campbell, W.J., and Orange, A.S., 1974. Contiuous sea and fresh water ice thickness profiling using an impulse radar system. In: Advanced Concepts and Techniques in the Study of Snow and Ice Resources. Monterey, Ca.

Campbell, W.J., Ramseier, R.O., Zwally, H.J., and Gloerson, P., 1980. Arctic sea ice variations from time lapse passive microwave imagery. In: Passive Radiometry of the Ocean, P. Reidel Publishing Company, Holland.

Central Intelligence Agency, 1978. Polar regions atlas. Washington, D.C.

Dietz, R.S. and Shumway, G., 1961. Arctic basin geomorphology. Geological Society of America Bulletin, 72.

Dorinin, Y.P., Smetannikova, A.V., and Gruskina, A.S., (in press). Utilization of the numerical method of calculation for the prognosis of autumn-winter ice conditions in the Arctic seas. In: Ice Forecasting Techniques for the Arctic Seas. New Delhi.

Eppler, D.T., 1982. Possible applications of Geosat-A radar altimeter data to ice forecasting in polar regions. NORDA Technical Note 177. Bay St. Louis, Miss.

Garrison, G.R., 1977. Oceanographic measurements in the Chukchi Sea and Baffin Bay-1976. Arctic Submarine Laboratory, Code 54. Naval Oceans Systems Center, San Diego, Ca.

General Physics Corporation, 1982. Arctic information study bibliography. Office of Naval Research, Washington, D.C.

Hall, R.T., 1975. Spatial variability of ice thickness distribution as determined from Landsat-A. AIDJEX, In: Proceedings of The International Symposium on Remote Sensing of Environment, 10th, Ann Arbor, Mich., Oct. 6-10 1975. Environmental Research Institute of Michigan, Center for Remote Sensing Information and Analysis, Ann Arbor, Mich.

Hatchwell, J.A., 1972. Concepts for data collection in the Arctic. Arctic Institute of North America, Washington, D.C.

Hibler, W.D. III, 1975. Characterization of cold-regions terrain using airborne laser profilometry. Journal of Glaciology, 15(73).

Hibler, W.D. III, 1975. Statistical variations in Arctic sea ice ridging and deformation rates. In: Ice Technology 75, Symposium on Icebreaking and Related Technologies, Montreal. Society of Naval Architects Marine Engineers., New York.

Hibler, W.D. III, 1980. Modeling a variable thickness sea ice cover. United States Army Cold Regions Research and Engineering Laboratory, Hanover, N.H., Monthly Weather Review.

Ketchum, R.D. Jr., Farmer, L.D., and Welsh, J.P. Jr., (in press). K-Band radiometric mapping of sea ice. NORDA, NSTL Station, Miss.

Knatiuk, J., Kovacs, A., and Hibler, W.D. III, 1978. A study of several pressure ridges and ice islands in the Canadian Beaufort Sea. Journal of Glaciology, 20(84).

Koerner, R.M., 1973. The mass balance of the sea ice of the Arctic Ocean. Journal of Glaciology, 12.

Kovacs, A., 1977. Iceberg profiling thickness. In: Proceedings of the fourth International Conference on Port and Ocean Engineering under Arctic Conditions, ed. D.B. Muggeridge, Memorial University of Newfoundland, St. John's, Newfoundland, Canada, Vol. II.

Kuhn, P.M., Stearns, L.P., and Ramseier, R.O., 1975. Airborne infrared Airborne infrared imagery of Arctic sea ice distribution. National Oceanic and Atmospheric Administration, Atmospheric and Chemistry Laboratory. Report No.: NOAA-TR-ERL-331, Boulder, Co.

Langleben, M.P. and Pounder, E.A., (in press). Sea ice thickness from Sea ice thickness from pulsed sonic methods. McGill University, Montreal, Canada.

LeSchack, L.A., 1975b. Potential use of satellite IR for ice thickness mapping. Development and Resources Transportation Co., Silver Spring, Md.

LeSchack, L.A., 1977. Probability of finding thin ice for ADOM deployment. Report to ADOM committee, unpublished.

Marko, J., 1975. Satellite observations of the Beaufort Sea ice cover. Beaufort Sea Technical Report #54. Department of the Environment, Victoria, B.C.

Maykut, G.A., 1982. Large scale heat exchange and ice production in the Central Arctic. Journal of Geophysical Research, 87(C10).

Maykut, G.A. and Untersteiner, N., 1969. Numerical prediction of the thermodynamic response of Arctic sea ice to environmental changes. The Rand Corporation, Santa Monica, Ca.

Maykut, G.A. and Untersteiner, N., 1971. Some results from a time-dependent thermodynamic model of sea ice. Journal of Geophysical Research, 76.

McLaren, A.S., 1984. The evolution of the Arctic submarine. The Journal of Navigation, 37(3).

McLeod, W.R. and Hodder, D.T., 1977. An examination of Longterm ice forecast and periodicities of the Beaufort Sea. In: Proceedings of the fourth International Conference on Port and Ocean Engineering under Arctic Conditions, ed. D.B. Muggeridge, Memorial University of Newfoundland, St. John's, Newfoundland, Canada, Vol. II.

McNutt, L., 1981. Ice conditions in the eastern Bering Sea from NOAA and Landsat imagery: winter conditions 1974, 1976, 1977, 1979. NOAA Technical Memorandum ERL PMEL-24, Washington, D.C.

Mock, S.J., Hartwell, A.D., and Hibler W.D. III, 1973. Spatial aspects of pressure ridge statistics. Journal of Geophysical Research, 77.

Morey. R.M.,1975. Airborne sea ice thickness profiling using an impulse radar. Geophysical Survey Systems Inc., Report No. USCG-D-178-75, Burlington, Mass.

Muggeridge, D.B.,1978. POAC Proceedings, Volumes I and II. Memorial University of Newfoundland, St. John's, Newfoundland, Canada.

National Science Foundation, (in press). Ice forecasting techniques for the Arctic Seas, Office of Polar Programs, Washington, D.C.

Overgaard, S., Wadhams, P. and Lepparanta, M., 1983. Ice properties in the Greenland and Barents Sea during summer. Journal of Glaciology, 29(101).

Potorsky, G.J. and Mitchell, P.A.,1972. First degree day and related theoretical ice thickness curves for selected Russian Arctic stations. Naval Oceanographic Office, Washington, D.C.

Ramseier, R.O., Vant, M.R., Arsenault, L.D., Gray, L., Gray, R.B., and Chuddbiak, W.J.,1975. Distribution of sea ice thickness in the Beaufort Sea. Beaufort Sea Technical Report #30. Department of the Environment, Victoria, B.C.

Reed, J.C. and Sater, J.E., 1974. The coast and shelf of the Beaufort Sea. Arctic Institute of North America, Washington D.C., In: Proceedings of Symposium on Beaufort Sea Coast and Shelf Research. Washington, D.C.

Rogers, J.C.,1977. A meteorlogical basis for long-range forecasting of summer and early autumn sea ice conditions in the Beaufort Sea. In: Proceedings of the fourth International Conference on Port and Ocear Engineering under Arctic Conditions, ed. D.B. Muggeridge, Memorial University of Newfoundland, St. John's, Newfoundland, Canada, Vol. II.

Rossiter, J.R. and Bazely, D.P.,1980. International workshop on the remote estimation of sea ice thickness, Proceedings. Memorial University of Newfoundland, Centre for Cold Ocean Resources Engineering Publication, St. John's, Canada.

Rossiter, J.R., Langhorne, P., Ridings, T., and Allan, A.J.,1977. Study of sea ice using impulse radar. In: Proceedings of the fourth International Conference on Port and Ocean Engineering under Arctic Conditions, ed. D.B. Muggeridge, Memorial University of Newfoundland, St. John's, Newfoundland, Canada, Vol. I.

Rothrock, D.A.,1978. Modeling sea ice features and processes. Polar Science Center, University of Washington, Seattle, Wa., In: The Symposium on Dynamics of Large Ice Masses, 21-25 August, 1978, Ottawa, Canada.

Rothrock, D.A. and Hall, R.T.,1975. Testing the redistribution of sea ice thickness from ERTS photographs. AIDJEX Bulletin, 29. University of Washington, Seattle, Wa.

Rothrock, D.A. and Thorndike, A.S.,1980. Geometric properties of the underside sea ice. Journal of Geophysical Research, 85(C7).

Rouse, J.W., Jr. and Schell, J.A.,1970. Radar studies of Arctic ice. In: Proceedings of a Seminar on Thickness Measurement of Floating Ice by Remote Sensing held at Defence Research Establishment, Technical Note No. 71-14, Ottawa.

Sater, J.E.,1969. The Arctic Basin. The Arctic Institute of North America, Washington, D.C.

Stigebrandt, A.,1981. A model for the thickness and salinity of the upper layer in the Arctic Ocean and the relationship between the ice thickness and some external parameters. Journal of Physical Oceanography, 11(10).

Thorndike, A.S., Rothrock, D.A., and Maykut, G.A.,1975. The thickness distribution of sea ice. Journal of Geophysical Research, 80(33).

Tucker, W.B. III and Govini, J.W.,1981. Morphological investigations of first-year sea ice pressure ridge sails. United States Army Cold Regions Research and Engineering Laboratory, Hanover, N.H., Cold Regions Science and Technology, 5(1).

Untersteiner, N.,1968. Natural desalination and equilibrium salinity profile of perennial sea ice. Journal of Geophysical Research 73(4).

Untersteiner, N., Maykut, G.,(in Press). Arctic Sea Ice. Washington University, Department of Atmospheric Sciences, Seattle, Wa.

Untersteiner, N. and others,1974. Annual Report No. 6. Washington University, Department of Atmospheric Sciences, Seattle, Wa.

Untersteiner, N. and others,1975. Annual Report No. 7. Washington University, Department of Atmospheric Sciences, Seattle, Wa.

Untersteiner, N. and others,1976. Annual Report No. 8. Washington University, Department of Atmospheric Sciences, Seattle, Wa.

Untersteiner, N. and others,1977. Annual Report No. 9. Washington University, Department of Atmospheric Sciences, Seattle, Wa.

Untersteiner, N. and others,1978. Annual Report No. 10. Washington University, Department of Atmospheric Sciences, Seattle, Wa.

U.S. Naval Oceanographic Office, 1951. Sailing directions for the East Coast of Siberia. H.O. Pub. 98., Washington, DC.

U.S. Naval Oceanographic Office, 1958. Oceanographic atlas of the polar seas Part II, Arctic, H.O. Pub. 705., Washington, D.C.

U.S.S.R. Ministry of Defense, Navy, 1980. Atlas Okeanov, Severnyj Ledovityj Okean (Atlas of Oceans, Arctic Ocean). Moscow.

Wadhams, P.,1975. Sea ice morphology in the Beaufort Sea. Beaufort Sea Technical Report #36, Dept. of the Environment, Victoria, B.C.

Wadhams, P. and Squire, V.A.,1983. An ice-water vortex at the edge of the East Greenland Current. Journal of Geophysical Research, 88.

Welsh, J.P., Wessel, R., Harr, P.A., and Pham, T.C.,1981. Report on FY81 effort for PIFS-N model. Naval Ocean

Research and Development Activity, NORDA Technical Note 123, Bay St. Louis, Miss.

Wittman, W.I. and MacDowell, G.P., 1964. Manual of short-term sea ice forecasting. United States Naval Oceanographic Office, Washington, D.C.

Wright, B.D., Knatiuk, J., and Kovacs, A., 1979. Multiyear pressure ridges in the Canadian Beaufort Sea. In: Port and Engineering under Arctic Conditions, Norwegian Inst. of Tech., Oslo.

Zakrzewski, W., 1982. Lody na Morzach. (Ice on Oceans). Gdan'sk.

INITIAL DISTRIBUTION LIST

		No. Copies
1.	Defense Technical Information Center Cameron Station Alexandria, VA 22314	2
2.	Library, Code 0142 Naval Postgraduate School Monterey, CA 93943	2
3.	Chairman (Code 68Mr) Department of Oceanography Naval Postgraduate School Monterey, CA 93943	1
4.	Chairman (Code 63Rd) Department of Meteorology Naval Postgraduate School Monterey, CA 93943	1
5.	Prof. R.H. Bourke (Code 68Bf) Department of Oceanography Naval Postgraduate School Monterey, CA 93943	5
6.	LCDR Robert P. Garrett Naval Oceanography Command Detachment Naval Air Station, Box 154 Cecil Field, FL 32215-0154	1
7.	Director Naval Oceanography Division Naval Observatory 34th and Massachusetts Avenue NW Washington, DC 20390	1
8.	Commander Naval Oceanography Command NSTL Station Bay St. Louis, MS 39522	1
9.	Commanding Officer Naval Oceanographic Office NSTL Station Bay St. Louis, MS 39522	1
10.	Commanding Officer Fleet Numerical Oceanography Center Monterey, CA 93940	1
11.	Commanding Officer Naval Ocean Research and Development Activity NSTL Station Bay St. Louis, MS 39522	1
12.	Commanding Officer Naval Environmental Prediction Research Facility Monterey, CA 93940	1

13. Chairman, Oceanography Department
U. S. Naval Academy
Annapolis, MD 21402 — 1

14. Chief of Naval Research
800 N. Quincy Street
Arlington, VA 22217 — 1

15. Office of Naval Research (Code 420)
Naval Ocean Research and Development Activity
800 N. Quincy Street
Arlington, VA 22217 — 1

16. Scientific Liaison Office
Office of Naval Research
Scripps Institution of Oceanography
La Jolla, CA 92037 — 1

17. Library
Scripps Institution of Oceanography
P.O. Box 2367
La Jolla, CA 92037 — 1

18. Library
Department of Oceanography
University of Washington
Seattle, WA 98105 — 1

19. Commander
Oceanographic Systems Pacific
Box 1390
Pearl Harbor, HI 96860 — 1

20. Commander (AIR-370)
Naval Air Systems Command
Washington, DC 20360 — 1

21. Commanding Officer
Naval Polar Oceanography Center, Suitland
Washington, DC 20373 — 1

22. Mr. Meyer Kleinerman (U04)
Naval Surface Weapons Center, NSWC
Silver Spring, MD 20902 — 1

23. Commander John King, USN
Naval Surface Weapons Center, NSWC
Silver Spring, MD 20902 — 1

24. Dr. W.F. Weeks
U.S. Army Cold Regions Research and Engineering Laboratory
Hanover, NH 03755 — 1

25. Library
U.S. Army Cold Regions Research and Engineering Laboratory
Hanover, NH 03755 — 1

26. Dr. Alan Beal (Code 54)
Arctic Submarine Laboratory
Naval Oceans Systems Center
San Diego, CA 92152 — 1

27. Dr. W.D. Hibler III
U.S. Army Cold Regions Research and Engineering Laboratory
Hanover, NH 03755 — 1

28. Dr. Ronald L. Woodfin
Div. 0333
Sandia National Laboratories
Albuquerque, NM 87185 — 1

29. Library
School of Oceanography
Oregon State University
Corvallis, OR 97331 — 1

30. Mr. Ken Pollak
Fleet Numerical Oceanography Center
Bldg. 13
Monterey, CA 93940 — 1

31. Capt. A.S. McLaren USN (Ret.)
1310 College Avenue, Suite 1104
Boulder, CO 80302 — 1

32. Dr. Warren Denner
SAIC
205 Montecito Ave.
Monterey, CA 93940 — 1

33. Director
Applied Physics Laboratory
Attn: Mr. Robert E. Francois
University of Washington
1013 Northeast 40th Street
Seattle, WA 98195 — 1

34. Chief of Naval Operations
Attn: NOP-02
Department of the Navy
Washington, DC 20350 — 1

35. Chief of Naval Operations
Attn: NOP-22
Department of the Navy
Washington, DC 20350 — 1

36. Dr. John L. Newton
10211 Rookwood Dr.
San Diego, CA 92131 — 1

37. Commanding Officer
Naval Submarine School
Box 700
Naval Submarine Base, New London
Groton, Connecticut 06340 — 1

38. Commander
Submarine Development Squadron Twelve
Naval Submarine Base, New London
Groton, Connecticut 06349 — 1

39. Commander Submarine Force
U.S. Atlantic Fleet
Norfolk, VA 23511 — 1

40. Commander Submarine Force
U.S. Pacific Fleet
N-21
FPO San Francisco, CA 96860 — 1

41. Mr. Beaumont M. Buck
Polar Research Laboratory
6309 Carpinteria Ave.
Carpinteria, CA 93013 — 1

42. Dr. James Wilson
c/o Polar Research Laboratory
6309 Carpinteria Ave.
Carpinteria, CA 93013 — 1

43. Dr. Ira Dyer
Dept. of Oceanography
Romm 5-212
Massachusetts Inst. of Technology
Cambridge, MA 02543 — 1

44. Dr. Drew A. Rothrock
Polar Science Center
4057 Roosevelt Way NE
Seattle, WA 98105 — 1

45. School of Oceanography, WB-10
University of Washington
Attn: Dr. L. K. Coachman
Seattle, WA 98105 — 1

46. School of Oceanography, WB-10
University of Washington
Attn: Dr. K. Aagaard
Seattle, WA 98105 — 1

47. School of Oceanography, WB-10
University of Washington
Attn: Dr. S. Martin
Seattle, WA 98105 — 1

48. Scott Polar Research Institute
University of Cambridge
Attn: Library
Cambridge, England
CB2 1ER — 1

49. Scott Polar Research Institute
University of Cambridge
Attn: Sea Ice Group
Cambridge, England
CB2 1ER — 1

50. Dr. Kenneth Hunkins
Lamont-Doherty Geological Observatory
Palisades, NY 10964 — 1

51. Science Applications, Inc.
Attn: Dr. Robin Muench
13400B Northrup Way
Suite 36
Bellevue, WA 98005 — 1

52. Institute of Polar Studies
Attn: Library
103 Mendenhall
125 South Oval Mall
Columbus, OH 43201 — 1

53. Institute of Marine Science
University of Alaska
Attn: Library
Fairbanks, AK 99701 — 1

54. Institute of Marine Science
University of Alaska
Attn: Dr. Joe Niebauer
Fairbanks, AK 99701 — 1

55. Bedford Institute of Oceanography
Attn: Library
P.O. Box 1006
Dartmouth, Nova Scotia
Canada
B2Y 4A2 — 1

56. Dr. Eddy C. Carmack
Dept. of the Environment
NWRI Branch
4160 Marine Drive
W. Vancouver, B. C. V7V 1N6 — 1

Thesis
G203
c.1

214255

Garrett
Temporal and spatial distributions of Artic sea ice thickness and pressure ridging statistics.

Thesis
G203
c.1

214255

Garrett
Temporal and spatial distributions of Artic sea ice thickness and pressure ridging statistics.

thesG203
Temporal and spatial distributions of Ar
3 2768 000 62966 1
DUDLEY KNOX LIBRARY